Auckland Regional Council
TE RAUHĪTANGA TAIAO

Mahurangi Estuary

Sedimentation History and Recent Human Impacts

June TR 2009/061

Auckland Regional Council
Technical Report No.061 June 2009
ISSN 1179-0504 (Print)
ISSN 1179-0512 (Online)
ISBN 978-1-877528-73-6

This report is part of a series of reports that were commissioned during the period 1993-1999 that were used to support the establishment of the Mahurangi Action Plan. They are being made available following a review of technical information.

Reviewed by:

Name: Amy Taylor

Position: Project Leader Land

Organisation: ARC

Date: 1/06/09

Approved for ARC Publication by:

Name: Grant Barnes

Position: Group Manager Monitoring & Research

Organisation: ARC

Date: 1/06/09

Recommended Citation:

Swales, A.; Hume, T. M.; Oldman, J. W.; Green, M. O.; etc. (1997). Title. Prepared by Organisation for Auckland Regional Council. Auckland Regional Council Document Type 2009/061.

Mahurangi Estuary: Sedimentation History and Recent Human Impacts

Andrew Swales
Terry M. Hume
John W. Oldman
Malcolm O. Green

prepared for

Auckland Regional Council

NIWA Client Report: ARC60201
June 1997

National Institute of Water & Atmospheric Research Ltd
PO Box 11-115, Hamilton
New Zealand
Tel: 07 856 7026
Fax: 07 856 0151

Contents

Reviewed by: *Approved for release by:*

R. B. Williamson J.C. Rutherford

Executive Summary

Estuaries infill with sediment from catchment and marine sources, the former inputs being most susceptible to human influences. Modification of estuaries following human settlement has been rapid in comparison to their prehistory. In New Zealand, soil erosion accompanying catchment deforestation and conversion to pasture from the 1800's, and more recently urban development, have permanently altered the quality and quantity of waters discharged to estuaries and led to accelerated estuary infilling and changes in the character of sediments deposited. These changes can have detrimental impacts on estuarine water quality, ecology, recreation, navigation and aesthetic values.

A study was made of the sedimentation history and present day sedimentation processes in the Mahurangi Estuary, to determine how the estuary has responded to historical changes in catchment sediment loads, associated with landcover changes following human settlement. The results serve as a guide to assessing how the Mahurangi Estuary will cope with future catchment development.

The Mahurangi Estuary (high tide area 24.7 km^2) is largely intertidal (65%). The *upper estuary* is a 6.4 km long tidal creek between Warkworth and Hamiltons Landing, bordered by dense stands of mangrove. Here, sedimentation is strongly influenced by freshwater discharge, particularly during floods. The *lower estuary*, seaward of Hamiltons Landing, is wide and deep, with numerous embayments and tidal arms, accounts for approximately 90% of the estuary's tidal volume. At low tide, extensive intertidal flats flank the main tidal channel.

Investigations included probing and coring the sediment column, stratigraphic analysis of the cores, assessing channel infilling from historical soundings, determining sediment accumulation rates from core stratigraphy and radiocarbon and pollen dating, examining records of historical land cover, estimating estuary sedimentation loads from estuary infilling - the proportion of the total load (suspended and bedload) deposited in the estuary. The potential for estuarine sediments to be reworked by waves and tidal currents was also modelled.

- At least 7300 years ago the Mahurangi Estuary was a deep subtidal basin, slowly infilling (0.3-0.8 mm/yr) with fine suspended sediment supplied by runoff from a native forest catchment. Up to 15 m of mud has been deposited in the lower estuary. During this time sedimentation predominated because the estuary was much deeper and therefore small, short period wind waves were much less effective at reworking sediments than today and only channel sediments were reworked by spring tide currents.

- Humans first arrived in the Mahurangi about 700 years ago. There is no evidence of catchment disturbance by the Polynesian in the sedimentary record. In contrast, rapid catchment deforestation following European settlement (1850-1900 A.D.) resulted in severe soil erosion and rapid deposition of thick sequences of gravel, sand, mud and vegetation in the upper estuary. Some 3 m of sediment have been deposited in the upper estuary since 1850 A.D. and a large proportion of this sediment (i.e., 2.2 m) has been deposited since the early 1900's. The narrow upper estuary therefore represents a 'sump' for coarse sediments eroded from the denuded catchments. In the much larger lower estuary the impact of catchment deforestation has been preserved as a relatively thin cap (i.e., average 0.3 m) of muddy sands on top of the Mahurangi Mud.

- The overall pattern of increased sedimentation in the estuary following catchment deforestation is similar to that documented in other Auckland estuaries. Background sedimentation rates of 0.3-0.8 mm/yr are similar to rates measured in Lucas (1 mm/yr), Brighams (0.5-0.8 mm/yr) and Hellyers Creeks (0.35 mm/yr) in the Upper Waitemata Harbour. Increased sedimentation in the lower estuary (2-4 mm/yr) during catchment deforestation is similar to that measured in the Upper Waitemata Harbour (3 mm/yr), although sedimentation rates in the upper Mahurangi Estuary are much higher (16-21 mm/yr). Since the early 1900's the rate of infilling in the lower estuary has declined moderately (average 2.2 mm/yr), while increased sedimentation in the upper estuary is partly attributed to the delayed delivery of coarse bedload sediments from catchment storage.

- Estuary sedimentation loads (that component of the total catchment sediment load deposited in the estuary) were computed from estuary sedimentation rates. They reveal that sedimentation loads were relatively low (120 tonnes/km^2/yr) prior to catchment deforestation (1850-1900 A.D.), which resulted in a 13-fold increase in sedimentation loads to about 1600 tonnes/km^2/yr. Some 75% of the total sedimentation load (9.6 million tonnes) associated with deforestation has been deposited in the lower estuary. Since 1900 A.D. the average annual sedimentation load has declined by 25% to 1170 tonnes/km^2/yr but is still an order of magnitude higher than sedimentation loads from the earlier forested catchment. In the lower estuary, where most of the suspended sediment is deposited, sedimentation loads have averaged 702 tonnes/km^2/yr since 1900 A.D.

- The estuary sedimentation load (average 702 tonnes/km^2/yr) deposited in the lower estuary since 1900 A.D. was compared with catchment suspended sediment loads over the last 20 years (average 448 tonnes/km^2/yr), computed using the Basin New Zealand (BNZ) model. The computed average sediment load is 64% of the long term value estimated from estuary sedimentation. These estimates are in remarkably good agreement, suggesting that catchment soil erosion has declined moderately since the early 1900's.

- Sedimentation in the Mahurangi Estuary is dominated by floods and infrequent large floods can deliver a large proportion (i.e., 98%) of the annual sediment load to the estuary. For instance, the May 1985 flood (50 year return period rainfall) delivered 75% of the annual average suspended sediment load (1976-1995). In fact the cumulative contribution of floods in 1985 was 3 times the annual average catchment load. If the May 1985 and total flood sediment loads for that year are distributed equally over the lower estuary this yields 1.3 mm and 3.7 mm of sedimentation. The average sedimentation rate in the lower estuary since 1900 A.D. has been 2.2 mm/yr.

- Sedimentation in the Mahurangi Estuary is also influenced by the mixing of river and sea water. In this partially-mixed state, the mixing of surface freshwater with the underlying saltwater drives a landward directed residual current near the bed which carries a proportion of the suspended sediment to the upper estuary. Consequently, in the vicinity of Hamiltons Landing there is a zone of high turbidity which also coincides with an area of rapid sedimentation over the last 150 years.

- Both tidal currents and waves rework and transport sediment in the Mahurangi Estuary today. Reworking by currents coincides with spring tides (cf. neap tides), which are strong enough to mobilise sediments in the main channel and on the lower intertidal flats over much of the tidal cycle. There is little reworking of sediment by tidal currents higher on the intertidal flats because here currents are weak, and also the flats are exposed for long periods.

- Wind waves are a far more important mechanism than currents for reworking intertidal sediments. Short period waves have high orbital velocities which are able to entrain sediments in the shallow water depths, although the window for reworking intertidal sediments is limited by the length of time the flats are inundated. Most of the sediment reworking occurs during extreme, intermittent periods of high winds which occur for several days/year. Westerly winds account for 50% of the local wind climate and intertidal sediments on the eastern half of the estuary are reworked more frequently than elsewhere. As a consequence more sandy sediments are found on the extensive intertidal flats north of Grants Island.

- Our studies show that the Mahurangi Estuary is very susceptible to the impacts of catchment soil erosion as evidenced by rapid estuary infilling and a change to much coarser sediment deposition in the last 150 years. Despite the fact that future catchment sediment loads will never be as extreme as occurred during catchment deforestation last century, sediment loads today are at least 5-6 times higher than prior to deforestation. Today the estuary has attained an advanced stage of infilling and although currents and waves appear to mitigate estuary infilling to some degree, sedimentation will continue to occur. In the upper estuary, continued rapid sedimentation is of concern, particularly in the vicinity of Hamiltons Landing. Infilling of the estuary has permanently and dramatically altered the capacity of the system to store and flush catchment sediment loads. For this reason we strongly recommend that future catchment development that is likely to expose catchment soils to erosion will have to be planned with particular care if further increases in estuary sedimentation and consequent adverse environmental effects are to be mitigated or avoided.

1. INTRODUCTION

1.1 Background

The Mahurangi Estuary (24.7 km^2) is located on the east coast of the Northland Peninsula, some 50 km north of Auckland. The *upper estuary* (termed estuary by Harris, 1993) is the 6.4 km long narrow tidal creek between Warkworth Falls and Hamilton's Landing (Fig. 1.1). The sinuous channel is bordered by extensive, dense stands of the mangrove *Avicennia marina* var. *resinifera*. Here, sedimentary processes are strongly influenced by freshwater discharge, particularly during floods (i.e., flood sedimentation and strong salinity gradients). The *lower estuary* (termed Harbour by Harris, 1993), seaward of Hamilton's Landing, is wide and deep with numerous side embayments and tidal arms, and accounts for approximately 90% of the estuary's tidal prism (40.54 x10^6 m^3; Harris 1993). At low tide, extensive areas of muddy-sand flats are exposed, flanking the main tidal channel, which are fringed by dense mangrove stands. Here, waves and tidal currents rework surficial sediments. The Mahurangi Estuary was formed some 6500 years ago when the sea rose to its present level, drowning the ancestral river valley. Since this time the estuary has been infilling with sediments.

The estuary is an important recreational resource used widely for boating and fishing and general water related pursuits. It is also the site of a large scale (120 ha) pacific oyster (intertidal rack culture) industry established in the early 1970's. Farms are located in the lower estuary in Dyers Creek, Browns and Huawai Bays, Te Kapa and Pukapuka Inlets (Fig. 1.1). This industry accounts for some 30% ($7.5 million) of the national export crop and locally employs some 80 full-time staff (Morrisey and Swales, 1996). Such uses come with the expectation of high environmental standards.

The estuary catchment (122 km^2) supports a variety of land use, including pastoral, forestry and urban activities. Runoff from 65% of the catchment drains into the upper estuary headwaters at Warkworth (Fig. 1.1). Over the next few years land use activities will change, primarily as a consequence of urban development and forestry activities. In the Mahurangi River Catchment, the first rotation of a 700 hectare exotic forest (9% of total catchment area) will be harvested in the next few years. On the eastern flank of the estuary, the Dawsons Creek sub-catchment has been zoned for future urban development in the Rodney District Plan (Auckland Regional Council, 1993).

Soil erosion and the resulting estuary sedimentation associated with changes in catchment landcover can have detrimental impacts on estuarine water quality, benthic ecology, recreation, navigation and aesthetic values. In New Zealand, soil erosion associated with catchment deforestation and conversion to pasture from the mid

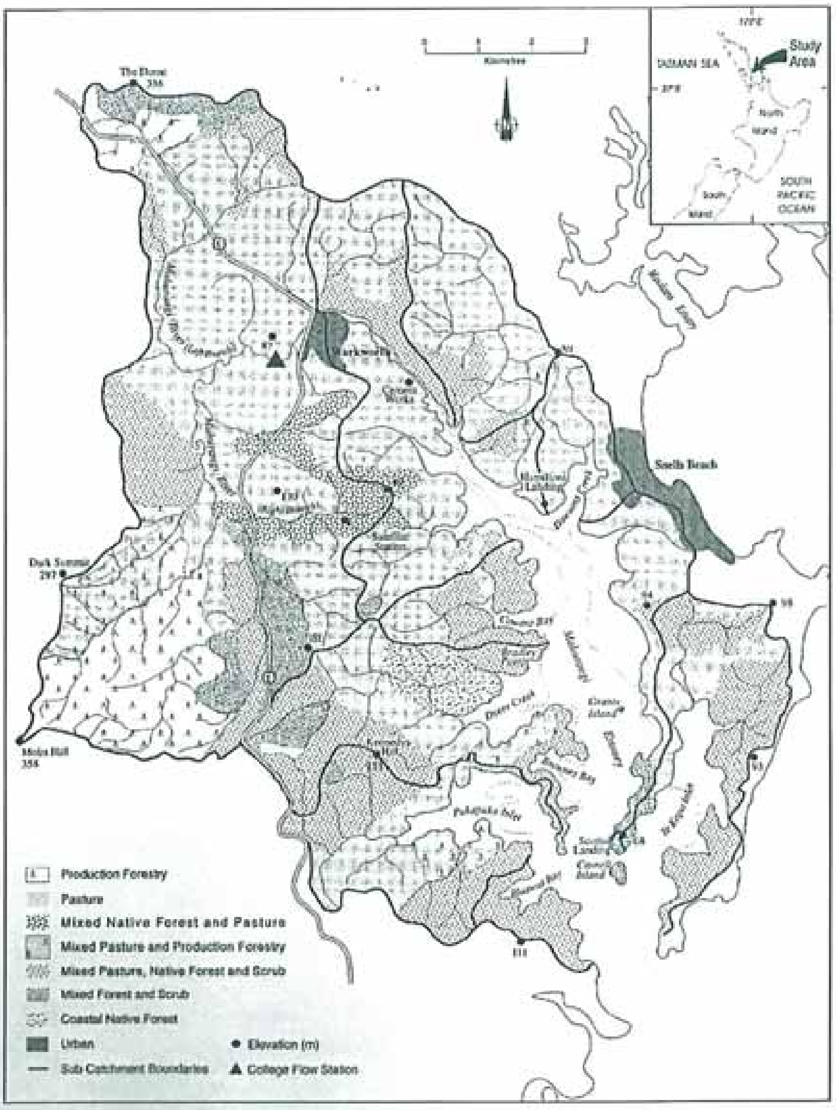

Fig. 1.1 Mahurangi Estuary location map and present day catchment landcover

1800's, and more recently urban development, have permanently altered the quality and quantity of runoff to estuaries and has the potential not only to accelerate estuary infilling but also to change the character of sediments deposited in estuaries (Curry, 1981; Gardner, 1987; GESAMP, 1993; Hume and Dahm, 1992; Hume and McGlone, 1986; Kingett Mitchell and Associates, 1988; Swales and Hume, 1994, 1995; Van Roon, 1981; Williams, 1976).

In the Mahurangi Estuary, oyster growers consider estuary sedimentation as a major environmental issue which has the potential to affect the future viability of the local industry. It has already been shown that sedimentation rates are enhanced in the vicinity of oyster farms (Forrest, 1991), where the accumulation of sediments is such that some farms have been extended into deeper water to maintain sufficient clearance between the oyster racks and the sea bed (Morrisey and Swales, 1996). The magnitude of the impact of changes in sediment loads associated with catchment development in the Mahurangi Estuary will depend very much on land management practices and the ability of an estuary to flush catchment sediment inputs.

This study investigates the sedimentation history and present day sedimentation processes in the Mahurangi Estuary, in order to estimate the potential future impacts of catchment landcover change on estuary sedimentation. It is part of a wider effort by the Auckland Regional Council to assess the potential effects of future landcover change on the Mahurangi Estuary and to formulate a management strategy to mitigate these effects.

1.2 Strategy and objectives

A measure of how the Mahurangi Estuary will cope with increasing sediment loads associated with future urban development and production forestry can be assessed by determining how the pattern and pace of sedimentation in the estuary has altered in historical times as the catchment was deforested during European settlement. In this study, this is achieved by coring the estuarine sediments and dating layers, and identifying changes in sediment type and sedimentation rates associated with individual historical catchment landcover phases. The fate of catchment sediment inputs to the estuary is predicted from field studies and numerical modelling of sediment entrainment by tidal currents and waves.

The specific objectives of this study are to:

- Quantify and compare estuary sedimentation prior to, during and subsequent to Polynesian and European catchment landcover changes to assess the relative rate of present day estuary infilling.
- Determine if the texture of sediments infilling the estuary has significantly altered following catchment deforestation last century to the present time.
- Assess the ability of tidal currents and waves to rework sediments in the Mahurangi Estuary.
- Assess the potential effects of future catchment landcover changes on sedimentation, and the character of sediments in the Mahurangi Estuary.

2. METHODS

A brief account of methods used in this study is presented in this chapter. Additional details of methods are presented in Appendix A.

2.1 Coring

The stratigraphy and sedimentation history of the estuary was assessed from cores, probes and records of catchment use in historical times. Long cores (to about 4 m length) were taken from 12 sites (Fig. 2.1) in channel, intertidal and subtidal environments using a Livingston piston corer from a moored vessel. The sediment thickness at the core sites was measured, up to least 7 m depth, by probing the sediment with steel rods.

2.2 Laboratory analyses

Stratigraphy

In the laboratory the cores were split, the stratigraphy (the various layers in the sediment) logged and key stratigraphic markers identified. The compression of sediments in the cores was calculated, and the uncompressed length of sediment used to calculate sedimentation rates. Sediments were sub-sampled for further analysis including, sediment texture, bulk density, radio-carbon dating of shell material and identification of pollen.

Sediment texture and bulk density

Sediment texture was determined on 10 mm thick slices taken from each of the major stratigraphic units in the core. The samples were pre-treated to remove organics (6% weight/volume hydrogen peroxide for 24 hours) then flushed with de-ionised water and dispersed (0.5% weight/volume sodium hexametaphosphate). The proportion of mud (< 0.0625 mm), sand (0.0625 - 2.0 mm) and gravel (> 2.0 mm) was determined by wet and dry sieving. Selected core samples were also analysed using a GALAI 'time of transition' laser technique to provide detailed particle size information. The sediment bulk density (mass/unit volume) was determined on 10 mm thick slices taken from each unit, by drying (24 hours at 120°C) and weighing.

Radiocarbon dating

Radiocarbon dating provides absolute ages on shell layers in the cores. This technique is suitable for material older than 250 years before present (B.P.) and therefore for dating layers further down in the core. The carbonate shells of benthic organisms, such as bivalves, are particularly suitable for analysis. Samples of shell

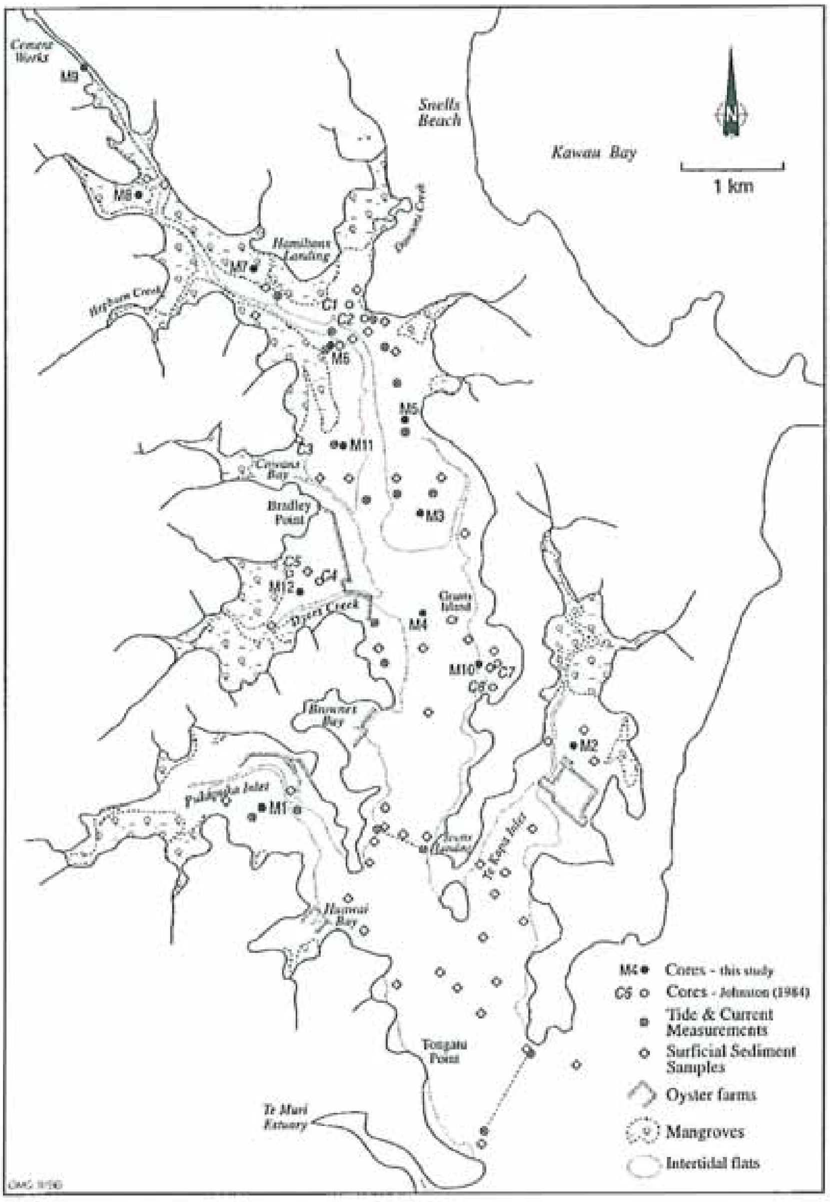

Fig. 2.1 Location of cores, surficial sediment samples, velocity and tide measuring stations, Mahurangi Estuary

material were selected from cores M1, M6, M8 and M9 where it occurred in relatively thin (10-15 cm) sand and shell units. Bivalve and gastropod species favoured for dating where *Austrovenus stutchburyi* (cockle), *Macomona liliana* (large wedge shell), *Paphies australis* (Pipi). In the distinctive, massive green-grey mud unit (which we term Mahurangi Mud), the turret shell *Maoriculpus roseus* is abundant. Radiocarbon dating and calibration of ages, was conducted by the University of Waikato Radiocarbon Dating Laboratory using a standard level of precision.

Pollen analyses

Landcover changes, such as catchment deforestation, alter the composition of the pollen that is delivered to an estuary and therefore laid down in sediments. Thus the types of pollen present at different levels in a core are indicative of catchment landcover at the time of sedimentation. The analysis of pollen in the cores in this study concentrated on the upper part of the sediment column. Samples were taken at 100 mm intervals down to the base of each core. Processing involved treatment with 10% HCl to remove carbonates, 10% KOH to deflocculate the samples and remove humic acids, 40% HF to dissolve silicates and a chlorine bleach to remove lignin and most organics, and finally a mixture of concentrated sulphuric acid and acetic anhydride to remove celluossic compounds. Following these treatments the HF resistant minerals, pollen, spores, charcoal and lignaceous material is mounted on glass slides and examined under a microscope. The general abundance of pollen types in samples (cores M1, M2, M3, M4, M6, M12) and a detailed count (pollen concentrations) of cores M1 and M8 was used to identify time horizons in the sediment column. Palynological analysis of the sediment column was conducted by Dr Matt McGlone of Landcare Research, Lincoln.

2.3 Catchment history

A chronology of catchment landcover changes was complied from historical records, and matched with core stratigraphy and the pollen signature.

2.4 Estuary Sedimentation Loads

Estuary sedimentation loads (that component of the total catchment sediment load deposited in the estuary) were calculated for the undisturbed native forest, deforestation and pasture/bush landcover phases from core (flats) and historical bathymetric (channel) data.

2.5 Catchment Flood Sediment Loads

The contribution of catchment floods to the estuarine sediment budget was assessed by calculating sediment loads associated with several recent floods (1985, 1994-1995) using flow and suspended sediment concentration data from the Mahurangi River Catchment and extrapolated to the entire estuary catchment by using BNZ, a basin model for simulation of long term average runoff, sediment and nutrient loads (Cooper and Bottcher, 1993).

2.6 Surficial sediments

Surficial sediments were taken by scooping the surface sediment at the 12 core sites and sediment texture determined by sieving. In addition, surficial sediments were sampled by grabbing at 53 sites by the Auckland Regional Council (Fig. 2.1) and particle size distributions determined using a MALVERN laser-diffraction system.

2.7 Tides, currents, waves and sediment entrainment

Tidal current velocity profiles were measured by current meter at the 12 long core sites and at a number of additional sites in the upper and lower estuary (Fig. 2.1). Water levels, salinity, turbidity and suspended sediment concentrations were also measured. Estuary bathymetry, water levels and our current measurements were used to set up and calibrate a 3-dimensional hydrodynamic numerical model of the estuary, as part of a related study (Oldman and Black, 1997). The model was used in this study to predict depth averaged tidal current velocities in 100x100 m grid cells throughout the Mahurangi Estuary.

Wind waves in the Mahurangi Estuary were modelled using a numerical wave model (3DD_WGEN). A twenty-four year wind record from Warkworth was used to analyse the local wind climate. On the basis of this analysis, 2 extreme wind-storm events (30 m/s northerly and 25 m/s westerly) were selected, and 3DD_WGEN used to compute significant wave height and period over a spring and neap tidal-cycle in 100x100 m grid cells throughout the estuary.

The hydrodynamic and wave models were then used to compute depth-averaged current velocity, water depth and shear-stress at the bed for each grid-cell. Critical thresholds for sediment entrainment (initial movement of surficial sediment) were calculated and compared to the shear stress exerted at the bed by tidal currents and waves. The modelling permitted mapping of the potential for sediment entrainment by tidal-currents and waves, in each grid cell, and an assessment of the likely fate of catchment sediment runoff to the estuary.

3. HOLOCENE SEDIMENTATION IN THE ESTUARY AND THE EFFECTS OF CATCHMENT LANDCOVER CHANGES

This chapter presents a reconstruction of sedimentation in the Mahurangi Estuary during the Holocene (10000 years B.P. to present), the period in which present day estuaries were formed, and examines the effects that changes in catchment landcover have had on the nature and rate of estuary sedimentation.

3.1. Catchment history

The catchment landcover history is reviewed to provide a basis for interpreting core stratigraphy and reconstructing the history of sedimentation in the estuary.

Early history (6500 to 700 years B.P.)

The land surrounding the estuary was covered by an undisturbed, mixed conifer-hardwood forest dominated by rimu, kahikatea, totara, matai, miro, hard beech, tree ferns and kauri (McGlone, 1994). A regional rise in kauri abundance commenced in the Auckland region some 6000 years B.P., climaxing some time after 3000 years B.P. (McGlone, 1994). This virgin native forest is the landscape that early Polynesian settlers viewed on their arrival in the Mahurangi.

Polynesian settlement (from c.700 years B.P.)

The chronology of Polynesian settlement in the Mahurangi is not well known. Elsewhere in the Auckland region, Hume and McGlone (1986) have inferred a date of 700 $\pm$100 years for an early phase of partial deforestation by the Polynesian and we adopt this timing for the Mahurangi. Forest clearance associated with Polynesian settlement was most likely localised and small scale in the Mahurangi, given the slash and burn method of agriculture commonly employed on coastal margins. It is also probable that this practice resulted in occasional accidental large scale forest fires, as appears to have occurred in the Coromandel Region (Hume and Dahm, 1992; Sheffield, 1991). In the Northland region, intense warfare between Northland tribes in the early 1800's may have led to forest burning as a defensive measure (Trotter, 1990).

In the Mahurangi, a large proportion of the conifer-hardwood forests remained intact until the mid-1800's when European settlement began. During a survey of the Mahurangi in 1840, Felton Mathew observed large tracts of undisturbed forest, with localised areas of bracken and fern, suggesting earlier clearance by the Polynesians, in the vicinity of Mahurangi Heads (i.e., Pa sites) and near the site of present day Warkworth (Johnston, 1984; Trotter, 1990).

European settlement and catchment deforestation (c.1850 to 1900)

Forest clearance by Europeans began in the Mahurangi as early as the 1820's when the Royal Navy established sites for the milling of kauri for ship spars. However, it was not until the 1840's that large scale deforestation began. Initially, timber stands adjacent to the lower estuary were logged and as these were depleted logging activities progressively moved further north towards the head of the estuary. In 1854, the settlement at Warkworth was established (Harris, 1993; Johnston, 1984; Trotter, 1990). Much of the milled timber was used in the construction of ships at Te Kapa Inlet and Dyers Creek. Between 1852 and 1880, when the last shipyard closed, 30 vessels were constructed (Johnston, 1984).

By the late 1800's only small remnants of the original conifer/hardwood forest remained in the Mahurangi Catchment, and at about this time large scale land clearance for farming began. The establishment of pasture involved the burnoff of scrub, following which exotic grasses were sown (Trotter, 1990). At this time road works occurred, with the Warkworth-Puhoi section of the Auckland-Warkworth road being completed in 1881 (Harris, 1993).

In many parts of the Northland and Coromandel Peninsulas, catchment deforestation was often followed by repeated burning of scrubland by gum-diggers in their search for kauri gum. Often these fires resulted in indiscriminate destruction of forest remnants (Bell and Fraser, 1912; Sale, 1978). The repeated removal of vegetation and exposure of soils to rainfall greatly increased soil erosion and subsequent sedimentation in receiving estuaries. The landcover changes affected by these activities were so large that their effects probably continued for years or decades following disturbance (Swales and Hume, 1995). Mahurangi historical records report such events, with gum-digging continuing nearby (15 km south) in the Silverdale area until the 1930's (Ferrar, 1934).

Pastoral land use and production forestry (c.1900 A.D. to present)

By the early 1900's pastoral farming, orcharding and cropping were the predominant catchment landuse activities, and small stands of pine were also planted at this time (Trotter, 1990). Mr Eric Barker, a long-time resident of the Mahurangi, recalls as a young boy (c.1910 AD) the hills around Pukapuka Inlet and Mahurangi West being covered in burnt tree stumps and 'rough grass' pasture.

Trotter (1990) has documented the logging of a small (< 1 ha) pine stand adjacent to the estuary in 1924. These small scale plantings would probably have had a very localised effect on the pollen record preserved in the estuarine sediments. In the Pukapuka Catchment 60 hectares of pine were planted as early as the mid 1930's on land bordering the southern shore of Pukapuka Inlet. This stand was first harvested in the mid 1950's, again in the mid 1980's, and is now in its third rotation (Mssrs Barker and Craig, Mahurangi West, pers. comm., 1996). The establishment of large-scale production forestry did not occur until the mid 1970's, when several hundred hectares of pine (mainly *Pinus radiata*) planted in the upper south branch of the Mahurangi Catchment. In the next few years the first rotation of this forest will be harvested.

How the catchment history is likely to be represented in the cores

On the basis of what has been observed in other estuaries (Hume, 1983; Hume and Dahm, 1992; Hume and McGlone, 1986; Kingett-Mitchell Limited, 1988; Sheffield, 1991; Swales and Hume, 1994, 1995) we would expect to see the following general signature of landcover changes in the estuary sediments.

Sediment loads from the forested catchment would have been low and therefore infilling of the estuary by muddy sediments slow. The pollen in basal core sediments will be representative of this virgin native forest. Polynesian settlement (from 700 years B.P.) is sometimes identified in estuary sediments by an increased abundance of pollen from secondary vegetation growth (i.e., bracken and fern) and a short period of increased sedimentation (Hume and Dahm, 1991). Catchment deforestation by Europeans (c.1850 to 1900) would have been accompanied by a significant increase in catchment sediment loads and therefore a marked increase in estuary sedimentation. The estuary sediments are also likely to have coarsened because removal of less weathered, and therefore more sandy, bedrock in the catchment would have occurred as soils were eroded. The pollen spectra should show a marked decrease in forest species and an increase in secondary growth. The establishment of pasture and production forestry (c.1900 to present) would have been accompanied by a gradual decline in catchment sediment loads and estuary sedimentation. However, the delayed yield of coarse bedload sediments from catchment storage probably continued for some time (i.e., years-decades) after deforestation as pasture and regenerating bush became established. In estuary sediments we would expect to see the virtual disappearance of forest species and replacement by exotic grasses, shrubs and trees.

3.2 Sediment stratigraphy

Geological background

Present day estuaries are relatively recent (in geological terms) coastal features. At the height of the most recent (Otirian) glaciation (16-18000 years B.P.) the sea was approximately 120 metres below its present level (Gibb, 1986). During the marine transgression that followed, the ancestral river valleys of Auckland's east coast were flooded by rising sea level, forming the numerous estuaries which indent this coastline today. During the Holocene (10000 years B.P. to present) at about 6500 years B.P., the sea reached its present level, with fluctuations (i.e., several decimetres) since this time (Gibb, 1986).

Seismic profiling shows that the Waitemata Group basement rocks occur 20 m below present sea level in the lower estuary and up to 15 m of unconsolidated sediment has been deposited over the last 10000 years or so (Trotter, 1990). In the vicinity of Cowans Bay (Fig. 2.1), the unconsolidated sediments (post 6500 years B.P.) are at least 7.5 m thick. As the sea was 15-20 m below its present level 8500 years ago (Gibb, 1986) sedimentation in the Mahurangi Estuary probably dates from about from this time.

Core data

The cores collected in this study are described in detail in Appendix B. Figure 3.1 summarises the stratigraphy of the Mahurangi Estuary, interpreted from cores. Sediment cores collected by Johnston (1984) and Trotter (1990) provide some additional evidence which is incorporated where appropriate. However, the value of these cores to our stratigraphic reconstruction is limited by the fact that the cores generally did not penetrate deep enough into the sediment column to sample sediment deposited prior to European settlement. Furthermore, neither absolute (e.g., ^{14}C) or relative (e.g., pollen) dating was undertaken by Trotter (1990), and Johnston (1984) only dated samples at two sites.

Our cores were mainly collected from intertidal and subtidal (flats) environments in the upper and lower estuary, where the sediments are least likely to be reworked by channels shifting back and forth. Core stratigraphy shows that the upper and lower reaches of the Mahurangi Estuary have infilled with markedly different sedimentary sequences over the last 6500 years.

Upper estuary stratigraphy

In the narrow upper estuary (cores M7, M8 and M9) the sediments are primarily inter-layered, poorly-sorted sand, mud, gravel (shell and rock fragments) and preserved vegetation. These are typical "flood sequences", the normal grading (upward fining) in the flood 'sets' show coarse gravels and sands are initially deposited from bedload, but as the flood runoff declines and salinity increases, the fine muds flocculate and settle out. This sequence is clearly shown at the upstream core site (M9).

In the gravel layers, shell fragments and dis-articulated valves of *Austrovenus stutchburyi* (Cockle) and *Macomona liliana* (Large Wedge Shell) frequently occur. These animals are typical of intertidal estuarine environments, with *Macomona lilliana* generally being more tolerant of muddy substrates (Morton and Miller, 1973). The poor state of preservation of this shell material indicates a high degree of reworking (e.g., high energy environment). At M9, lateral channel migration is suggested by inclined, alternating sand and mud layers at 2.66 m depth.

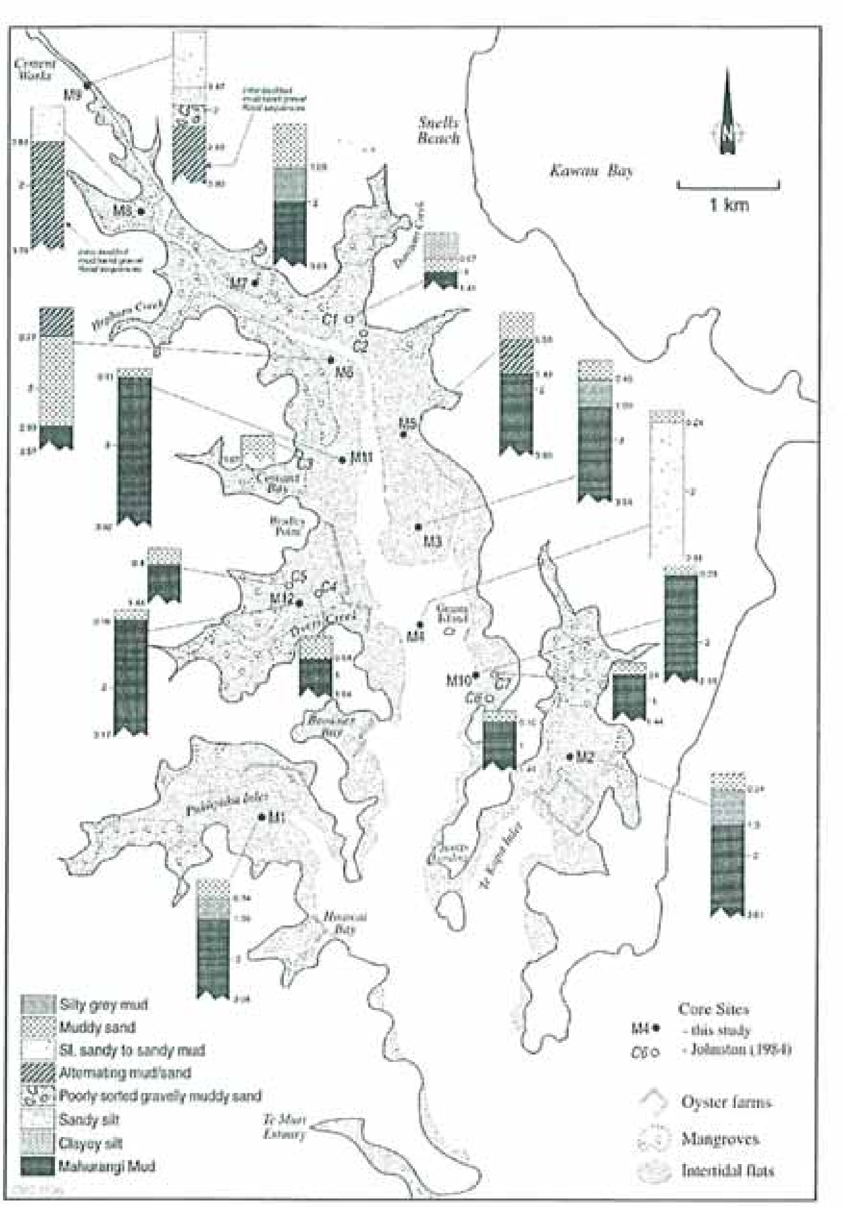

Fig. 3.1 Generalised stratigraphy of Mahurangi Estuary cores, this study and Johnston (1984).

Lower estuary stratigraphy

In the lower estuary, the sediment column is largely composed of a distinctive homogenous, low density (dry 0.8-1.0 g/cm^3), clay-rich, green-grey mud (Fig. 3.1) which we have termed the **Mahurangi Mud**. This mud was cored to 3.9 m (e.g., M11) and probing with steel rods indicates that it is at least 7 m thick and nowhere is the basement rock contacted. Particle size analysis of the Mahurangi Mud (cores M1, M3 and M10) at 2.3-2.8 m depth shows that the mean particle size is very small (1.0-1.2 µm) with 90% of the particles being less than 2 µm in size. Particle size gradually increases towards the top of the sediment column: at 1.05 m depth (core M3) the mean particle size is 4.6 μm, with 90% of particles being less than 7 μm. In the upper 80-100 cm of the sediment column, the sand fraction progressively increases (5-30%) (Appendix B). Johnston's (1984) cores sampled the very top of the Mahurangi Mud, which are described as an 'olive-grey, clayey silt' and 'with kaolinite, smectite and illite being the main clay types present'. Mahurangi Mud is absent from the sediment column in the upper estuary.

Associated almost exclusively with the Mahurangi Mud are fossils of the turret shell, *Maoriculpus roseus*, a deposit feeding gastropod found in sub-tidal and outer estuary environments in water depths of up to 100 metres (Batham, 1969; Morton and Miller, 1973; Powell, 1979). The close association of *Maoriculpus* with the Mahurangi Mud gives an indication of the early sedimentary environment in the Mahurangi Estuary. *Maoriculpus* is very abundant and well preserved in the Mahurangi Mud suggesting that it lived in the estuary and was not transported into the estuary by tidal currents. The abundance of *Maoriculpus* declines towards the head of the estuary, being common near the entrance (i.e., M1, M10 and M3) and rare in the upper estuary at M7, where the Mahurangi Mud terminates (Fig. 3.1). Today *Maoriculpus* lives on sediments at the mouth of the estuary and in adjacent coastal waters (Johnston, 1984). The occurrence of *Maoriculpus* as fossils in the Mahurangi Estuary suggests that the sedimentary environment was one of gradual sedimentation in a deep subtidal basin.

On the intertidal flats a relatively thin veneer (average 0.3 m; range 0.11-0.90 m) of muddy (fine-medium) sand caps the Mahurangi Mud. The sand layer is thin at the seaward end of the estuary, but thickens in the vicinity of Hamiltons Landing. The cores show that a rapid increase in grain size occurs in the upper 1.0 m of the sediment column, grading from the Mahurangi Mud to a silty sand (75% sand) at the surface. A similar sequence is also seen in Johnston's (1984) cores. This coarsening of sediments towards the surface is widespread in the estuary and suggests a major change in sediment supply and/or sorting of sediments in the estuary.

Figure 3.2 presents the generalised estuary stratigraphy for a longitudinal cross-section of the intertidal flats. This shows the relative thickness of the Mahurangi Mud, overlain by a thin sequence of recent sandy sediments (<0.5 m thick) in the lower estuary and a much thicker sequence of sandy flood sediments (up to 4-5 m) in the upper estuary.

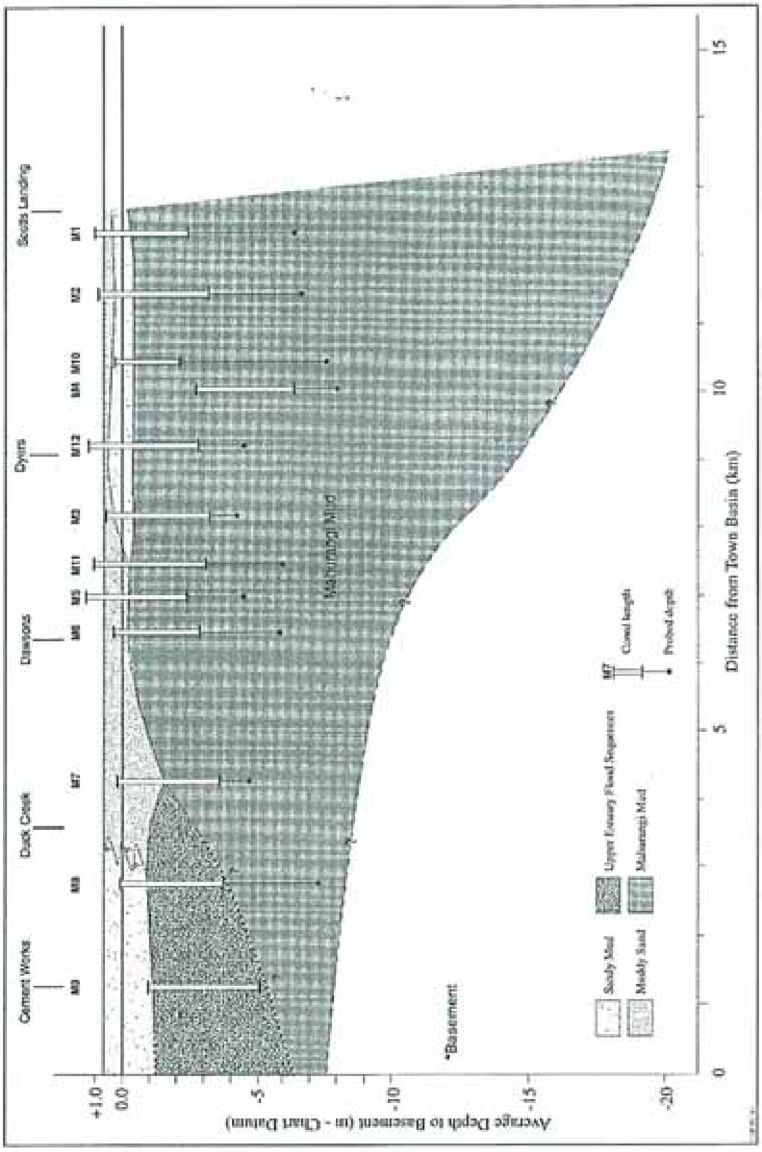

Fig. 3.2 Schematic longitudinal cross-section of estuary stratigraphy, showing the position and depth of cores and probes with the approximate depth to basement rock along the channel axis (source, this study and Trotter, 1990).

3.3 Radiocarbon dating of core material

The calibrated radiocarbon ages for shell material taken from 4 cores are given in Table 3.1.

Table 3.1: Ages of shell samples determined by radiocarbon dating.

Core	Depth to shell (mm)	Age of shell lower-mid-upper (years B.P.)	Comments
M1	3110	6433-6735-7037	
M6	1280	1687-1904-2122	reworked?
M6	3010	2380-2549-2717	
M8	2070	974-1085-1195	reworked?
M8	3610	931-1031-1130	
M9	2880	7200-7323-7445	reworked ?

Note: Calibrated upper, **middle** and lower ages (years B.P.- where present = 1950 A.D.) were calculated for 2σ (2 standard deviations) using the probability distribution technique (Stuvier and Pearson, 1986). The mid-range values were used to calculate net sedimentation rates. Standard errors in dated shell samples are low (± 45-130 years).

At M6, M8 and M9 there is evidence from the pollen record that older shell had been reworked to higher levels in the sediments, and therefore the age of the dated shell does not represent the age that the sediments were deposited. In most situations we have more confidence in pollen dating of sediments because reworking of a single dated shell can produce an erroneous age for the entire sediment layer, whereas mixing of the entire sediment column would be required to blur or erase the pollen record. Disturbance of shell from its original stratigraphic position is always a potential problem when dating shells from "active" environments. The dates derived from the shallow shell layers in cores M6, M8 and M9 therefore represent maximum ages for the sediment and were not used in calculating sedimentation rates. A more detailed discussion of radiocarbon and pollen dating techniques is presented in Appendix A.

3.4 The pollen record

The pollen assemblages identified in the sediment cores are presented in table 3.2 and a detail spectra for core M1 illustrated in Fig. 3.3. Appendix C includes a full report made by McGlone (1994). The excellent preservation of pollen grains and spores in the cores provides a high degree of confidence in the results. The catchment landcover history is matched to the results of pollen analysis to reconstruct the sedimentation history of the Mahurangi Estuary.

Table 3.2: Relative pollen abundance in sediment cores where detailed pollen counts were not made. "5" indicates a high proportion of total pollen found in a sediment sample, and "1" indicates a low percentage (1-5%). A "+" indicates the pollen type was seen, but probably not in enough quantity to be registered as a percentage. "-" indicates pollen type absent.

Core/depth (cm)	Pine	Grass and Weeds	Bracken	Kauri	Other Forest	Zone
M2						
10	5	5	4	+	1	A
20	+	+	5	4	4	B
30	-	-	5	4	4	B
40	-	-	-	5	5	C
M3						
10	5	5	2	+	1	A
20	2	4	3	4	4	A
30	-	-	-	5	5	C
40	-	-	-	5	5	C
M4						
1	5	5	3	+	2	A
5	+	+	3	2	4	B
10	+	+	3	3	4	B
20	-	-	2	5	4	B
30-50	-	-	1	5	5	C
60	-	-	-	5	5	C
M6						
10	4	4	3	+	2	A
20	3	4	3	+	2	A
30	3	3	4	+	2	A
40	2	3	4	+	3	A
50	+	+	4	3	4	B
60-100	+	-	4	3	4	B
200	-	-	-	5	5	C
300	-	-	-	1	5	D
M12						
10	5	4	2	1	1	A
20	+	+	2	4	5	B
30	+	-	-	5	5	C
40	-	-	-	5	5	C

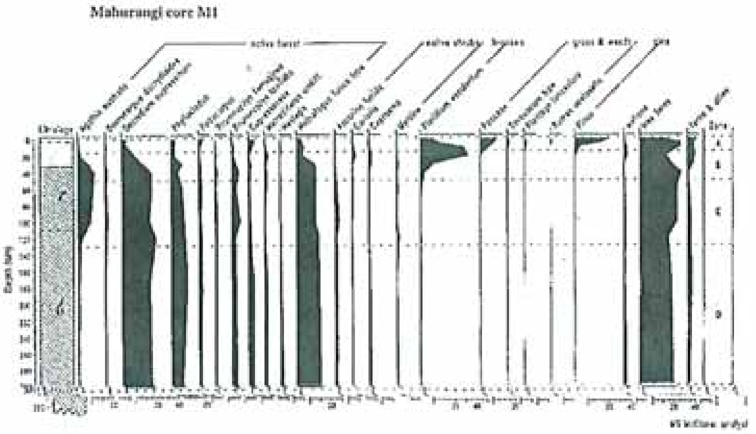

Figure 3.3: Pollen assemblage in Pukapuka Inlet (core M1), Mahurangi Estuary. Pollen types as percentage of total pollen count.

Four major pollen assemblages were identified in the estuarine sediments associated with a distinct landcover phase:

Zone A: 1900 A.D. to present - recent pasture/bush
Zone B: 1850 A.D. to 1900 - catchment deforestation
Zone C: 3000 years B.P. to 1850 A.D. - undisturbed forest with abundant kauri
Zone D: 6000 to 3000 years B.P. - undisturbed conifer/hardwood forest

Zone A: In the upper part of the sediment column (i.e., 0.15-2.2 m depth) the abundance of pine, grasses and weeds of arable land (e.g., plantain, sorrel, clover) increase, while bracken decreases, as the catchments were converted for pasture from the early 1900's. In the upper estuary (M8) the abundance of Macrocarpa (*Cupressus macrocarpa*) pollen records the planting of this species for farm hedging and plantations. The continued abundance of corrosion resistant tree fern spores near the top of cores indicates continued disturbance and erosion of catchment soils, probably associated with agriculture. Fern spores are associated with top soils and are delivered to the estuary with soil runoff.

Zone B: In this zone the abundance of all forest dominants rapidly declines, while the abundance of disturbance indicators such as bracken and tutu (*Coriaria*) increase rapidly. Traces of pine pollen also occur in Zone B. This pollen signature is indicative of widespread logging of native forest catchments, initially for kauri in the mid 1800's, and by 1900 A.D. much of the original forest cover had been removed.

Zone C: Pollen assemblages of this zone are similar to that of Zone D, with the exception that kauri and matai have become more common. Note that pollen assemblages characteristic of the Polynesian settlement phase (from about 700 years B.P.) are absent from the upper part of this zone, indicating the Polynesian impact on catchment landcover and sediment loads was negligible, although increased bracken abundance in the Pukapuka Inlet sediments (core M1) may be indicative of localised forest clearance by Polynesian.

Zone D: Prior to 3000 years B.P. the undisturbed forest landcover was dominated by forest trees and tree ferns, but with low abundance of kauri (*Agathis australis*). Dominant canopy species were rimu (*Dacrydium cupressinum*), kahikatea (*Dacrycarpus dacrydioides*), totara (*Podocarpus*), matai (*Prumnopitys taxifolia*), miro (*Prumnopitys ferruginea*), hard beech (*Northofagus fusca* type), and kauri. Therefore, basal core sediments (Zone D) are representative of an early conifer/hardwood forest landcover phase prior to a regional rise in kauri. A similar forest dominated the region from about 10000 years B.P.

In Pukapuka Inlet (core M1) pine pollen abundance increases sharply (0-30%) in the upper 20 cm of the sediment column, suggesting a local pollen source. By contrast, the pollen spectra for pine at M8 (upper estuary) increases gradually from 240 cm depth to 20% at the surface, suggesting pollen input from both regional and local sources. The source of pine pollen at Pukapuka is thought to be the plantings of 60 hectares of pine on the southern margin of the inlet in the mid-1930's. Thus a time horizon of c.1945 A.D. for the beginning of Zone A is represented by the pine pollen there, which differs from that used elsewhere in the estuary (i.e., 1900 A.D.) when pasture was first established in the catchment.

3.5 Hydrographic surveys, channel shifts and estuary infilling

Naval charts provide a record of channel shifts and sedimentation in historical times. The 1836, 1904/5 and 1975 charts have been analysed by Johnston (1984) and the 1904/5 and 1975 charts by Harris (1993) to assess sedimentation patterns in the estuary. We undertook no further analysis but summarise the findings, particularly those of Harris who conducted a thorough and extensive analysis. Comparing the surveys led Johnston (1984) to believe that the position of the channel in the main harbour was stable, and that in the area between Browns Bay and the entrance there was a period of sedimentation prior to 1904 followed by erosion after that time is contrary to our findings and those of Harris (1993). The results of Harris's (1993) work are summarised in Figure 3.4, showing the average depth reduction in various sectors of the harbour. Between 1904/5 and 1975 there have been substantial changes in channel depth with a distinct trend towards accretion. Along the entire length of the lower estuary channel the average accretion over the 70 year period has been 67 cm (nearly 10 mm/yr). Near the entrance there has been little siltation (0-20 cm accretion). In the vicinity of Hamilton Landing/Cowans Bay the channel has infilled by upwards of 290 cm of sediment (about 40 mm/yr). Our cores in intertidal sites in this area also indicate this is an area of rapid sedimentation.

The lack of soundings over much of the intertidal flats and the errors involved in comparing these old surveys (Harris, 1993) does not permit similar estimates of sedimentation to be made from hydrographic data for the intertidal flats where a large proportion of catchment sediments have been deposited.

Seaward of Hamilton's Landing, where the estuary widens, there is evidence from core stratigraphy and historical bathymetric surveys for shifts in the position of the main channel. At core M6 a thick layer of sandy mud (a slightly sandy version of the Mahurangi Mud) in the base of the core, is overlain by 2.8 m of weakly graded (i.e., particle size increases towards surface) muddy medium-coarse shelly sand, with a thin silty, organic rich mud at 0.55-0.77 m depth, which in turn is capped by a fine sandy mud. While the surface unit is typical of intertidal sediments, the underlying layer is typical of a tidal channel environment, and near the base of the core the sediments suggests a subtidal flat environment. This sequence is evidence for lateral shifts in the channel axis, which appears to have migrated from east to west several times over the last several thousand years. Prior to 3000 years B.P. the channel axis was probably located near its present position to the east of M6 (Fig. 3.5). After this time it migrated to the west to about the position of M6 where it remained until the late 1800's. During this time sediment slowly accumulated (i.e., 0.8 mm/year). The channel may have altered course from east to west over a relatively short period between the late 1800's and early 1900's, but by the early 1900's it had migrated back to the east and "stabilised" in its present position. Harris (1993) also found an eastward shift in channel position in the vicinity of Dawsons Creek from comparison of the 1904/5 and 1975 hydrographic surveys, with about 1 m of sediment infilling the channel between Bradley Point and Dawson's Creek.

3.6 Estuary sedimentation rates derived from cores and hydrographic surveys

Net sedimentation rates calculated for the major land cover phases based on the stratigraphic, radiocarbon and pollen data are presented in Table 3.3. Figure 3.6 summarises estuary sedimentation rates associated with subsequent catchment landcover phases.

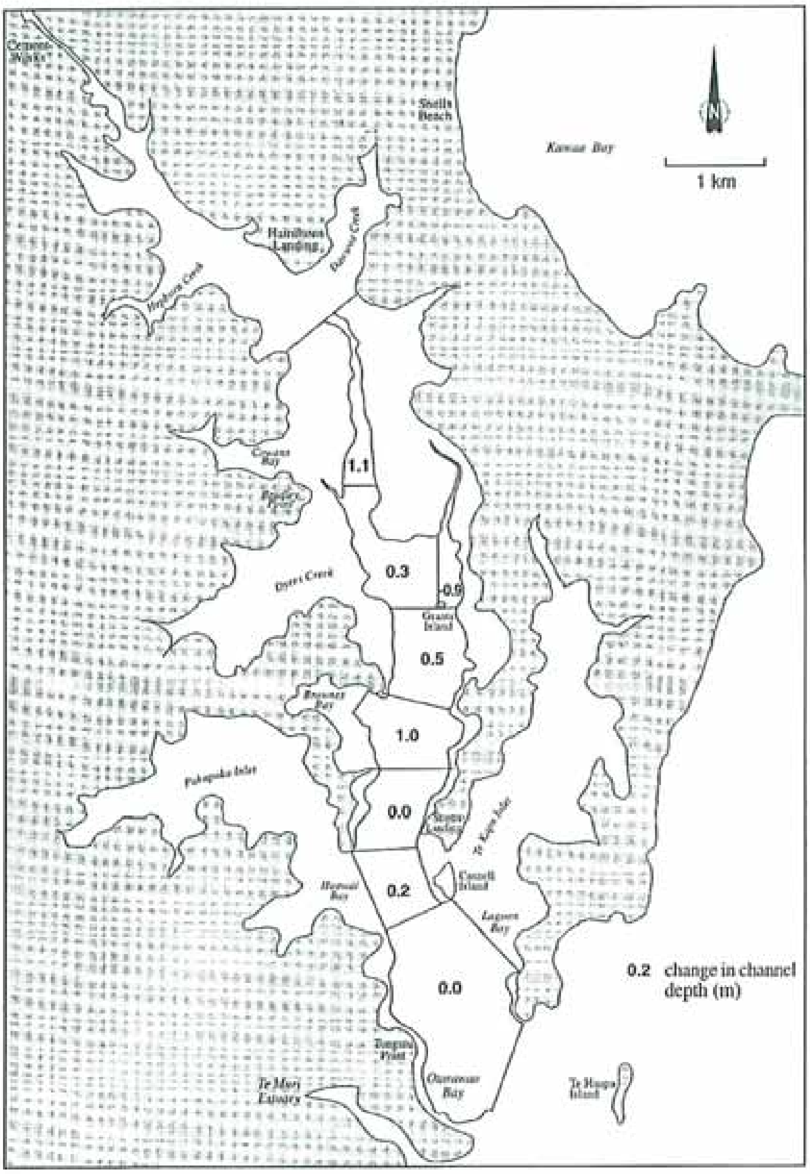

Fig. 3.4 Changes in channel depth from comparison of 1904/5 and 1975 hydrographic surveys, Mahurangi Estuary. Positive values inducate infilling and negative values scouring (m) (after Harris 1993).

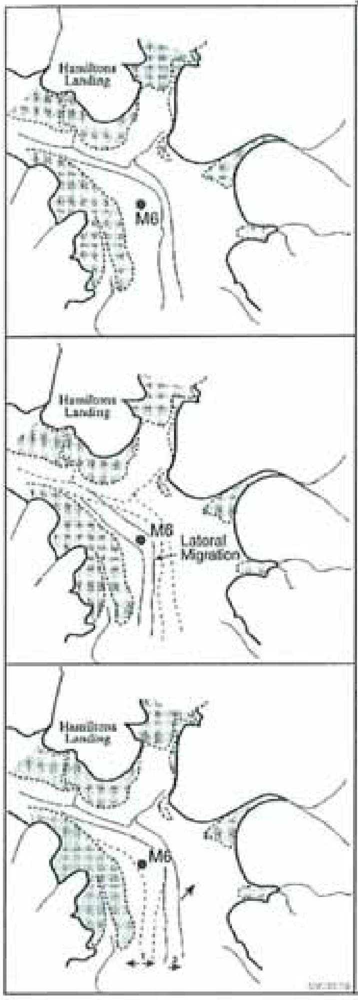

(A) **Pre-3000y B.P.** : Main tidal channel located to east of core site M6

(B) **3000y B.P. to late 1800's A.D.** : After 3000y B.P. the tidal channel migrates west to vicinity of core site M6. Remains approximately in this ailignment until the late 1800's (A.D.).

(C) **Late 1800's to present** : Some evidence of rapid (1) (decadal) channel shifts to west and east and from early 1900's (2) channel migration east, to present position.

1 km

Fig. 3.5 Postulated sequence of channel migration in the vicinity of Hamiltons Landing, 3000 years B.P. to present (source, core M6).

Table 3.3: Estimates of average sedimentation rates based on pollen (P) and radiocarbon (C14) dating (mid-range values) of cores.

Core	Dating Method	Depth range (mm)	Time Period	Landcover Phase	Net Sedimentation Rate (mm/yr)
M1	P	200-0	1945-1993	Pastoral/bush	4.1
	P	500-200	1850-1945	Deforestation	3.15
	P	1300-500	3000 y BP-1850	Kauri forest	0.3
	P	1290-1016	3000-6500 y BP	Conifer/H.wood	0.77
	C-14	3110-500	6635 y BP-1850	Native Forest	0.39
M2	P	150-0	1900-1993	Pastoral/bush	1.6
	P	350-150	1850-1900	Deforestation	4.0
M3	P	250-0	1900-1993	Pastoral/bush	2.7
	P	??-250	1850-1900	Deforestation	??
M4	P	50-0	1900-1993	Pastoral/bush	0.54
	P	250-50	1850-1900	Deforestation	4.0
M6	P	450-0	1900-1993	Pastoral/bush	4.8
	P	1500-450	1850-1900	Deforestation	21.0
	P	2500-1500	3000 y BP-1850	Kauri forest	0.34
	C14	3010-1500	2449 y BP-1850	Kauri forest	0.62
M8	P	2200-0	1900-1993	Pastoral/bush	23.7
	P	3000-2200	1850-1900	Deforestation	16.0
	C14	3610-3000	3000 y BP-1850	Kauri forest	0.77
M9	C14	2880-0	7223 y BP-1993	Native forest-pastoral	0.39
M12	P	150-0	1900-1993	Pastoral/bush	1.6
	P	250-150	1850-1900	Deforestation	2.0

Notes: The depth range is the depth below surface of the dated horizons. The average sedimentation rate is for the period between these two horizons. Depths are corrected for core compression. Time periods are in years AD unless specified otherwise. Mid-range radiocarbon dates are used in the calculations of sedimentation rates.

Native forest phase (before 1850 AD)

Radiocarbon dating of shell in cores shows that sedimentation in the estuary began prior to 6500 years B.P. as the sea inundated the river valley. For example, dated turret shell in core M1 at 3.1 m depth were deposited 6735 years B.P. and the sediment column here is at least 7 m thick. This indicates that sedimentation in the Mahurangi Estuary is likely to have commenced several thousand years prior to 6500 years B.P. Average sedimentation rates in the estuary during the native forest landcover phase are low (i.e., 0.3-0.77 mm/year).

In the estuarine sediments there is little evidence for accelerated sedimentation associated with Polynesian land clearance (i.e., slash and burn agriculture), save for the slightly elevated abundance of bracken in Pukapuka Inlet sediments (M1), although this could also be due to some localised natural disturbance in the catchment (e.g., slope failure).

Catchment deforestation phase (c.1850-1900 A.D.)

Average sedimentation rates during catchment deforestation were much greater than for the preceding native forest phase and range between 2-21 mm/year. In the lower estuary sedimentation rates, averaging 2-4 mm/year, are probably more representative of the estuary as a whole. Rapid sedimentation in the estuary coincides with catchment deforestation and soil erosion.

In the upper estuary, rapid infilling in places (16 mm/year at M8, 21 mm/year at M6,) with flood sequences of inter-layered gravel-rich sands and muds was underway by the late 1800's. The average sedimentation rate was about 20 times that associated with the preceding native forest phase. The large amount of coarse sediment evident in the upper estuary cores (i.e., M7-M9) indicates that much of the coarse sediment load from the Mahurangi River was trapped there. The widening of the estuary in the vicinity of Hamilton's Landing would also result in a substantial reduction in current velocities associated with ebb tides and flood runoff, favouring sedimentation in the upper estuary.

Pastoral/regenerating bush phase (1900 A.D.-recent)

Since 1900 A.D. sedimentation rates in the lower estuary have declined moderately (range 0.5-4.1 mm/yr) from the preceding catchment deforestation phase. The declining rate of infilling is attributed to reduced sediment loads from the mainly pasture landcover and/or declining sediment trapping efficiency of the estuary. The latter possibility is examined in chapter 5.

In the upper estuary sedimentation rates substantially increased (24 mm/yr at core M8). At M8 some 2.2 m of sediment have been deposited since 1900 A.D. or approximately 30% of total depth of sediment deposited since 6500 years B.P. The upper 0.5-0.7 m of the sediment column becomes progressively finer in the upper estuary (Appendix B)., changing from the distinctive flood sequences of inter-layered gravel, sand and mud to finer, sandy muds. Possible explanations for this change in sediment texture include: (1) delivery of mainly muddy sediments from catchments converted to pasture and regenerating bush remnants (i.e., less soil erosion) and/or (2) a tailing off in the delivery of coarser bedload sediment that was slowly released from catchment storage, following deforestation. A potential lag in the delivery of coarse sediments to the estuary may have persisted for years or decades after 1900 A.D. Meade (1982) documents this process in catchments draining to estuaries on the Atlantic coast of the United States.

3.7 Comparison with other estuaries

The overall pattern increased sedimentation following catchment deforestation in the Mahurangi Estuary is similar to that documented in other New Zealand estuaries, which gives us some confidence in our findings.

Net sedimentation rates of 0.3-0.77 mm/year in the Mahurangi associated with native forest cover are similar to rates measured in Lucas (1 mm/year), Brighams (0.5-0.8 mm/year) and Hellyers (0.35 mm/year) Creeks, Upper Waitemata Harbour (Hume 1983; Hume and McGlone, 1986; Vant et al., 1993). Background (i.e., native forest phase) sedimentation rates in a number of Coromandel estuaries were even lower; averaging 0.1-0.3 mm/year (Hume and Dahm, 1992; Sheffield, 1991; Swales and Hume, 1994, 1995).

In the Mahurangi Estuary there is scant evidence of catchment disturbance by the Polynesian in the estuary sediments. Any evidence that did exist has subsequently been erased by physical and biological reworking of the sediment column. Hume and Dahm (1992) report slight increases in sedimentation rates in Whangapoua Harbour and Firth of Thames sediments coincident with Polynesian settlement. In contrast Swales and Hume (1994, 1995) found no evidence of the Polynesian settlement phase preserved in the sediments of Whangamata and Wharekawa Estuaries.

During catchment deforestation (1850-1900 A.D.) sedimentation rates in the Mahurangi Estuary increased to 2-4 mm/year in the lower estuary and up to 21 mm/year in the upper estuary. Sedimentation rates in the Upper Waitemata Harbour also increased from their pre-deforestation rates to 3 mm/year (Hume and McGlone, 1986; Vant et al., 1993). In the Mahurangi, sedimentation rates measured in the upper estuary for the deforestation phase are much higher than in the Upper Waitemata Harbour (e.g., Lucas Creek). This difference in part may be a result of the larger catchment area, increased elevation (Mahurangi up to 358 m, c.f. 120 m for Lucas Creek Catchment), hillslope steepness, and susceptibility of catchment soils to erosion.

Since 1900 A.D. the rate of infilling in the lower estuary has generally declined, although rapid sedimentation (e.g., core M8, 24 mm/year) has occurred in the narrow upper estuary, which represents a 'sump' for coarse catchment sediments. Sedimentation rates in the lower estuary (0.5-4.1 mm/year) are in the range reported for other Auckland estuaries today. Hume and McGlone (1986) estimated sedimentation rates of 1-2 mm/year from a largely pastoral/bush catchment for Lucas Creek. Vant et al. (1993) measured rapid sedimentation (2.7-9 mm/year) in Brighams Creek (1970-present). In Hellyers Creek, sedimentation rates have averaged 6 mm/year following catchment urbanisation since the late 1960's (Hume, 1983).

3.8 Reconstruction of estuary sedimentation history

Originally the Mahurangi Estuary was a deep subtidal basin, slowly infilling with fine suspended sediments of catchment and marine origin. Seismic surveys show that up to 15 m of sediment has been deposited in the lower estuary, much of this prior to human settlement (Trotter, 1990). The catchment was covered by an undisturbed, mixed conifer-hardwood forest dominated by rimu, kahikatea, totara, matai, and miro, with tree ferns and lesser amounts of kauri (McGlone, 1994). The sedimentary environment was much different from today. The Mahurangi Mud represents the long period of slow estuary infilling with fine clay-rich muds, supplied by catchment runoff, prior to catchment deforestation.

As infilling of the Mahurangi Estuary reached an advanced stage, the sedimentary environment was permanently altered; with the change from a largely subtidal basin to an intertidal estuary. Infilling of the lower estuary constructed the extensive intertidal flats, about 1000 years B.P, although cores show that upper estuary remained subtidal until the rapid sedimentation associated with catchment deforestation occurred. Since the mid-1800's the estuary has progressively infilled with coarser sediments, reflecting the supply of coarse sediments due to soil erosion and increasingly effective reworking of sediments by waves and currents in a shallow intertidal estuary (refer chapter 5).

Very different sedimentary sequences have been deposited in the upper and lower estuaries.

In the narrow upper estuary sedimentation was slow (0.77 mm/year) prior to catchment deforestation and fine suspended sediments characterised sedimentation. There was also sporadic deposition of sand, associated with flood events. The most upstream appearance of the Mahurangi Mud in the vicinity of Hamilton's Landing marks the boundary of 2 distinct sedimentary environments, the lower estuary was much deeper and fine suspended sediments accumulated in a low energy environment. The rapid catchment deforestation (<50 years) which followed European settlement in the mid-1800's appears to have resulted in severe soil erosion and rapid deposition of "flood sequences" of inter-layered, poorly-sorted gravel, sand, mud and preserved vegetation. A large proportion of these coarse sands and gravels appear to have been trapped in the upper estuary. At M8 some 3 m of sediment have been deposited since 1850 A.D. and a large proportion of this sediment (i.e., 2.2 m) has been deposited since the early 1900's. The upper estuary therefore represents a 'sump' for coarse sediments eroded from the denuded catchment. It is likely that similar sequences of sediments are likely to be found at the head of many of the small inlets that fringe the estuary.

In the much larger lower estuary the impact of catchment deforestation has been preserved as a relatively thin cap (average 0.3 m) of muddy sands on top of the Mahurangi Mud.

4. COMPARISON OF PAST AND PRESENT ESTUARY SEDIMENTATION LOADS AND THE CONTRIBUTION OF FLOODS TO ESTUARY INFILLING

In this chapter historical changes in catchment sediment loads delivered to the estuary are assessed as well as the contribution of river floods to the estuarine sediment budget. An estimate of catchment sediment loads, associated with each landcover phase, is calculated from the estuary **sedimentation load**, that component of the total catchment sediment load deposited in the estuary.

4.1 Total sediment mass deposition and estuary sedimentation load

The mass of sediment deposited in the Mahurangi Estuary was estimated for the native forest and deforestation landcover phases using core data. The total mass deposited in the estuary since 1900 A.D. was estimated for the (1) lower estuary using a combination of core (tidal flats) and bathymetric data from the 1904/5 and 1975 surveys (channels) and (2) in the upper estuary primarily using core data.

Calculation methods

The total mass (M in tonnes) of sediment deposited in the estuary (or part thereof), based on the cores was calculated as:

$$M = A.t.d$$

where A = area (m^2) of the estuary or part thereof, t = the average thickness (m) of sediment deposited in the area in the time period of interest and d = the average dry bulk density (tonnes/m^3) of the sediment in the core for that time period.

The area of estuary channel and intertidal compartments (A) was measured from hydrographic charts, t from the cores (flats) and bathymetric data (main channel) for the lower estuary, and d from the core data. Because d varies widely, and therefore strongly influences the mass calculation, we calculated a range of values for M based on ± 2 standard deviations ($\pm 2\sigma$) of dry bulk sediment density.

The high tide area of the upper estuary was taken as 2.03 km^2 and the lower estuary 22.7 km^2. In the lower estuary 8.5 km^2 is subtidal and 14.2 km^2 is intertidal. However, in computing mass deposition in the lower estuary since 1900 A.D. not all of the subtidal area is accounted for by the hydrographic surveys, such as tributary channels draining inlets and embayments (2.2 km^2). Consequently, in the lower estuary 2.2 km^2 is added to the intertidal area for calculating mass sedimentation. In addition, the most seaward channel compartment (2.3 km^2) of Harris (1993) was not included in our calculations because much of the sediment deposited in this compartment is likely to be of marine origin and changes in bed elevation associated with tidal inlet processes rather than deposition of catchment sediments.

Total mass deposited in the upper and lower estuary were computed separately because there are large differences in the data "quality" between the two areas. In the upper estuary only 3 cores (M7-M9) were collected with considerable variability in sediment bulk density. By comparison, in the lower estuary there is much more comprehensive spatial coverage of sediment stratigraphy (9 cores this study; 6 cores Johnston, 1984) and lower variability in sediment bulk density. Therefore, sediment mass estimates for the lower estuary are considered more reliable than for the upper estuary.

Native forest phase (3000 years B.P.-1850 AD)
For the native forest phase an average 0.5 mm/year sedimentation rate was applied to the entire estuary (at that time sub-tidal), which equates to a sediment thickness of t = 1.45 m. A dry bulk density of 1.2 tonnes/m^3 ($2\sigma = \pm 0.42$) was used to compute sediment mass.

Deforestation phase (1850-1900 A.D.)
For the deforestation phase we used t = 0.2 m and d = 1.56 tonnes/m^3 ($2\sigma = \pm 0.34$) for the lower estuary, and t = 0.9 m and d = 1.38 tonnes/m^3 ($2\sigma = \pm 0.68$) for the upper estuary. These values are applied to the entire upper and lower estuary areas to derive mass estimates.

Pasture/bush phase (1900-1993 A.D.)
For the pasture/bush landcover phase the mass (M) deposited in the lower estuary was the sum of sedimentation in the channel derived from bathymetric data and core bulk density and on the intertidal flats from core data only.

In the lower estuary, the sediment mass was calculated for the main channel and the tidal flats in the following manner. Harris (1993) computed average depth changes in eight channel compartments. We used this data, along with the channel area for each compartment, to calculate the total sediment volume deposited in each channel compartment. The error in the sounding data ($\pm$0.5 m) provided an upper/lower range of volume estimates. The bulk density values used to compute sediment mass in the channel were derived from the top 0.2 m of intertidal flat cores in the lower estuary (mean 1.65 tonnes/m^3 $2\sigma = \pm 0.52$, n=9). The sediment mass in each channel compartment was computed for all nine combinations of bulk density (mean, $\pm 2\sigma$) and depth change (mean, $\pm$ 0.5 m) and then summed to provide mass estimates for the lower estuary channel (i.e., high-average-low). The large range in the mass estimates is due to variability in the sediment bulk density and the error term ($\pm$ 0.5 m) associated with the hydrographic surveys (Table 4.1). Negative lower values reflects these errors. On the intertidal flats (16.4 km^2) a uniform sediment thickness (0.2 m) and bulk density of 1.65 tonnes/m^3 ($2\sigma \pm 0.52$) was used to compute sediment mass.

In the upper estuary, the sediment mass was calculated using core data (t = 2.2 m, d= 1.18 tonnes/m^3, $2\sigma = \pm 1.02$, n=21) and upper estuary area (2.03 km^2). The sedimentation rate derived from the cores is consistent with apparent channel shoaling (1.4-2.9m) determined from the 1904/5 and 1975 hydrographic surveys (Harris, 1993). Given the limited number or cores (3) and large variation in sediment bulk density the mass calculation for the upper estuary has a much larger error in comparison to the lower estuary (Table 4.2).

Errors in estimates of M arise from (1) using historical hydrographic surveys which may have measurement errors of as much as $\pm$ 0.5 m (Harris, 1993) and (2) the range of bulk density values in cores, particularly in the upper estuary. Overall the mass estimates for the pasture/bush landcover phase are better than those for the preceding phases because this sedimentary unit has a relatively uniform depth (0.15-0.25 m), and is more comprehensively cored and dated. Because a proportion of the catchment sediment load is probably flushed from the estuary then the estuary sedimentation loads will underestimate actual catchment soil erosion.

Table 4.1: Total sediment mass deposited in the Mahurangi Estuary, and estuary sedimentation load since 1900 A.D.

	Upper estuary	Lower estuary channel	Lower estuary intertidal flats	Lower estuary channel+flats
Mass (10^6 tonnes)				
upper	9.83	6.82	7.13	13.95
average	5.27	2.52	5.42	7.94
lower	0.72	-0.66	3.71	3.06
Sedimentation load (t/ km^2/yr)				
upper	1320			1235
average	708			702
lower	96			271

Notes: The total sedimentation load for the lower estuary is derived from the total mass deposited in the channel compartments and on the flats, divided by the total catchment area.

The annual average estuary sedimentation load was calculated for each landcover phase by dividing the total sediment mass in the estuary by the catchment area (for upper and lower estuaries taken as 80 km^2 and 121.5 km^2 respectively), and the time period during which sedimentation occurred. The mass estimates for estuary sedimentation since 1900 A.D. are presented in Table 4.1 and sedimentation loads associated with each landcover phase presented in Table 4.2.

Table 4.2: Total mass of estuary sedimentation in the Mahurangi Estuary, average annual sedimentation and catchment sedimentation loads (lower-**average**-upper values) for each historical landcover phase.

Site	Landcover phase	Total sediment mass (tonnesx10^6)	Average annual sedimentation (tonnesx10^3/yr)	Sedimentation load (tonnes/km^2/yr)
Upper estuary	pastoral	0.7-**5.3**-9.8	7.7-**56.7**-105.7	96-**708**-1320
	deforestation	1.3-**2.5**-3.8	25.6-**50.4**-75.2	320-**630**-940
	native forest	2.5-**3.72**-5.0	0.8-**1.2**-1.6	10-**15**-20
Lower estuary	pastoral	3.06-**7.9**-14.0	32.9-**85.4**-150.0	271-**702**-1235
	deforestation	5.5-**7.1**-8.6	110.8-**141.6**-172.6	912-**1165**-1420
	native forest	27.9-**43.4**-55.8	8.9-**13.6**-18.4	73-**112**-151
Entire estuary	pastoral	3.8-**13.2**-23.8	40.6-**142.1**-255.7	334-**1170**-2105
	deforestation	6.8-**9.6**-12.4	136.4-**192**-247.8	1122-**1580**-2039
	native forest	30.4-**47.1**-60.8	9.7-**14.8**-20	80-**122**-165

Notes: Sedimentation load for entire estuary calculated from total mass deposited in the lower and upper estuary divided by the total catchment area.

4.2 Historical changes in estuary sedimentation loads

The dramatic increase in estuary mass sedimentation as a consequence of catchment deforestation is illustrated by figure 4.1. Mass sedimentation in the estuary from native forest averaged 15x10^3 tonnes/yr and increased to 192x10^3 tonnes/yr during the deforestation landcover phase. Since 1900 A.D. average mass sedimentation in the estuary has declined (142x10^3 tonnes/yr), although it is an order of magnitude higher than prior to catchment deforestation. It is also apparent that sedimentation in the upper estuary has continued to increase.

Estuary sedimentation loads for the undisturbed native forest landcover phase averaged about 120 t/km^2/yr. Catchment deforestation resulted on average in a 13-fold increase in sedimentation load to about 1600 t/km^2/yr. Some 75% of the total sedimentation load (9.6 million tonnes) associated with catchment deforestation (1850-1900 A.D.) was deposited in the lower estuary (Table 4.2).

Since 1900 A.D. the average annual sedimentation load has declined by 25% to 1170 t/km^2/yr but still remains an order of magnitude higher than 'background' rates associated with native forest landcover (Table 4.2). A comparatively large proportion

(40%, mostly sand and gravel) of the total sedimentation load since 1900 has been

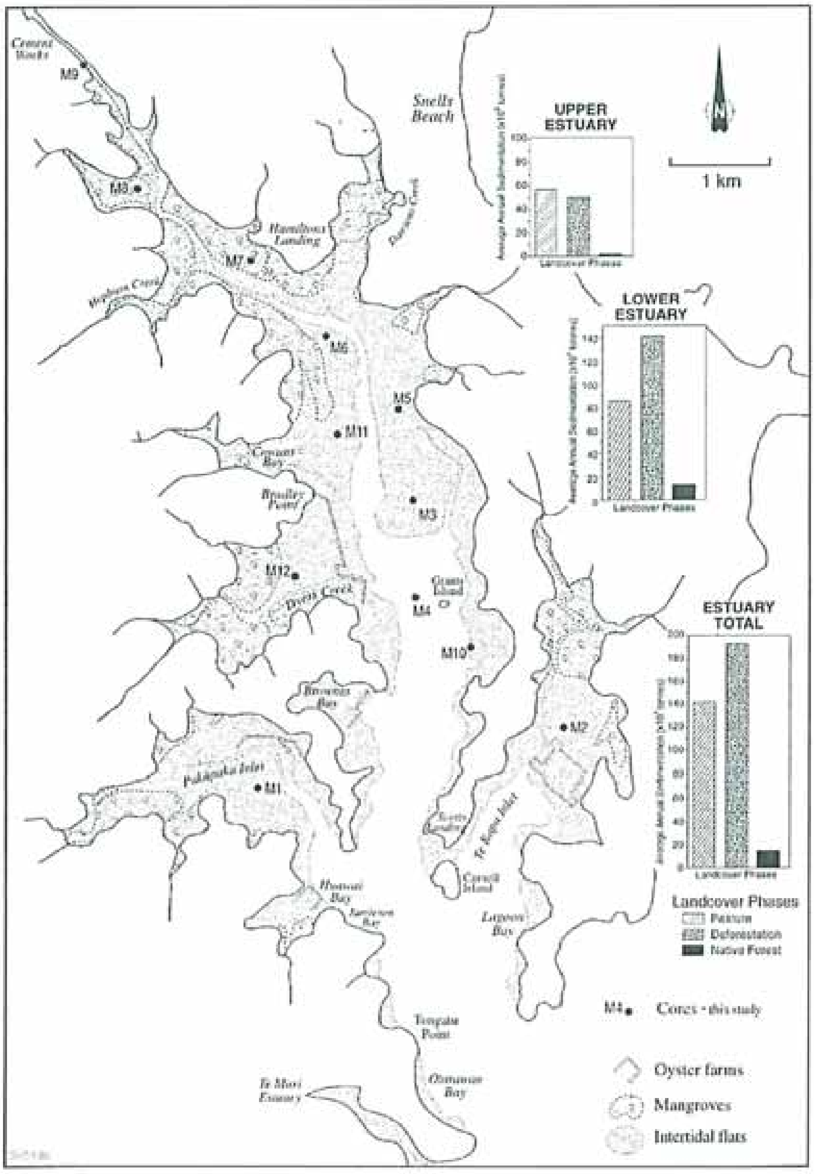

Fig. 4.1 Annual average sedimentation load (tonnes x10^3/year) deposited in the Mahurangi Estuary during the native forest (pre-1850 A.D.), catchment deforestation (1850-1900 A.D.) and pasture (1900-1993 A.D.) landcover phases.

deposited in the upper estuary, although it only accounts for 8% of the total estuary's high tide area. In the upper estuary, the average sedimentation load has increased from 630 to 708 t/km^2/yr and cores show that a substantial proportion of these sediments are sands and gravels. We hypothesise that this increased deposition represents a lag in the delivery of coarse (i.e., bedload) sediment stored in stream channels, eroded during catchment deforestation and/or continued rapid soil erosion after pasture was established. The delivery of coarse sediments from the catchment to the upper estuary may have lag their initial erosion by years or decades. Therefore, sedimentation in the lower estuary is considered more representative of soil erosion from a mainly pasture/bush catchment since 1900 A.D.

4.3 Comparison of estuary sedimentation load with catchment model predictions

The BNZ (Basin New Zealand) model (Stroud and Cooper, 1997) was used to estimate annual catchment sediment loads for a 20 year period (1976-1995). The model has been calibrated with a continuous 1 year record (1994/95) of flow and suspended sediment loads measured at several sites in the Mahurangi Catchment.

Figure 4.2 illustrates the annual variability in suspended sediment load (1976-1995) from the estuary catchment, which relates to the intensity and duration of rainfall. Importantly, rain-storms in 1979, 1985 and 1988 (e.g., Cyclone Bola) generated sediment runoff 2-3 times the annual average suspended sediment load (448 t/km^2/yr) for the 1976-1995 period (Fig 4.2). This indicates that sediment loads delivered by large infrequent storms make a significant contribution of to the estuary's long-term sediment budget.

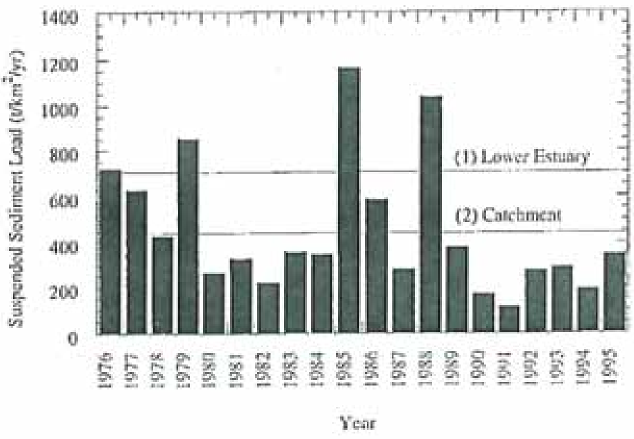

Figure 4.2: Comparison of average (1) lower estuary sedimentation load (post-1900A.D.) and (2) catchment suspended sediment loads (BNZ model), (1976-1995).

Comparing catchment model predictions with estuary sedimentation shows that the average suspended sediment load predicted by the model (448 tonnes/km^2/year; 1976-1995) is 64% of the long term (post-1900 A.D.) estuary sedimentation load derived from cores (702 t/km^2/yr) (Fig. 4.2). We compare estimates of sedimentation load from the lower estuary only, because (1) coarse bedload sediments account for a significant proportion of sediments deposited in the upper estuary, (2) of which a proportion are likely to have been eroded during the earlier catchment deforestation and (3) we speculate that most of the suspended sediment load is deposited in the lower estuary.

The similarity of the average catchment (1976-1995) suspended sediment load and estuary (1900-1993 A.D.) sedimentation load is remarkable given that the estimates relate to different periods of time (i.e., 20 versus 90 years) and were made using very different methods. The lower catchment suspended sediment load over the last 20 years suggests that catchment soil erosion has declined since the early 1900's as pasture was established and bush remnants regenerated.

4.4 Comparison of hindcast sedimentation loads with other Auckland catchments

Table 4.3 compares sedimentation loads for the Mahurangi Estuary with suspended sediment loads from other catchments in the Auckland region. The comparisons have to be made with some caution because the data have been derived in different ways and represent different time periods. The Mahurangi data are measured from estuary sedimentation while suspended sediment loads from other Auckland catchments are based on stream flow and suspended sediment measurements and statistical analysis to derive long term average yields (notably Hicks, 1994).

Table 4.3: Comparison of Mahurangi Estuary sedimentation loads and catchment suspended sediment loads associated with various landcover types in the Auckland region

Catchment	Landcover	Sediment load ($t/km^2/yr$)	Source
Mahurangi	pastoral/bush	271-702-1235	this study[1]
(lower estuary)	deforestation	912-1165-1420	
	native forest	73-112-151	
U.W.H.C.[2]	urban	210	Van Roon (1980)
	pastoral	223-349	
	bush	197	
Alexandra	urbanising	2370	Hicks (1994) [3]
	pastoral	58	
Wairau	urban	100	Hicks (1994)
	urbanising	2000	Strachan (1977)
Botany	urbanising	157	Swales (1989)[4]
	pastoral	46	Hicks (1994)
Pakuranga	urban	22	Hicks (1994)

Notes: (1) lower-**mid**-high values for the lower estuary (Table 4.2), for the deposited suspended sediment load, (2) Upper Waitemata Harbour Catchment, (3) 20 year average annual sediment runoff (Hicks, 1994) and (4) for a 6 month (January-July) period (1988).

Comparing sedimentation loads derived from core data for the lower estuary with suspended sediment loads measured in catchments elsewhere in the Auckland region, shows that the Mahurangi Estuary sedimentation load prior to deforestation (120 $t/km^2/yr$), is the same order as suspended sediment loads from present day bush (197 $t/km^2/yr$), pasture (46-349 $t/km^2/yr$) and urban (22-210 $t/km^2/yr$) catchments (Table 4.3). The sedimentation load deposited in the lower estuary during catchment deforestation (1165 $t/km^2/yr$) is also similar to suspended sediment loads from urbanising catchments (157-2370 $t/km^2/yr$). The average annual load deposited in the lower estuary since 1900 A.D. (702 $t/km^2/yr$) is twice the maximum load measured from pasture/bush catchments elsewhere in the Auckland region. The modelled average catchment sediment load for the last 20 years (448 $t/km^2/yr$) suggests that soil erosion in the Mahurangi may have declined since 1900 A.D.

These data indicate that the Mahurangi Estuary sedimentation loads are high in comparison to suspended sediment loads from catchments elsewhere in the Auckland region and that the Mahurangi Estuary Catchment is susceptible to soil erosion. Furthermore, the fact that sedimentation loads remain much higher today than prior to catchment deforestation suggests that deforestation has affected a long term change in catchment sediment loads. The Whangaripo clay soils that mantle much of the catchment have a low infiltration capacity and consequently the erosivity of rainfall is high. In addition a large proportion of the catchment is steepland pasture and in combination these factors will promote catchment soil erosion. Future catchment development that is likely to expose catchment soils to erosion will have to planned with particular care if periods of potentially increased estuary sedimentation and consequent adverse environmental effects are to be mitigated or avoided.

4.5 Contribution of floods to the Mahurangi Estuary sediment budget

Numerous studies indicate that a large proportion of catchment sediment loads to estuaries is contributed by floods (e.g., Curry, 1981; Dyer, 1986; Hume, 1983; Fahey and Coker, 1992; Nichols, 1977; Schubel and Pritchard, 1986; Swales, 1989). For example, in Chesapeake Bay, U.S.A., at least 50% (0.53 m) of sedimentation since 1900 AD has been contributed by two major storm events in 1936 and 1972 (Schubel and Pritchard, 1986). In Lucas Creek, Upper Waitemata Harbour, Hume (1983) found that the Cyclone Sina flood event (March 1980, 6 days) accounted for about 90% of the annual sediment load delivered to the estuary.

Flood suspended sediment loads

The contribution of catchment floods to the estuarine sediment budget was assessed by calculating sediment loads associated with several recent floods (i.e., May 1985, July 1994 and March 1995).

Suspended sediment loads for the 1994-1995 floods were estimated from the Mahurangi River flow and suspend sediment concentration data (i.e., college site) (Fig. 1.1),which receives runoff from a 46.8 km^2 catchment. Flood sediment loads from the entire catchment where estimated by scaling the results by the total catchment area (i.e., scale factor 2.6). Modelling suggests that other sub-catchments deliver more sediment to the estuary than the Mahurangi River, therefore our total catchment estimate is conservative. Appendix A.5 outlines the techniques used to derive flood sediment loads.

To estimate the suspended sediment load for the May 1985 flood we applied the discharge-suspended sediment relationship for the Mahurangi River at the college site (peak flow 139 m^3/s), used in catchment modelling (Cooper and Stroud, 1997).

July 1994 Flood

For the July 1994 flood (2.2 year return period) the flood peak (63 m^3/s) was initiated by 104 mm of rainfall in the preceding 30 hours (Fig. 4.3a and b), with 1600 tonnes of suspended sediment delivered to the estuary (Fig. 4.3c). We estimate that at least 4200 tonnes of sediment was delivered from the entire catchment or 8% of the annual average suspended load (1976-1995).

March 1995 Flood

The March 1995 flood (9 year return period) was a much larger (peak discharge 137.6 m^3/s) and more concentrated flood (Fig. 4.4a-c), initiated by 153 mm of rainfall, of which 80% occurred during a 9 hour period. The suspended sediment load delivered to the estuary by the Mahurangi River was 5088 tonnes, most of which (99%) was delivered in 14 hours (Fig. 4.4c). We estimate that at least 13.2 $x10^3$ tonnes of sediment was delivered from the entire catchment or 24% of the annual average suspended sediment load (1976-1995).

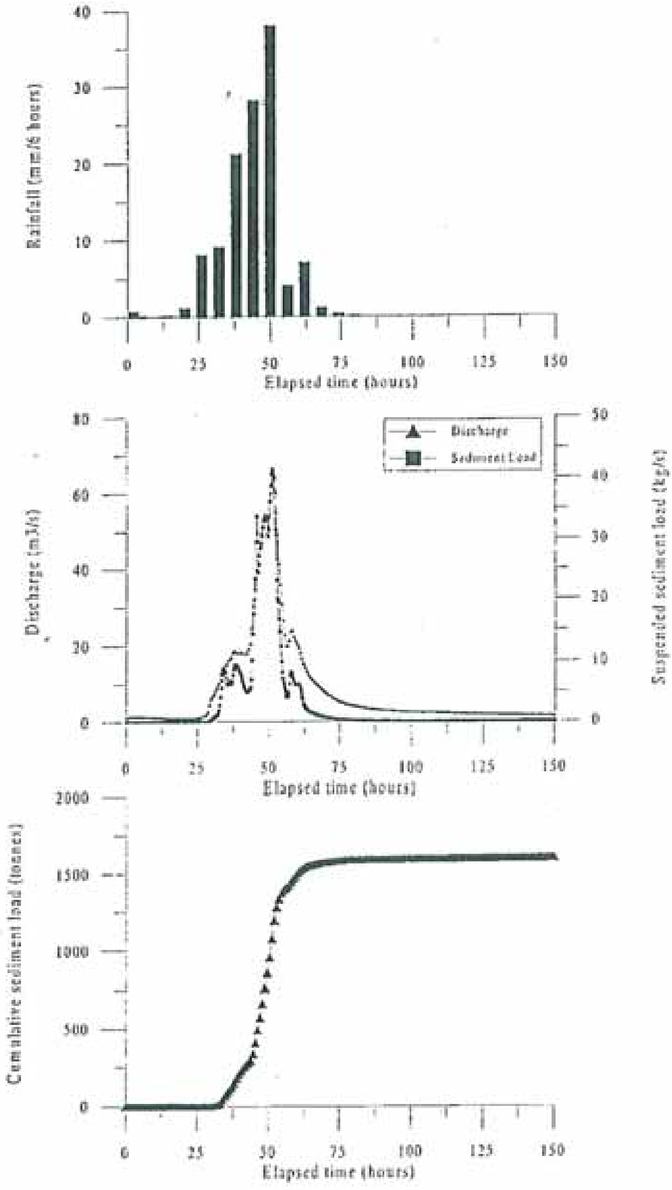

Figure 4.3: a) Rainfall, (b) runoff and (c) cumulative suspended sediment load, 23-27 July 1994 flood at the college site, Mahurangi River.

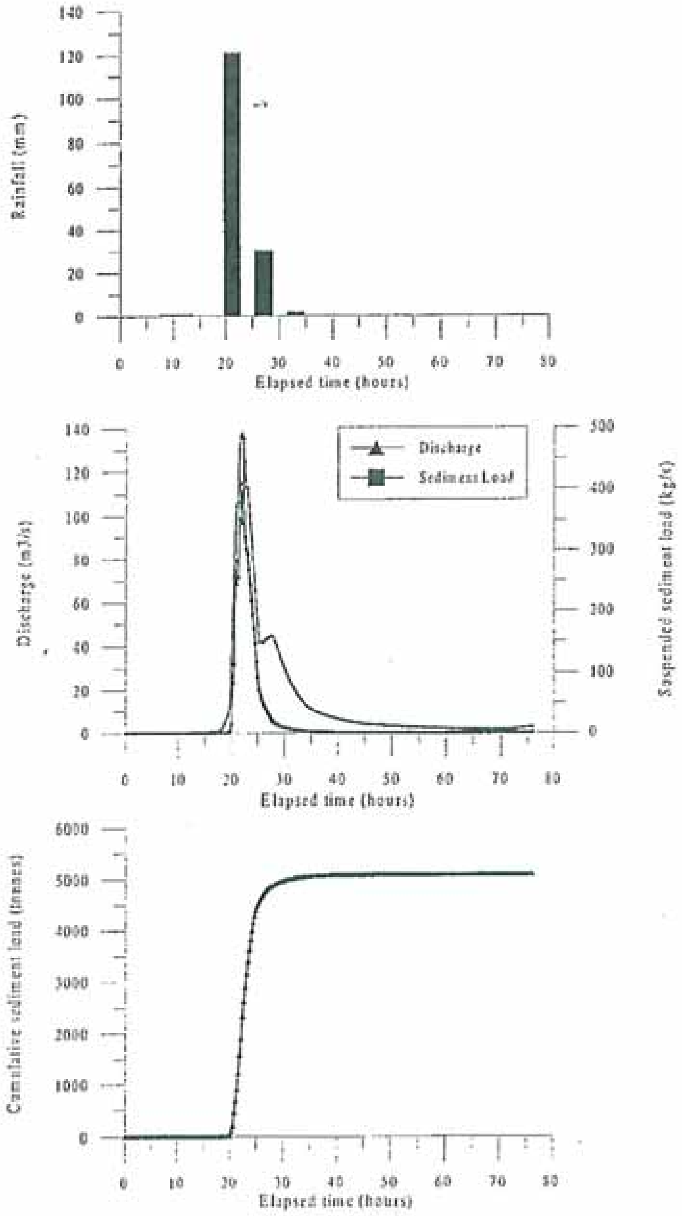

Figure 4.4: a) Rainfall, (b) runoff and (c) cumulative suspended sediment load, 28-29 March 1995 flood at the college site, Mahurangi River.

May 1985 Flood

Annual loads in 1985 and 1988 account for a large proportion of the sediment delivered to the estuary over the last 20 years, much of which was delivered by large floods. The May 1985 flood highlights the large contribution that extreme events make to the estuarine sediment budget.

The May 1985 flood was caused by a depression, which delivered some of the highest rainfall ever recorded in the Mahurangi Catchment. At Warkworth, 12 hour (170 mm) and 24 hour (200 mm) rainfalls had estimated return periods of about 50 years (Auckland Regional Water Board, 1986). The peak discharge measured at the Mahurangi River college site was 205 m^3/s (c.f. March 1995 flood peak of 137.6 m^3/s). Erosion of the Whangaripo clay-loam hill soils which mantle a large area of the Mahurangi Catchment was common and occurred mainly as shallow slips in saturated soils (Auckland Regional Water Board, 1986). We estimate that at least some 41.5 $x10^3$ tonnes of suspended sediment was delivered to the estuary from the entire catchment or 75% of the annual average suspended load (1976-1995). The total suspended sediment load delivered to the estuary during 1985 was also exceptional, with $120x10^3$ tonnes, most of which was delivered by floods. The total load in 1985 was 3 times the 1976-1995 annual average.

The relative contribution of floods to the estuarine sediment budget is also shown by considering the amount of sediment delivered by low flows, which occupy more than 90% of the flow duration (average discharge of 1 m^3/s and a ssc of 10 g/ m^3). Low flows deliver about 850 tonnes/yr, or 2% of the annual average suspended sediment load. Floods account for more than 90% of the catchment suspended sediment load delivered to the Mahurangi Estuary.

Potential estuary sedimentation of flood sediment loads

If we assume that all of the suspended sediment load associated with floods is deposited in the lower estuary (22.7 km^2) then estimates of flood sedimentation can be compared to average annual sedimentation rates measured from cores.

From cores, the average dry bulk density of surface sediments is 1.41 tonnes/m^3, which yields volumes of 2980 m^3 (July 1994), 9360 m^3 (March 1995) and 29500 m^3 (May 1985) for the flood sediment loads. Distributing this volume equally over the lower estuary yields 0.13 mm, 0.4 mm and 1.3 mm of sedimentation respectively. For the total 1985 sediment load the equivalent volume is 85106 m^3, equivalent to a layer 3.7 mm thick in the lower estuary.

By the same method, the average annual suspended sediment load over the last 20 years (448 t/km^2/yr) is equivalent to an average sedimentation rate of 1.7 mm/yr. This is about 75% of the post-1900 A.D. average sedimentation rate derived from cores (2.2 mm/year). Therefore, the flood sedimentation attributable to the 1994 (0.13 mm), 1995 (0.40 mm) and 1985 (1.3 mm) events represents 8%, 24% and 75% of the average sedimentation (1976-1995) in the lower estuary. Sedimentation during 1985 is equivalent to 2 years average sedimentation in the lower estuary.

Sedimentation in the Mahurangi Estuary is dominated by the cumulative contribution of small frequent floods (i.e., annual) and infrequent large floods can deliver an entire years average sediment load to the estuary.

5. ESTUARY HYDRODYNAMICS AND SEDIMENT ENTRAINMENT

The impacts of future catchment development on sedimentation in the Mahurangi Estuary will depend in part on the ability of the estuary to flush sediment inputs. In this chapter field measurements of physical parameters (i.e., tidal currents, sediment grain size and density), hydrodynamic modelling of tidal currents and wind waves and the estuary sedimentation history (cores) are used to develop a conceptual understanding of the role currents and waves play in reworking (i.e., entrainment) estuary sediments.

5.1 Estuary bathymetry, tides and waves

The Mahurangi Estuary is largely intertidal (65% of high tide area) and indented with numerous shallow inlets and embayments (Fig. 5.1). At the entrance, the channel is up to 20 m deep, progressively shoaling landwards of this point. In the upper estuary, the main channel is narrow and shallow (1-2 m deep at low tide).

A consequence of the river-like shape and shallow nature of the estuary is that circulation is primarily back and forth along the channels. Tidal currents on the intertidal flats decline in strength away from the channel and are very weak in shallow embayments and inlets where they are damped by friction (Fig. 5.2). The short cross-estuary fetch (<2-3 km) and extensive intertidal area also limits the development of waves by the prevailing westerly wind.

Currents in the estuary are primarily driven by the tide, the dominant constituent of which is the lunar semi-diurnal (M2) tide which has a periodicity of 12.42 hours. Average neap (1.4 m) and spring (3.1 m) tides have tidal prisms of 33×10^6 m^3 and 50×10^6 m^3 respectively (Harris, 1993). A consequence of the large differences in tidal range for sediment entrainment is that spring tide current velocities can be 50% higher than during neap tides (Fig. 5.2) and therefore have a much greater capacity to entrain estuarine sediments.

Waves in the estuary are primarily generated by wind action on the water surface, although some swell does enter the entrance on occasions. Small wind waves up to 0.5 m height and about 2-3 sec period have been observed (this study and Davies-Colley and Nagels, 1995) propagating across (west-east) the lower estuary. During strong westerly winds, sediments on the eastern intertidal flats are re-suspended by waves (Davies-Colley and Nagels, 1995). Orbital motions of the water under waves extend to about half the wave length, so these small waves have the potential to stir sediment over much of the intertidal areas where the water is shallow (<3 m), particularly in the lower estuary where the fetch is greater. The short-lived (few

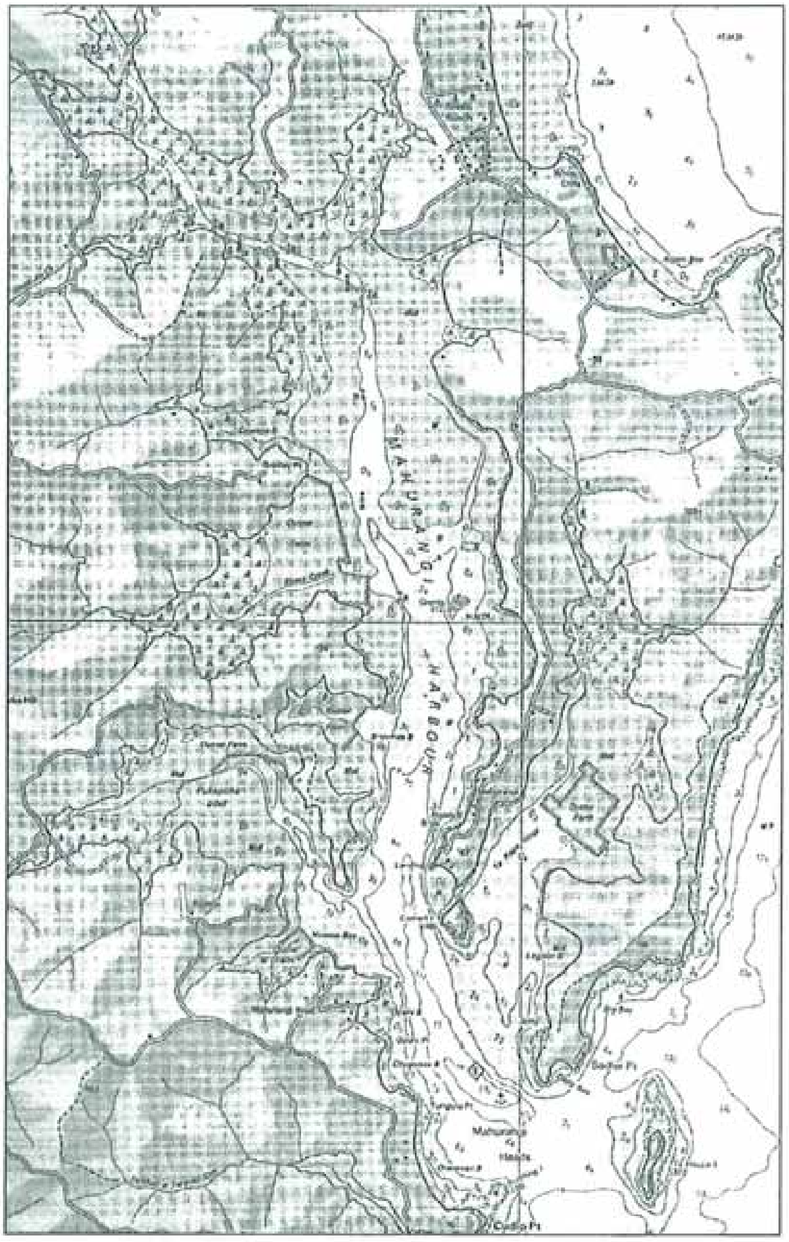

Fig. 5.1: Bathymetry of the Mahurangi Estuary (chart NZ5321, 1978).

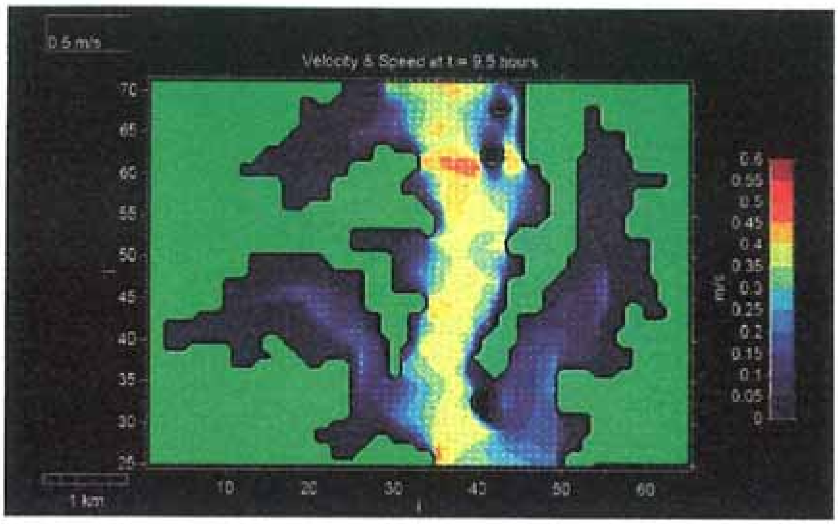

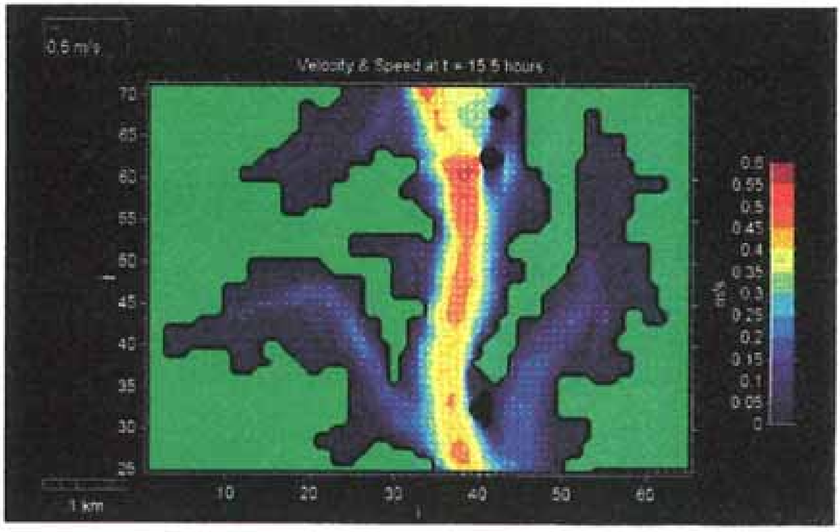

(A)

Figure 5.2: 3DD Hydrodynamic model vector plot showing peak flood and ebb current velocities for average (a) spring and (b)neap tides, lower estuary.

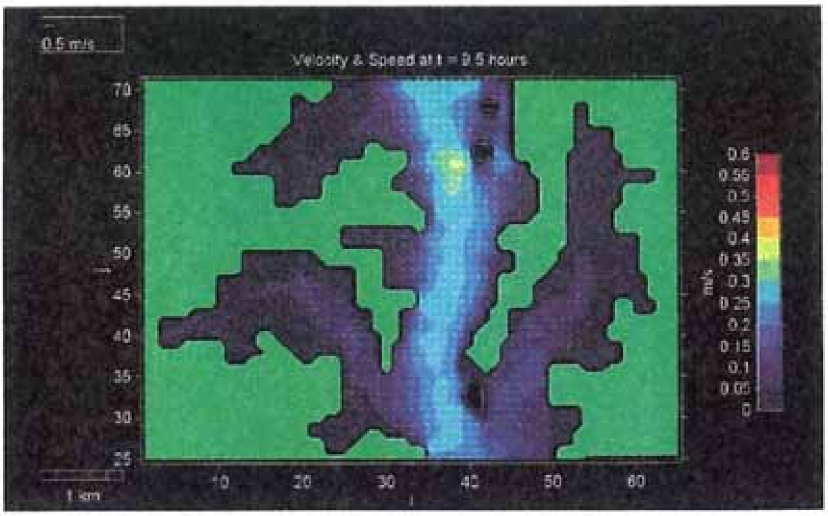

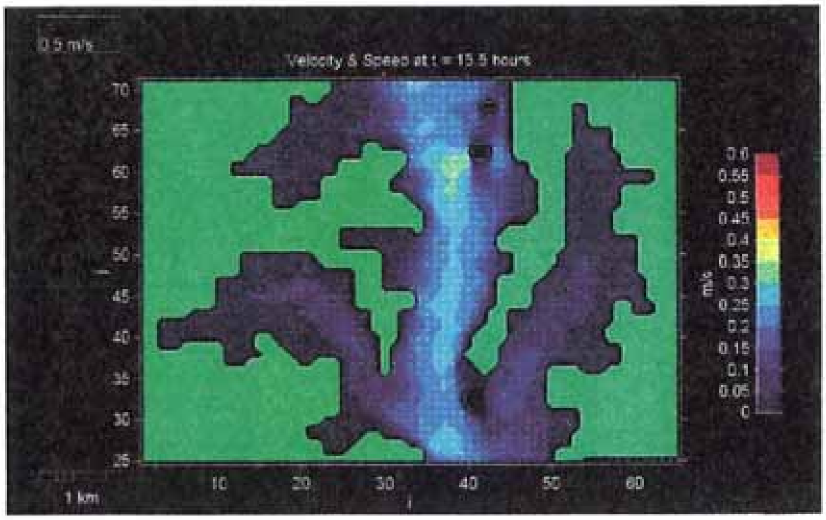

(B)

hours/days) effect of waves on water turbidity (Davies-Colley and Nagels, 1995) indicates that sediments are rapidly re-deposited and/or flushed from the estuary by tidal currents.

5.2 Freshwater runoff and estuary stratification

In addition to tidal currents and waves, sediment transport and deposition in the Mahurangi Estuary is also influenced by density differences (stratification) between the saline tidal waters and lower density river water. In the upper estuary the freshwater flows seawards at the surface, over the denser saltwater, becoming increasingly mixed downstream. Figure 5.3a shows the partially-mixed salinity structure of the estuary during a period of low freshwater flow. The mixing of fresh and saltwater downstream is indicated by the declining vertical and horizontal salinity gradients. Mixing of the water column results in a loss of mass in the near-bottom saltwater layer, which is compensated for by a corresponding inflow of salt water near the bed (i.e., residual current). Fine suspended sediments in the surface freshwater eventually settles into the more saline water below and are transported to the head of the estuary by residual and tidal currents. In partially-mixed estuaries suspended sediment concentrations, as well as sedimentation rates, are generally higher in the upper reaches than elsewhere. In the Mahurangi Estuary, suspended sediment concentrations are generally highest in the vicinity of Hamiltons Landing (e.g., Fig. 5.3a). This zone is termed the turbidity maximum and is a feature of partially mixed estuaries.

Changes in water salinity and turbidity associated with floods shows that the Mahurangi Estuary responds rapidly to freshwater pulses. Davies Colley and Nagels (1995) measured salinity and suspended sediment concentrations at 7 stations for 2 weeks following the July 1994 flood. The data (Fig. 5.3b-d) show that initially the estuary was highly stratified, with a low salinity (i.e., salinity <25 ppt, flocculation complete at 25 ppt) surface layer extending downstream to Dyers Creek. In the lower estuary, settling of flocculated sediments was probably occurring below the surface freshwater layer. In the upper estuary, the high suspended sediment concentrations near the bed suggests that a landward directed residual bottom flow was present. Some 24 hours later (Fig. 5.3C) the turbidity maximum had moved seawards and suspended sediment concentrations had declined. The rapid seaward decline in ssc suggests that sediment was being deposited and/or diluted by sea water. Thirty six hours after the flood peak a partially mixed salinity structure was becoming re-established (Fig. 5.3D). By then the flood sediment load had been deposited and/or flushed from the estuary. What we can say is that during floods, water flows, and therefore sediment transport, is predominantly seaward. In the lower estuary, turbulent mixing of fresh and salt water produces a partially stratified structure and settling of flocculated solids occurs (Davies-Colley and Nagels, 1995). The presence of a turbidity maximum in the vicinity of Hamiltons Landing suggests that this should be an area of rapid sedimentation. This is consistent with the pattern of recent sedimentation (post-1900 A.D.) we see in the Mahurangi Estuary.

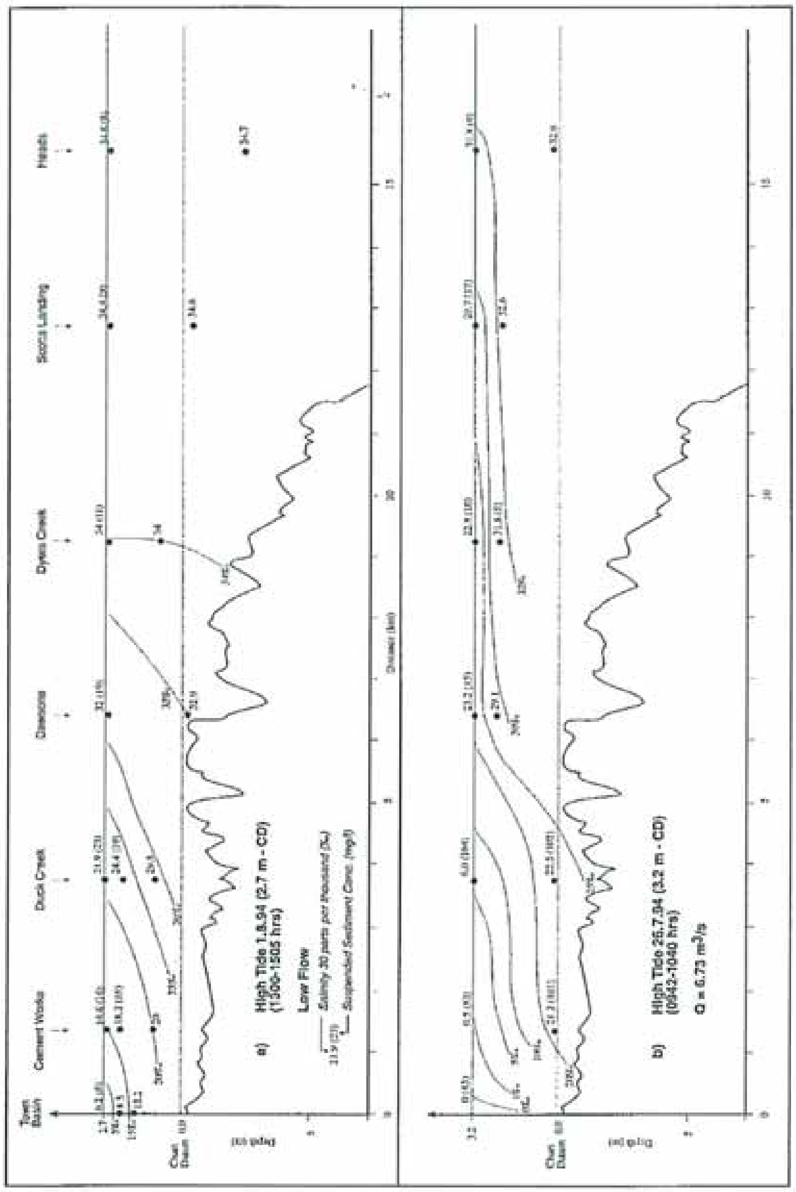

Fig. 5.3a-d Longitudinal-vertical salinity and turbidity of the Mahurangi Estuary, from Warkworth seaward to the Mahurangi Heads, for (a) low flow (partially mixed estuary) and during the July 1994 flood at (b) high tide 26.7.94, (c) low tide 26.7.94, and (d) high tide 27.7.94.

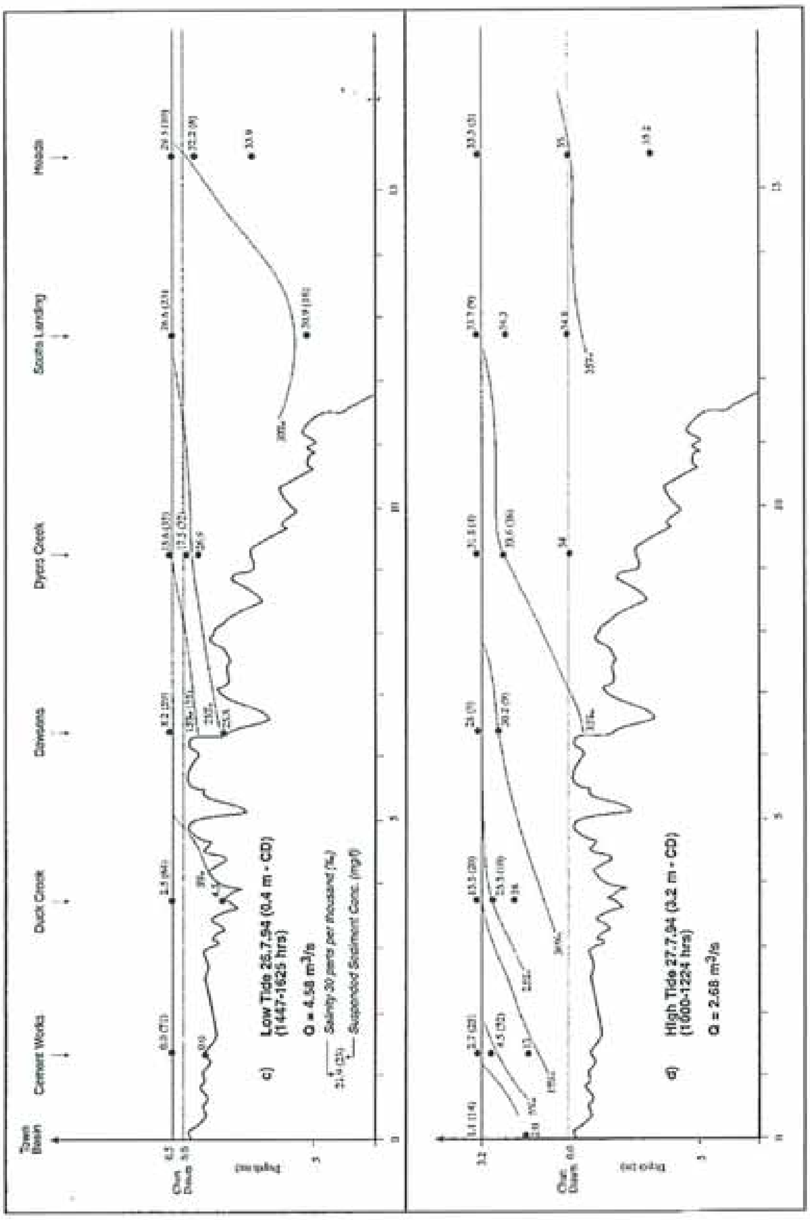

5.3 Surficial sediments

Figure 5.4 shows the distribution of surficial sediment grain size in the estuary. In the upper estuary, sediments on the tidal flats are muds that contain <10% fine sand, 60-70% silt and 20-30% clay, while in the channel there are sandy muds and muddy sands with coarse rock fragments (Johnston 1984). Where the estuary widens at Hamiltons Landing, the sediments coarsen and are commonly about 20-35% fine sand, 50-60% silt and about 20-25% clay. In the lower estuary and upstream of Scotts Landing, the sediments are coarser with 60-70% fine sand, 20-40% silt and 10%clay.

In Te Kapa Inlet the sediments are highly variable in particle size. Near the estuary mouth the sediments contain 80-90% sand and little silt and clay, and in the channel, carbonate gravel lag (i.e., shell and shell hash) is common.

Overall, the surficial sediments are very fine grained, and they become more muddy towards the head of the estuary, although a large quantity of sand and gravel was deposited here following catchment deforestation (1850-1900 A.D.). These fine surface sediments, particularly those in the upper estuary, contain enough clay and/or biological material (e.g., mucus, faecal pellets etc.) to 'glue' the sediments making them cohesive, thereby inhibiting entrainment by waves and currents.

5.4 Sediment entrainment by currents under present day conditions

The 3DD hydrodynamic model (Black, 1995) was used to compute depth-averaged tidal currents for mean neap and spring tides. These predicted currents were then compared to threshold values for sediment entrainment and provide an estimate of sediment entrainment in various estuary sub-environments (i.e., channel, subtidal and intertidal flats etc.). This procedure ignores sediment cohesion, which at present cannot be satisfactorily modelled. Appendix A.6.2 describes the techniques used to predict sediment entrainment in the Mahurangi Estuary.

Results

Figures 5.5a&b show the peak (depth-averaged) tidal current velocities in the Mahurangi Estuary for average spring and neap tides, as predicted by the HD model.

On spring tides, current velocities are concentrated in the main channel, between Hamiltons Landing and Cowans Bay and reach 0.5-0.6 m/s in the channel and 0.4-0.6 m/s on the fringing subtidal flats (Fig. 5.5a). Elsewhere, currents are weak over most of the intertidal flats and in the inlets and embayments fringing the estuary. On the neap tide, peak currents are weak throughout the entire estuary (Fig. 5.5b). Currents exceeding 0.1 m/s are restricted to the main tidal channel and fringing intertidal flats. In sheltered embayments and the large inlets (i.e., Te Kapa and Pukapuka) peak tidal current velocities are very low (<<0.1 m/s).

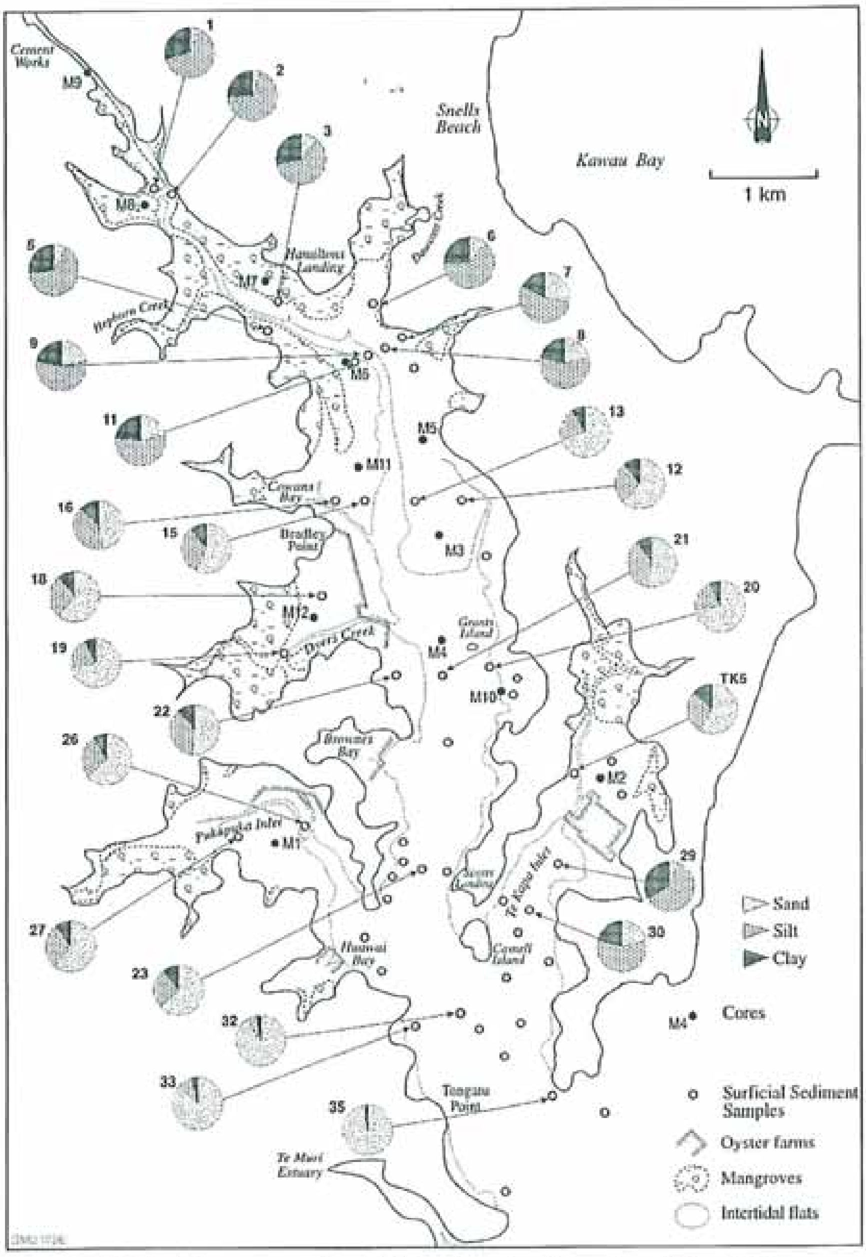

Fig. 5.4 **Surficial sediment texture (% sand/silt/clay) at selected locations, Mahurangi Estuary**

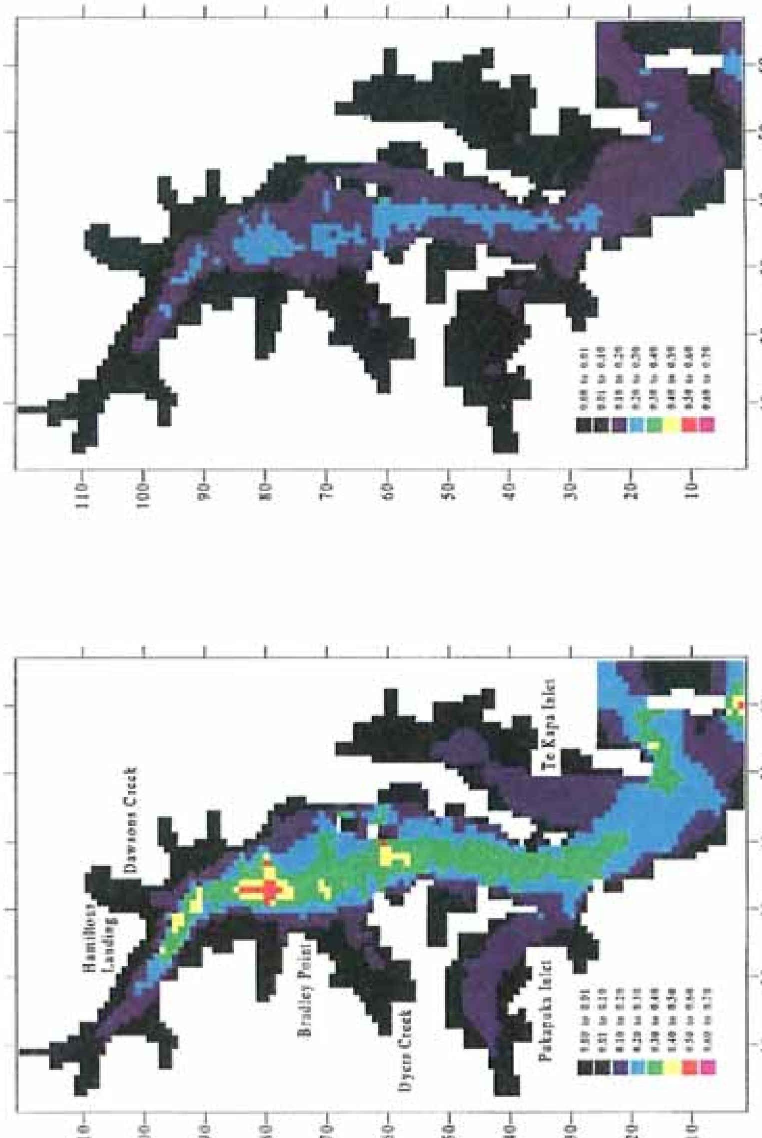

Figure 5.5a-b: Peak depth-averaged spring (a) and neap (b) tide current velocities (m/s). Note that the predicted peak currents occur at different times and locations in the estuary.

Figures 5.6a&b present model predictions for the duration (%) of each tidal cycle that current velocities exceed thresholds for sediment entrainment under neap and spring tide conditions, and how this varies throughout the estuary.

For neap tides the potential for sediment entrainment is restricted to a small region of the main tidal channel and lower intertidal flats between Hamiltons Landing and Grants Island (Fig. 5.6a). By comparison, spring tide currents potentially entrain sediment over a much larger area (Fig. 5.6b). Current velocities exceed thresholds along the entire tidal channel from Hamiltons Landing, seawards to Casnell Island

and on the intertidal flats close to the main channel. The modelling also suggests that current velocities exceed thresholds for short periods at isolated patches in side embayments (e.g., Te Kapa Inlet).

The strength and duration of currents in the channel near Hamiltons Landing indicates that conditions are unfavourable for sedimentation. At first this result appears to be at odds with the rapid channel sedimentation indicated from comparison of the 1904/5 and 1975 hydrographic surveys (e.g., 1.1 m $\pm$ 0.5 m between Hamiltons Landing and Bradley Point). However, hydrographic and core data show that there has been significant lateral (west to east) channel migration in the vicinity of Hamiltons Landing. Sediment is being deposited on the western flank of the channel, over time reducing the channel depth and width (i.e., volume). Although some scouring has probably occurred on the eastern channel flank this is much less than accretion on the western flank. The net reduction in channel width will locally increase current velocities. However the channel sediments are muddy (e.g., average size 30-61 µm) and will have higher thresholds for entrainment than predicted. Modelling also indicates that the durations of flood and ebb tide entrainment are similar (i.e., no net direction of movement).

Flood/Ebb Tide Asymmetry

The net direction of sediment transport by tidal currents can be estimated from the areal extent and duration (% of tidal cycle) that current velocities exceed thresholds during flood and ebb phases of the tide. Only the spring tide was modelled because this is primarily when sediments are mobilised by currents.

The modelling indicates that in the main channel and on the fringing intertidal flats there is a net ebb directed movement of sediment. Comparison of figure 5.7 a-b shows that at any one place the duration of ebb tide entrainment exceeds the flood. During the ebb tide channel current velocities exceed thresholds on average for 50-75% of the time (Fig. 5.7a), whereas current velocities exceed thresholds for only 25-50% of the flood tide (Fig. 5.7b). On the lower intertidal flats, ebb tide (25-75% duration) entrainment exceeds that on the flood tide (25-50% duration) (Figs. 5.7a and b). However in some locations (e.g., between Hamiltons Landing and Bradley Point) the duration of ebb and flood tide entrainment are similar. Therefore modelling suggests a net seaward directed movement of sediment.

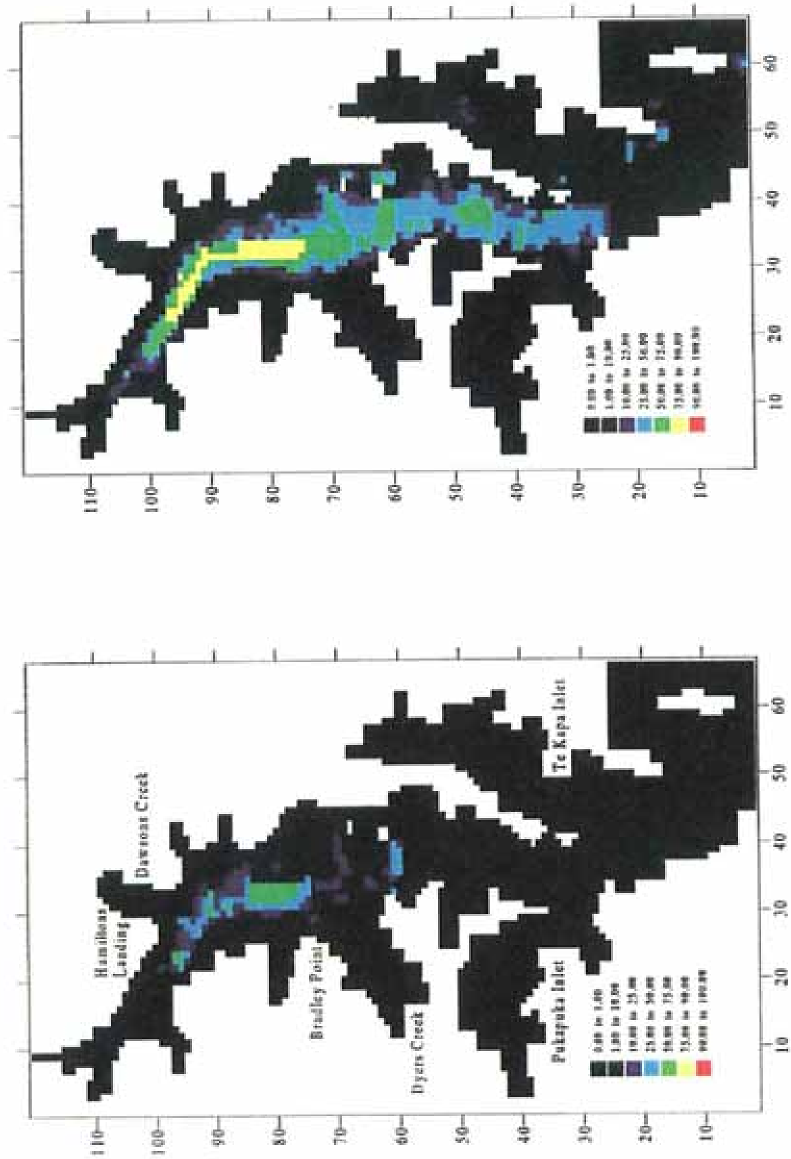

Figure 5.6a-b: Duration (% of tidal cycle) of neap (a) and spring (b) tide sediment entrainment under peak tidal currents, Mahurangi Estuary.

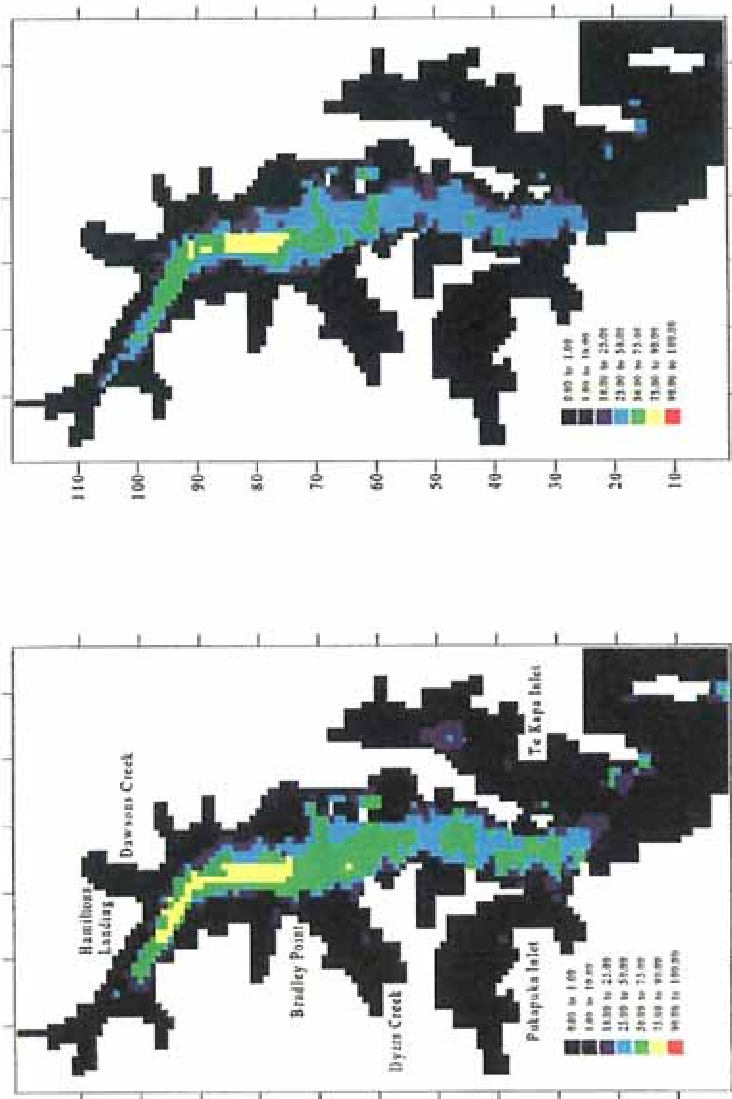

Figure 5.7a-b: Duration (% of tidal cycle) of ebb (a) and flood (b) tide sediment entrainment under peak spring tidal currents, Mahurangi Estuary.

5.5 Sediment entrainment by currents and waves under present day conditions

Waves are more effective than tidal currents at entraining bed sediments, and waves acting in combination with currents are the most effective mechanism of all. The hydrodynamic model and 3DD_WGEN wave model were used to compute the tidal currents and bed-orbital currents generated by waves for 4 selected combined tidal/wave scenarios. These predictions were then compared to threshold currents for sediment entrainment computed in each model cell, and so provide an estimate of sediment entrainment in the estuary by combined currents and waves.

Background

Combined wave and current flows greatly enhance the fluid forces imposed on bed sediments. The bed shear stress is maximum when the wave propagates in the direction of current flow and minimum when the wave propagates perpendicular to the current flow. However, waves will always enhance the shear stress imposed by a unidirectional current.

In the Mahurangi Estuary the regular exposure and inundation of the intertidal flats by the tide continually changes water depth and fetch. At low tide, the generation of waves, particularly across the estuary (west-east), will be attenuated because of the much reduced fetch and water depth. On the ebb tide, waves will begin to break on the intertidal flats and progressively closer to the main channel as water depth decreases. At high tide, cross-estuary fetch and depth will be maximised, although the bed orbital velocities may be greater at an intermediate depth, depending on the wave period and amplitude. The available fetch along the axis of the estuary (north-south) is up to 5 times the cross-estuary fetch and waves of increased height and period will be generated by a wind of constant speed and direction. The extensive intertidal flats will also significantly attenuate waves propagating along the axis of the estuary, except within a narrow 'window' along the channel. The peak bed orbital velocity imposed by waves in the deeper channel will be less than that on the adjacent (shallow) intertidal flats because orbital velocities decline with depth under waves. Therefore, sediment re-suspension by waves will be most effective on the flats fringing the channel.

Model scenarios

Scenarios were selected to predict whether sediment entrainment occurred under "extreme" wind storms. Two wind scenarios were selected from a 24 year record (1972-1996) at the nearby Warkworth Satellite Earth Station; a 30 m/s (108 km/h) northerly and a 25 m/s (90 km/h) westerly wind. The northerly wind has an occurrence probability of 2% (7.3 days/year), and the westerly 1% (3.7 days/year). The four combined tide-wave scenarios considered are shown in Table 5.1.

Table 5.1 Combined tide and wind-wave scenarios for modelling sediment entrainment in the Mahurangi Estuary.

Scenario	Tide	Wind speed (m/s)	Direction
1	spring	30	Northerly
2	neap	30	Northerly
3	spring	25	Westerly
4	neap	25	Westerly

Results

The modelling showed that wave heights of up to 0.8 m with short periods (<2-3 s) characterise waves in the estuary under strong winds. However, for most of the time (between wind storms), waves are much smaller or entirely absent. Also because wave periods are short, high bed-orbital velocities only rework sediment in shallow waters, on the intertidal flats and on the flanks of channels.

The results of the model runs are presented in Figures 5.8 to 5.11a-c. In each case plot 'a' maps peak bed-orbital velocities (cm/s) in each model cell, plot 'b' maps where tidal currents have the capacity to entrain sediment and where the combined action of currents and waves are required to entrain sediment, and plot c maps the duration (% of tidal cycle) of sediment entrainment by currents and/or waves.

Scenario 1: Northerly Wind + Spring Tide

- In the lower estuary and larger inlets, bed orbital velocities on intertidal flats are 20-60 cm/s (Fig 5.8a) and less than 1-10 cm/s in the main channel. The orbital velocities are high enough to re-suspend intertidal sediments but not in the deeper channel.

- As already shown, tidal currents alone will exceed sediment entrainment thresholds in the main channel and on the fringing intertidal flats (yellow zone) (Fig. 5.8b). Waves are required to suspend sediments on much of the upper intertidal flats and in the side embayments (red zone).

- The duration of potential sediment entrainment by combined tidal currents and waves varies from 50-90% for the main channel, to 50-75% for the lower intertidal flats, to 25-50% for the mid intertidal flats (Fig. 5.8c). Near the shore, thresholds are rarely exceeded (<1% duration); and this zone corresponds to the present-day distribution of mangrove in the estuary. The duration of potential sediment entrainment declines with distance from the main channel in direct proportion to the time inundated.

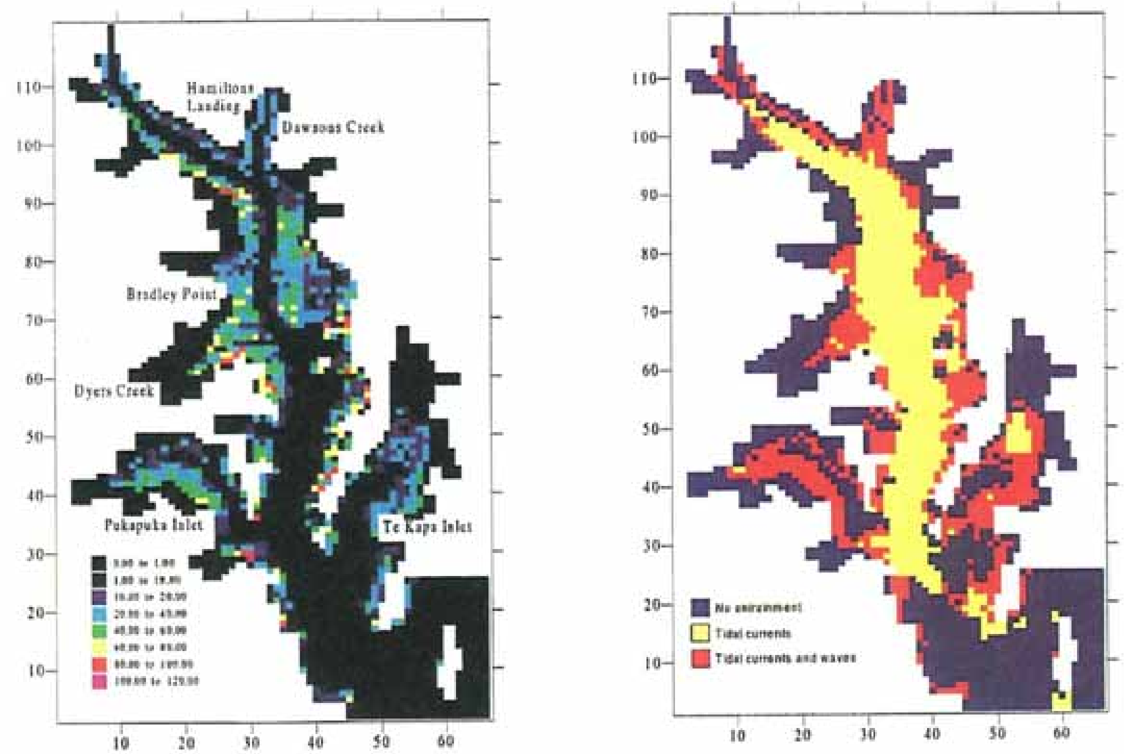

Figure 5.8a-b: (a) Peak bed-orbital velocities under a spring tide and northerly wind (30 m/s); (b) Sediment entrainment under peak spring tidal currents (yellow zone) and where combined tidal currents and waves are required to entrain sediment (red zone). Mahurangi Estuary. In the blue zone sediment entrainment does not occur under peak combined currents and waves.

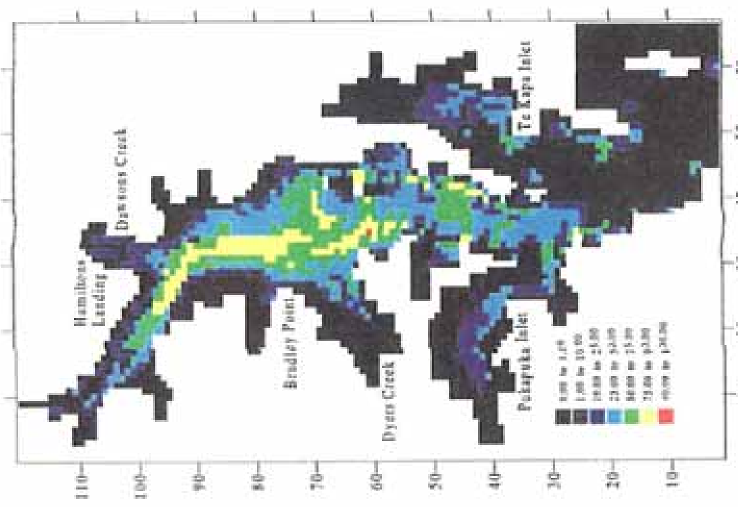

Figure 5.8c: Duration (% of tidal cycle) of sediment entrainment under combined peak spring tide currents and bed-orbital velocities (northerly wind 30 m/s). Mahurangi Estuary.

Scenario 2: Northerly Wind + Neap Tide

- Bed orbital velocities show a similar pattern to the spring tide, although orbital velocities are higher (40-60 cm/s) over a larger intertidal area (fig. 5.9a). The increased water depth at low tide and time of inundation on the intertidal flats during neap tides increases the fetch and therefore effectiveness of waves.

- Potential sediment entrainment by the combination of tidal currents and waves is much reduced during neap tides. In the main channel, tidal currents exceed thresholds (yellow zone) only occur landward of Grants Island (Fig. 5.9b). By comparison, waves (red zone) may still suspend sediment over a large proportion of the intertidal flats and in the larger inlets.

- Although the overall extent of neap tide sediment entrainment on the intertidal flats is less in comparison to that of spring tides, the duration is much longer (e.g., +25% duration). On the large intertidal flats north of Grants Island sediments may be suspended by waves for much longer periods than during spring tides (fig. 5.9c).

Scenario 3: Westerly Wind + Spring Tide

- Despite the much smaller fetch, bed orbital velocities on the intertidal flats are generally higher than those associated with the northerly wind scenarios, especially on the eastern (downwind) intertidal flats. By comparison sediments on the western side of the estuary are sheltered from wave action (fig. 5.10a).

- As for the northerly wind scenario, tidal currents alone are sufficient to entrain sediments (yellow zone) along the main tidal channel and fringing intertidal flats

(Fig. 5.10b). On the upper intertidal flats, in the side embayments and in the large inlets waves (red zone) are required to entrain sediment.

- The overall difference, in comparison to northerly winds, is for longer duration of sediment entrainment on the large eastern flats north of Grants Island, and for less entrainment seaward of this area (fig. 5.10c).

Scenario 4: Westerly Wind + Neap Tide

- As with the northerly wind scenario, entrainment mainly occurs north of Grants Island, but the duration is shorter especially on the western intertidal flats (Fig 5.11a).

- Because of the limited cross-estuary fetch, potential sediment entrainment by waves on the intertidal flats mainly occurs east of the main channel (Fig. 5.11b). In Pukapuka and Te Kapa Inlets waves are the primary mechanism by which sediments are suspended.

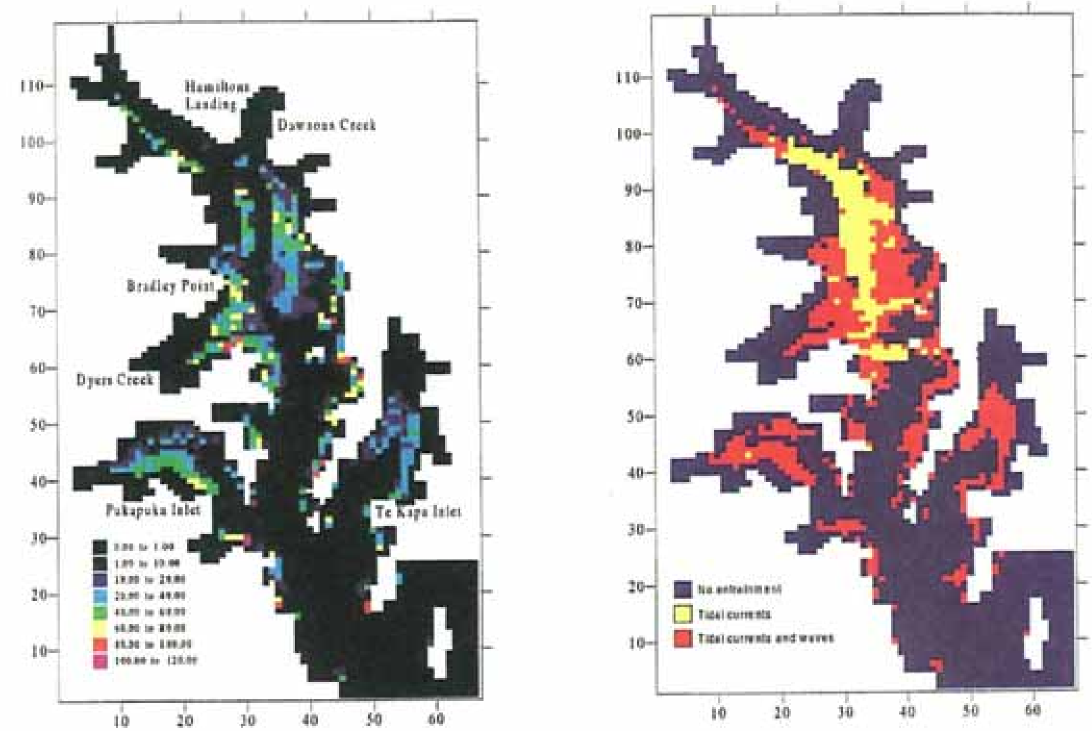

Figure 5.9a-b: (a) Peak bed-orbital velocities under a neap tide and northerly wind (30 m/s); (b) Sediment entrainment under peak neap tidal currents (yellow zone) and where combined tidal currents and waves are required to entrain sediment (red zone), Mahurangi Estuary. In the blue zone sediment entrainment does not occur under peak combined currents and waves.

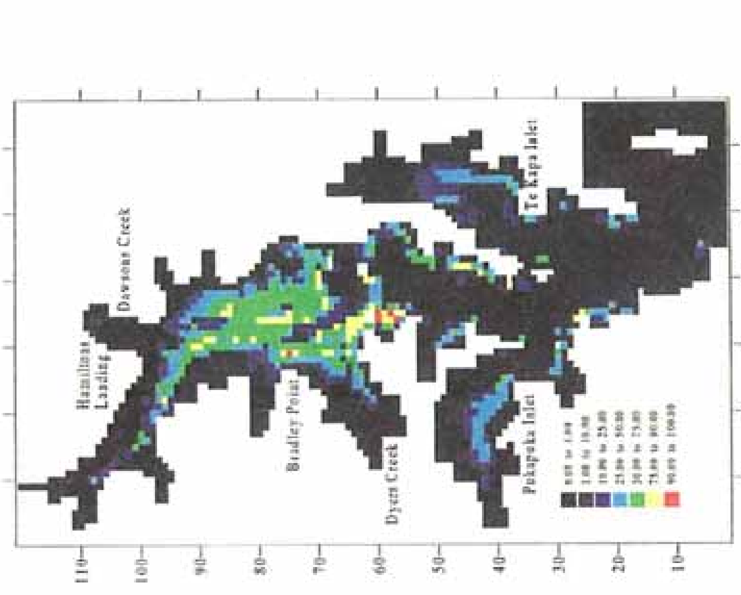

Figure 5.9c: Duration (% of tidal cycle) of sediment entrainment under combined peak neap tide currents and bed-orbital velocities (northerly wind 30 m/s), Mahurangi Estuary.

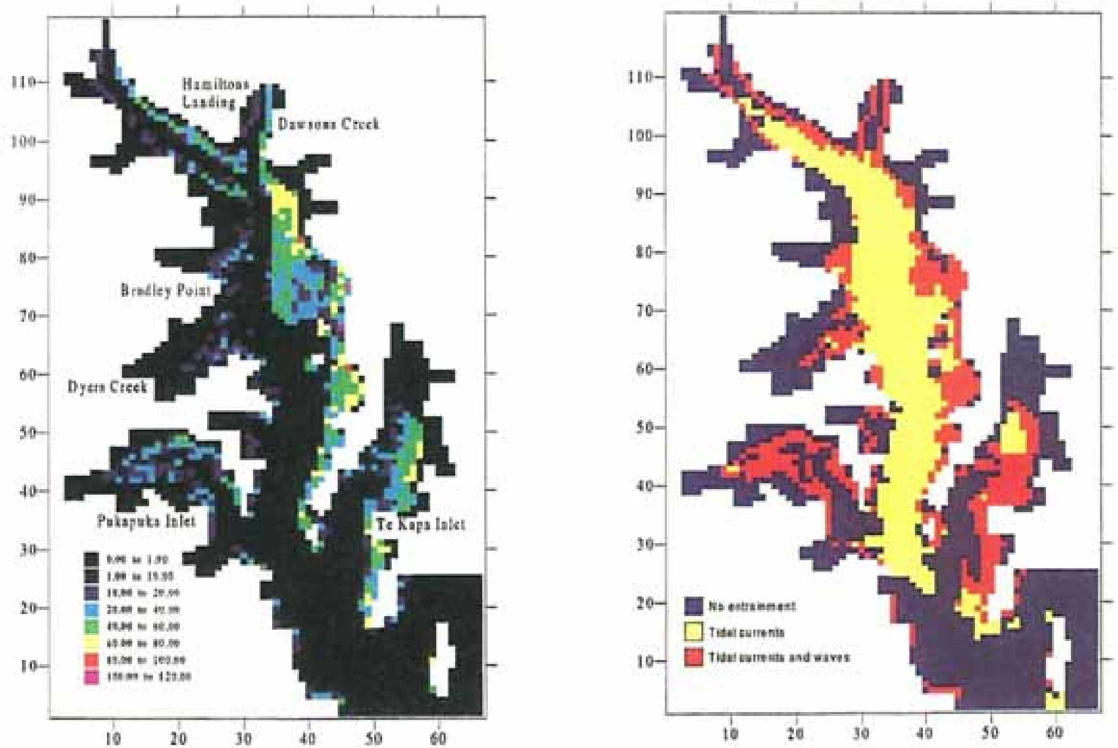

Figure 5.10a-b: (a) Peak bed-orbital velocities under a spring tide and westerly wind (25 m/s); (b) Sediment entrainment under peak spring tidal currents (yellow zone) and where combined tidal currents and waves are required to entrain sediment (red zone), Mahurangi Estuary. In the blue zone sediment entrainment does not occur under peak combined currents and waves.

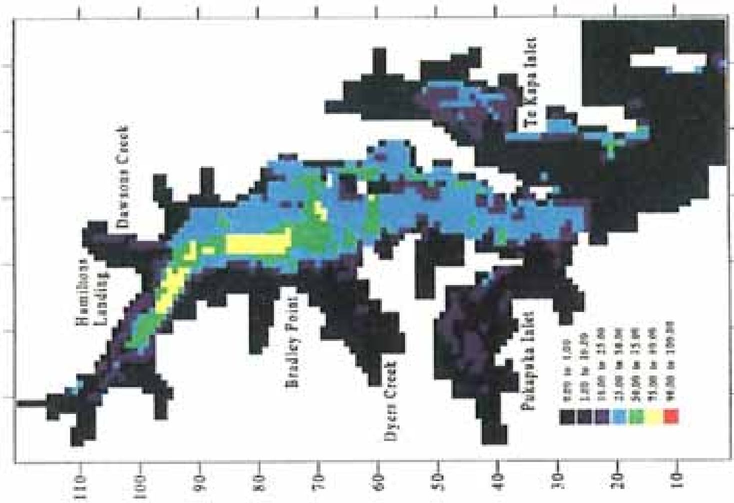

Figure 5.10c: Duration (% of tidal cycle) of sediment entrainment under combined peak spring tide currents and bed-orbital velocities (westerly wind 25 m/s), Mahurangi Estuary.

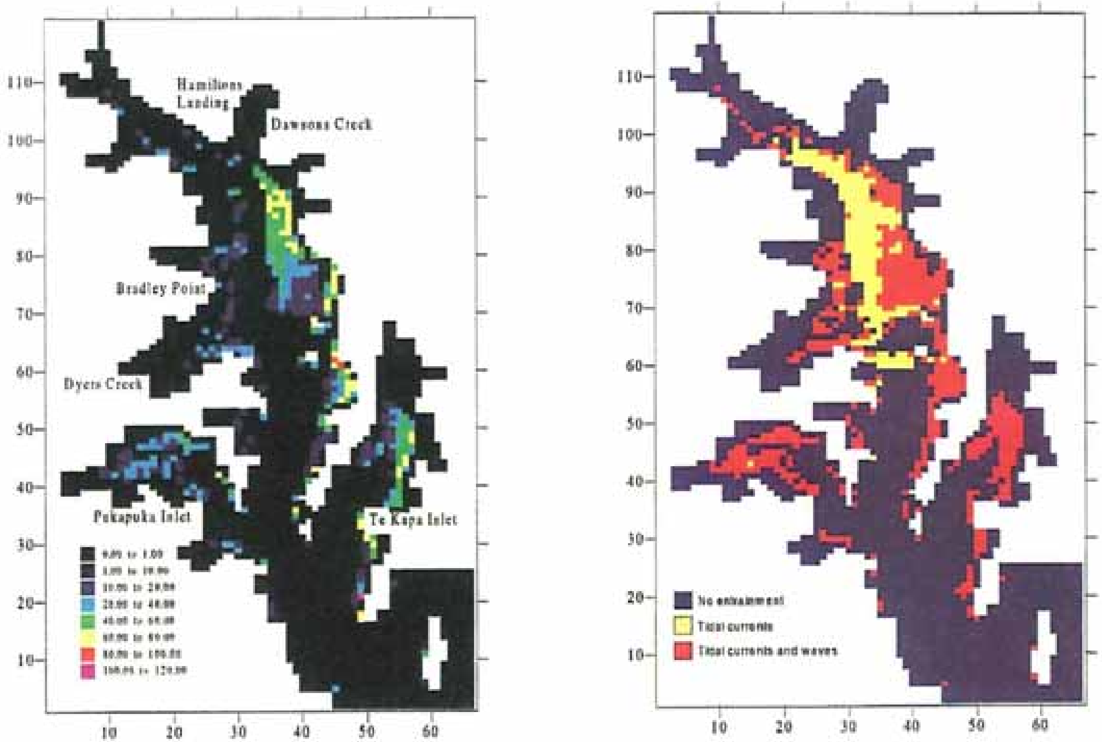

Figure 5.11a-b: (a) Peak bed-orbital velocities under a neap tide and westerly wind (25 m/s); (b) Sediment entrainment under peak spring tidal currents (yellow zone) and where combined tidal currents and waves are required to entrain sediment (red zone). Mahurangi Estuary. In the blue zone sediment entrainment does not occur under peak combined currents and waves.

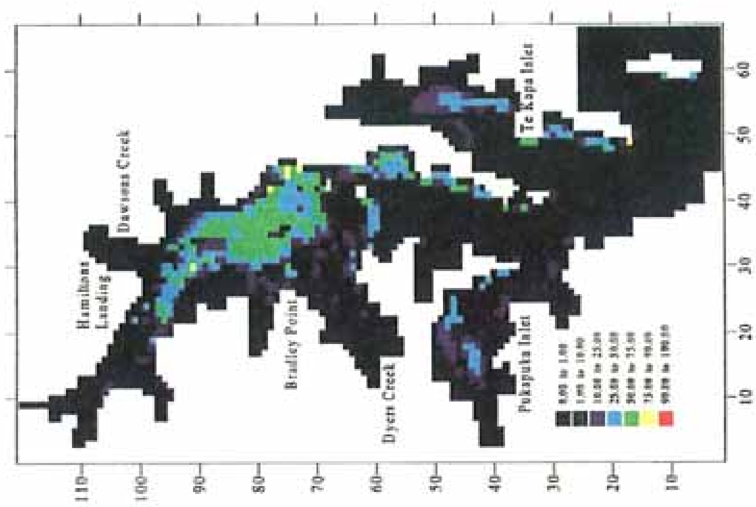

Figure 5.11c: Duration (% of tidal cycle) of sediment entrainment under combined peak neap tide currents and bed-orbital velocities (westerly wind 25 m/s), Mahurangi Estuary.

5.6 Summary

The modelling has served to highlight that:

- The potential for sediment entrainment by currents is directly related to the tidal range. The much larger spring tide generates stronger currents that potentially entrain sediment almost along the entire length of the main channel and fringing intertidal flats. By comparison, neap tide currents may only entrain sediments in a small section of the channel between Grants Island and Hamiltons Landing.

- Waves enhance sediment entrainment by tidal currents in the channel and fringing intertidal flats and are predicted to initiate entrainment high on the intertidal flats, in embayments and inlets where tidal currents are very weak. Waves are potentially effective in these environments despite their sheltered aspect and limited fetches.

- In the Mahurangi westerly winds (WNW-WSW) prevail, accounting for 50% of the local wind climate (1972-1996) (cf. easterly winds make up 20% of the total). In addition, winds from the westerly quarter are on average stronger. We would expect therefore for sediments on the eastern tidal flats to be more reworked than those on the west. The higher sand content of intertidal sediments east of the main channel, north of Grants Island (Fig. 5.4), seems to bear this out.

- Although waves may suspend sediment on the intertidal flats, our cores show that this process has not prevented infilling of these areas to date. These areas represent long term sinks for eroded catchment soils.

- While modelling indicates that sediments are not entrained by tidal currents in most intertidal areas, waves can enhance the pattern imposed by the tidal currents. Where waves do entrain intertidal sediments, there will be a net ebb directed movement of sediment.

5.7 Sediment entrainment by currents and waves, past and future.

Mahurangi Estuary at 3500 years B.P.

In reconstructing the sedimentation history of Mahurangi Estuary, we postulate that resuspension of sediments by waves would have become increasingly frequent as the estuary infilled and shallowed. To provide some indication of the relative importance of sediment entrainment by tidal currents and waves in a formerly deeper subtidal estuary, the four combined wave and current scenarios (Table 4.1) were modelled for a deeper estuary. For this purpose the model grid-cells were uniformly deepened by 3 m (channels and flats) which is the amount of infilling that has occurred in the last 3000 years. We assumed the same tidal boundary and sediment conditions as the present day.

The results of the modelling suggests that:

- Peak spring and neap current velocities north of Grants Island were much lower, and current velocities seawards of Grants were higher (Fig. 5.12a&b), than those of the present day.

- Under spring tides the pattern of sediment entrainment in the deeper estuary (yellow zone) was broadly similar to that of today, although currents exceed thresholds over a much wider area near the mouth of the estuary and less in the area now occupied by extensive intertidal flats north of Grants Island (cf Figs 5.12c & d, with 5.8b & 5.10b).

- In the deeper estuary, waves were less effective at re-suspending estuarine sediments.

- Under neap tides, current velocities exceed thresholds (yellow zone) in very few areas (cf. Figs. 5.12 d & f with 5.9b and 5.11b).

In the deeper estuary of 3000 years B.P. sediment entrainment by currents and waves largely coincided with spring tides. Spring tidal currents entrained sediment in the main channel and fringing subtidal zone. Only spring tides produced water depths shallow enough over the subtidal flats for waves to suspend sediment. Neap tidal currents and waves were too weak to entrain sediment and once deposited most sediment would not be disturbed, at least until the next spring tide. Therefore, the fate of catchment sediment runoff delivered to the estuary by floods could have been more strongly dependent on the spring-neap tidal cycle than it is today. The overall effect of this would have been for more complete trapping of any sediment entering the estuary. The reduced effectiveness of sediment resuspension by currents and waves during neap tides suggests that average water turbidity in the estuary may have been lower than today, although more variable.

Future infilling

Our core data (section 3.6) showed that the Mahurangi estuary is infilling much more rapidly in recent times than prior to catchment deforestation. Over the last 90 years, net sedimentation rates have been 0.5-4.1 mm/year in the lower estuary and much higher in the upper estuary. Assuming that this trend continues, then 0.05-0.4 m of sediment will be deposited in the estuary over the next 100 years or so. Locally, sedimentation rates in some parts of the estuary (e.g., upper estuary) could be higher.

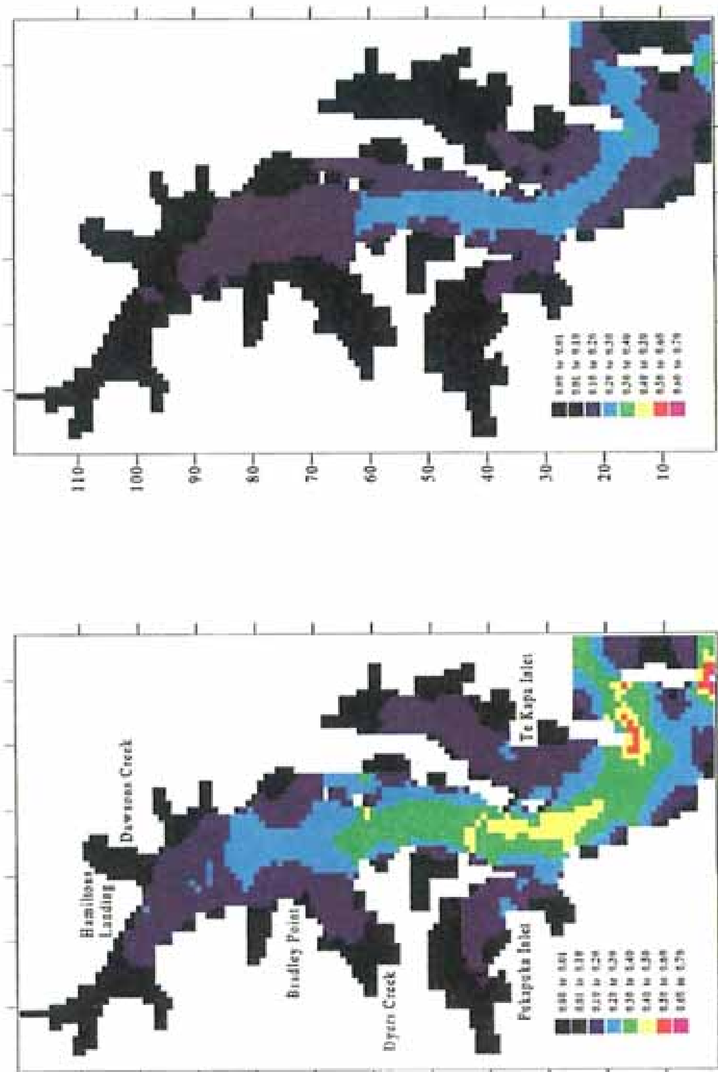

Figure 5.12a-b: Peak depth-averaged spring (a) and neap (b) tide current velocities (m/s) in a deeper subtidal estuary (3500 yr B.P.). Note that the predicted peak currents occur at different times and locations in the estuary.

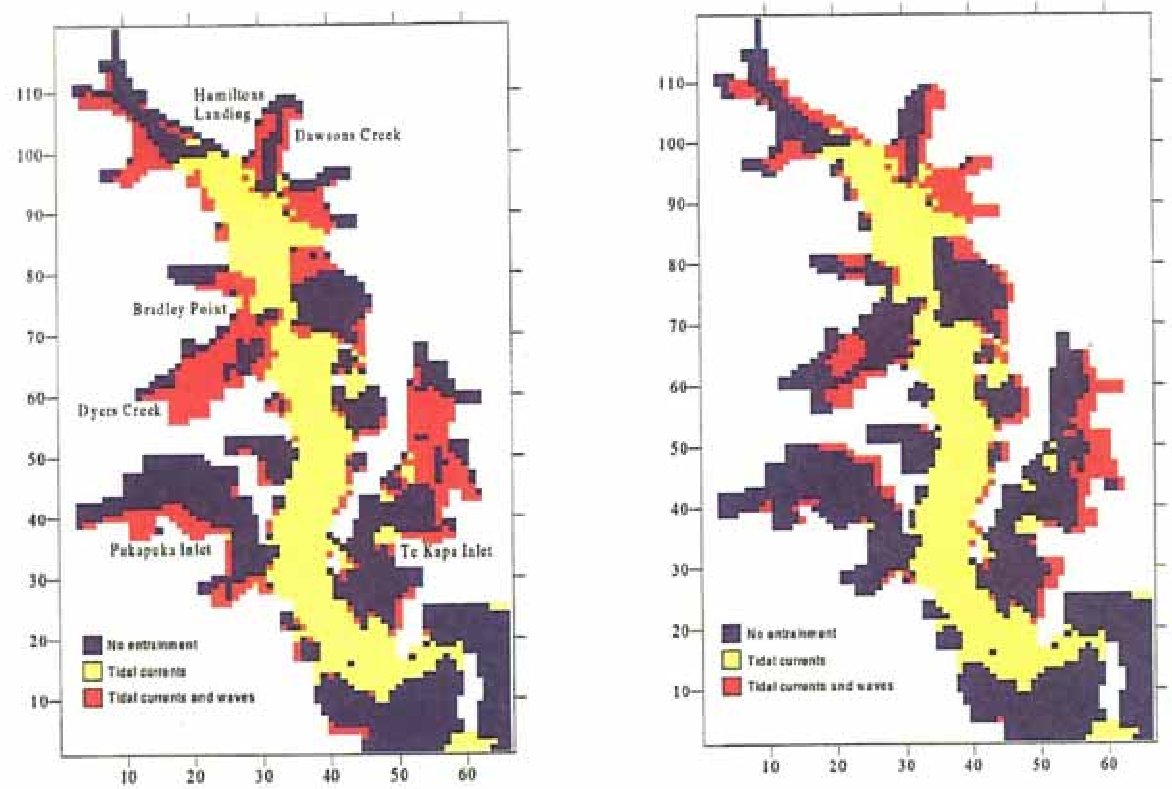

Figure 5.12c-d: Sediment entrainment under combined currents and bed-orbital velocities for a (c) spring tide and northerly wind (30 m/s) and (d) spring tide and westerly wind (25 m/s) in a deeper subtidal estuary (3500 yr B.P.). In the blue zone sediment entrainment does not occur.

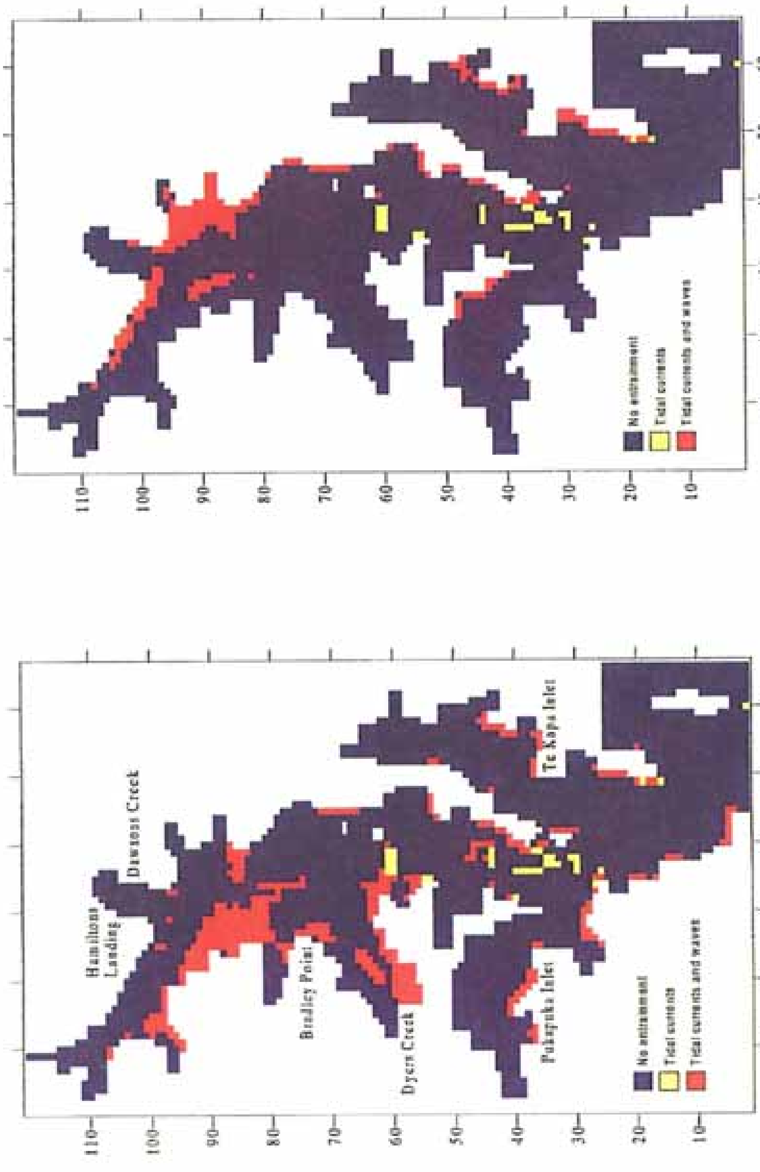

Figure 5.12e-f: Sediment entrainment under combined currents and bed-orbital velocities for a (e) neap tide and northerly wind (30 m/s) and (f) neap tide and westerly wind (25 m/s) in a deeper subtidal estuary (3500 yr B.P.). In the blue zone sediment entrainment does not occur.

To assess the potential effects of estuary infilling on patterns of sediment entrainment by currents and waves 100 years from now, the model estuary bed was uniformly raised by 0.25 m. This is equivalent to the amount of infilling predicted to occur in the next 100 years, assuming present sedimentation rates. We assumed the same tidal boundary conditions and surficial sediment characteristics as the present day.

The modelling predicts:

- Peak spring and neap tidal current velocities would increase slightly in the main channel and on the fringing intertidal flats landward of Grants Island (Fig. 5.13a & b). In the large inlets and embayments (e.g., Pukapuka Inlet) a significant reduction in current velocities is likely as a consequence of the smaller tidal prism.

- The pattern of sediment entrainment by tidal currents is similar to the present day, with the largest potential for entrainment being during spring tides in the channel and on the intertidal flats (Fig. 5.13c & d).

- Waves would play an increasingly significant role in suspending surficial sediments, particular on the intertidal flats (Fig. 5.13c & d).

Waves will continue to be the primary means by which sediments on the upper intertidal flats and in the large inlets and embayments are entrained (Fig. 5.13c & d). However, further infilling of the estuary will reduce the duration of tidal inundation in those environments and therefore the amount of time available to rework sediment. The net result will be for the intertidal flats to increasingly become long term sinks for eroded catchment soils. Sedimentation on the channel margins will be offset to some degree because as infilling proceeds waves will become more effective.

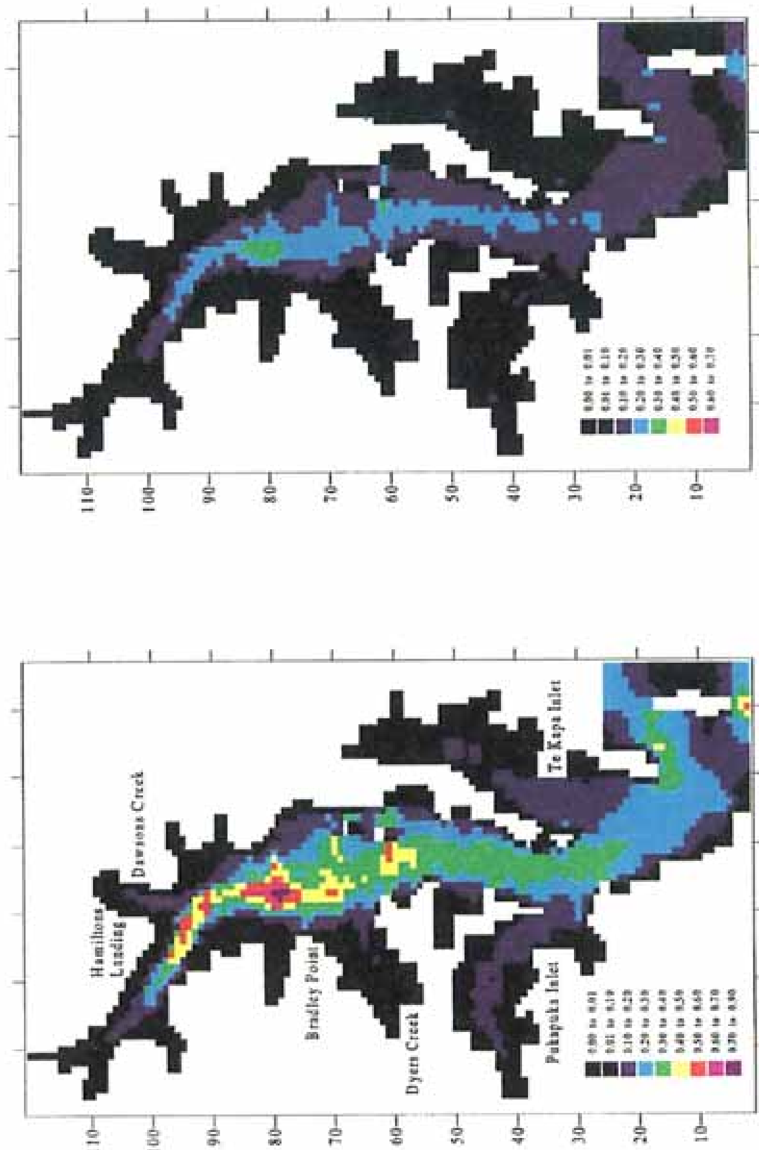

Figure 5.13a-b: Peak depth-averaged spring (a) and neap (b) tide current velocities (m/s) in a shallower intertidal estuary. Note that the predicted peak currents occur at different times and locations in the estuary.

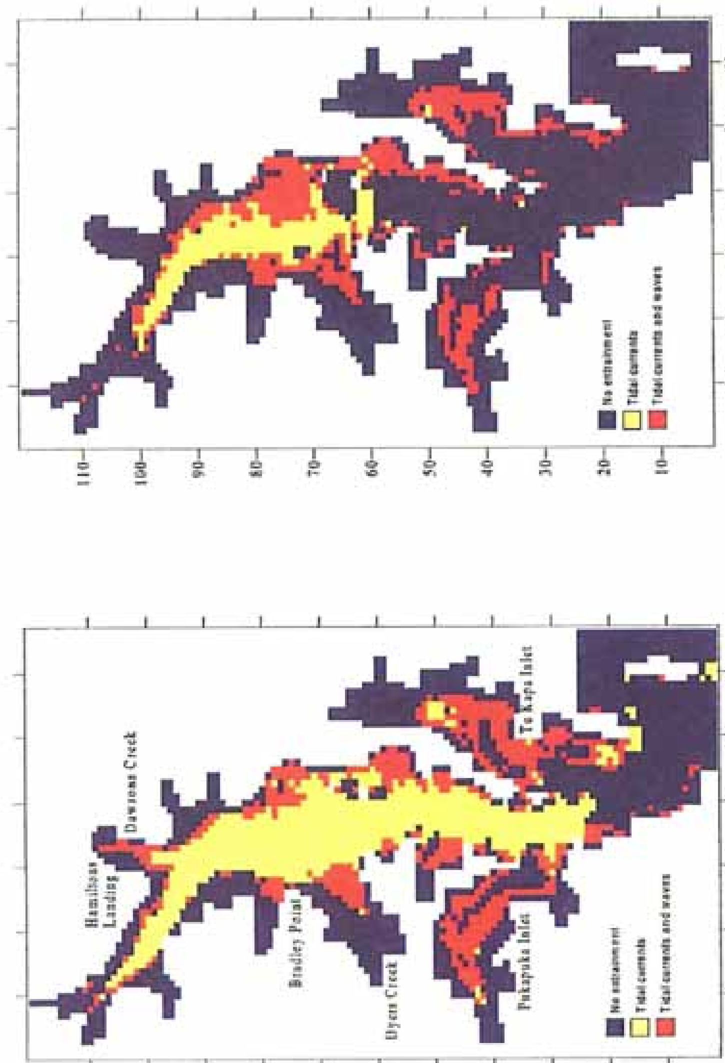

Figure 5.13c-d: Sediment entrainment under combined currents and bed-orbital velocities for a (c) spring tide and northerly wind (30 m/s) and (d) neap tide and westerly wind (25 m/s) in a shallower intertidal estuary. In the blue zone sediment entrainment does not occur.

6. CONCLUDING COMMENTS

At least 7300 years ago the Mahurangi Estuary was a deep subtidal basin, slowly infilling with fine suspended sediments of catchment and marine origin. Since that time up to 15 m of mud have been deposited in the lower estuary, much of this prior to human settlement. In the last thousand years the sedimentary environment has dramatically and permanently altered to a largely intertidal estuary which has infilled with increasingly coarse sediments. In historical times (i.e., last 150 years), estuary infilling has been dramatically accelerated by catchment deforestation and subsequent soil erosion accompanying European settlement. The coarser sediments deposited in the estuary, particularly since the mid-1800's, reflects the increased supply of coarse sediments due to catchment soil erosion as well as increasingly effective sediment reworking by waves and currents as the estuary has infilled. On the intertidal flats, it is likely that muds are winowed by wave action, which is suggested by the coarser texture of sediments on the extensive eastern flats. Figure 6.1, a conceptual model of past and present estuary and catchment conditions, summarises the main findings of the study.

The average sedimentation load in the lower estuary since 1900 A.D. (702 tonnes/km^2/yr) is twice the maximum sediment load measured for pasture/bush catchments elsewhere in the Auckland region. Although modelling indicates that the average catchment sediment load has declined in the last 20 years to 448 t/km^2/yr, it is highly unlikely that catchment sediment loads and therefore estuary sedimentation rates will return to the very low levels that existed prior to catchment deforestation.

Our results indicate that estuary sedimentation loads are high in comparison to suspended sediment loads from catchments elsewhere in the Auckland region and that the Mahurangi Estuary Catchment is susceptible to soil erosion. Furthermore, the fact that sedimentation loads remain much higher today than prior to catchment deforestation suggests that deforestation has affected a long term change in catchment sediment loads. Future catchment development that is likely to expose catchment soils to erosion will have to planned with particular care if periods of potentially increased estuary sedimentation and consequent adverse environmental effects are to be mitigated or avoided.

In the next 100 years an additional 0.25 m of sediment will be deposited in the lower estuary if infilling continues at present rates (i.e., post-1900 A.D.). In the upper estuary sedimentation rates could be higher. Overall, modelling indicates that at the 'moderate' infilling rates expected in the next 100 years, estuary hydrodynamics and therefore sedimentation patterns will not be drastically different than today. This assumes that catchment sediment loads do not significantly increase.

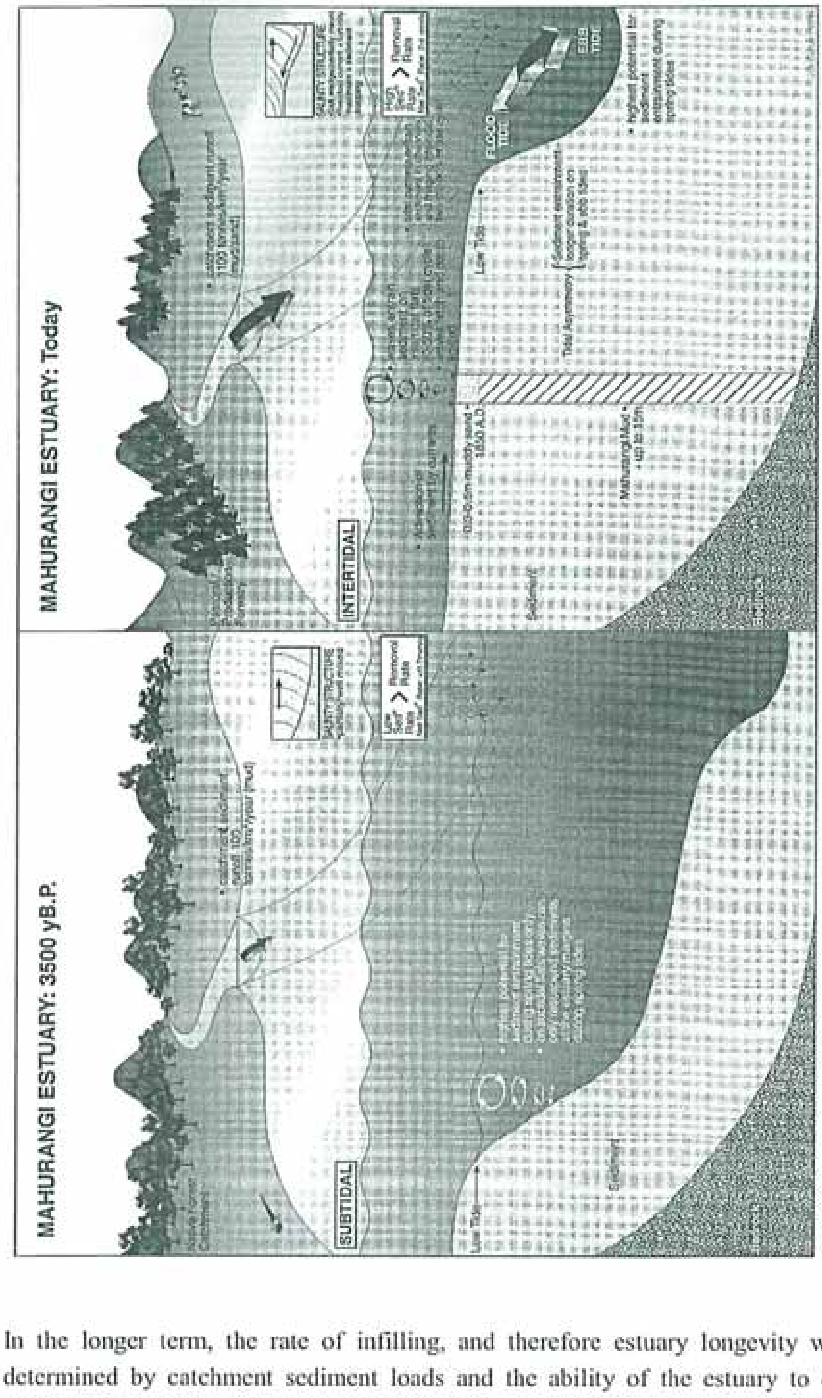

Fig. 6.1 Conceptual model of past (3500 y B.P.) and present catchment inputs, sedimentation and the relative importance of sediment reworking by currents and waves in the Mahurangi Estuary

In the longer term, the rate of infilling, and therefore estuary longevity will be determined by catchment sediment loads and the ability of the estuary to export sediment inputs. Two alternative responses to future infilling are presented, based on past estuary response to catchment sediment inputs and modelling of estuary sediment reworking by waves and currents.

Alternative 1: The rate of estuary infilling will accelerate, primarily as a consequence of loss of tidal prism, thereby reducing the ability of currents and waves to rework and export sediment:

- Based on sedimentation rates in the recent past (post-1900 A.D.), modelled catchment suspended sediment loads and assuming catchment landcover does not alter and/or intensify, we estimate that the estuary will continue to infill at 2-4 mm/year. Locally, sedimentation rates could be much higher, particularly in the upper estuary and in the vicinity of Hamiltons Landing.

- Ultimately, with the continued loss of tidal prism, the ability of currents to remobilise sediment will decline. Furthermore, estuary infilling will increasingly exclude waves from reworking intertidal sediments. Consequently, the rate of estuary infilling will accelerate. The estuary would be progressively infilled and replaced by freshwater marsh at its landward end and a tidal lagoon-mangrove swamp in the lower estuary. Freshwater runoff would be discharged via a network of channels, tidally influenced at their seaward margin.

Alternative 2: A more likely alternative is that the rate of estuary infilling will be maintained at present levels or decline, as a dynamic balance between catchment sediment loads and the estuary's ability to export sediment is reached:

- As the estuary infills, wind waves and currents will become increasingly effective at reworking sediments. On the intertidal flats, wave stirring will winnow fine muddy sediments, maintaining the coarser sandy texture of intertidal sediments. By this process the eroded mud will accumulate in low energy environments (i.e., sheltered inlets) or exported from the estuary by tidal currents. These predictions are consistent with modelling results and field work in the estuary.

- Reconstruction of historical sedimentation in the estuary shows that the Mahurangi Estuary is progressively infilling from the landward end. This process is 'shortening' the estuary in that the effective discharge point of sediment delivered to the estuary during floods is displaced further seaward. Consequently, an increasingly large proportion of flood sediment loads are likely to be exported from the estuary.

By these processes sedimentation in estuaries is retarded and the longevity of an estuary can be extended for a considerable period of time. However, in the Mahurangi Estuary we cannot confidently predict how long the present hydrodynamic and sedimentary environment will be maintained. Modelling suggests that no significant changes will occur over the next 100 years, at present rates of estuary infilling.

Future catchment development that exposes soils to erosion has the potential to increase catchment sediment loads and consequently estuary infilling. The high sedimentation load computed from cores for the pasture/bush landcover phase shows that catchments draining to the Mahurangi Estuary have a high potential for soil erosion. In the long term, land use activities that repeat the cycle of catchment disturbance and soil erosion will have a larger influence on estuary sedimentation than 'one-off' activities (e.g., urban development) that have a relatively short period of disturbance. However, on-going exposure of relatively small catchment areas to erosion, typical of urban development, could also represent long term source areas for soil erosion.

7. ACKNOWLEDGEMENTS

The authors acknowledge the assistance of ARC staff with field work for this study, in particular Mr Ken Becker, Resource Quality Scientist. We also acknowledge Dr Matt McGlone (Landcare Research) and Dr Tom Higham (Waikato University Radiocarbon Laboratory) for palynological and radiocarbon dating, Max Oulton (Geography Department, University of Waikato) for cartographic services, John Nagels (NIWA) for field assistance, Morag Stroud (NIWA) for sediment load data and Dr Bruce Williamson (NIWA) for constructive comments.

8. REFERENCES

Auckland Regional Council, 1993, Review of Mahurangi Catchment, Estuary and Harbour Water Quality. Technical Publication No. 27, Environment and Planning Division, Auckland Regional Council.

Auckland Regional Water Board, 1986, Report on the storm, 22 May to 23 May 1985. Technical Publication No. 40, Auckland Regional Water Board.

Batham, E.J., 1969, Benthic Ecology of Glory Cove, Stewart Island. *Transactions of the Royal Society, Biological Sciences*, 11(5):73-81.

Bell, J.M. and Fraser, C., 1912, The geology of the Waihi-Tairua Subdivision, Hauraki Division. Bulletin No.15 (New Series). New Zealand Department of Mines, Geological Survey Branch, Wellington.

Black, K.P., 1995, The hydrodynamic model 3DD and support software. *Occasional Report No. 19 Department of Earth Sciences, University of Waikato.* 53 pp.

Cooper, A.B. and Bottcher, A.B., 1993, Basin-scale modelling as a tool for water resource planning. *Journal of Water Resources Planning and Management*, 119(3): 306-323.

Curry, R.J., 1981, Hydrology of the catchments draining to the Pauatahanui Inlet. *Water and Soil Tech. Pub. 23.*

Davies-Colley, R.J. and Nagels, J.W., 1995, Optical water quality of the Mahurangi Estuarine System. NIWA Consultancy Report.

Davis, J.C., 1986, Statistics and Data Analysis in Geology, Second Edition. John Wiley and Sons.

Dyer, K.R., 1986, Coastal and estuarine sediment dynamics. John Wiley and Sons.

Fahey, B.D. and Coker, R.L., 1992, Sediment production from forest roads in Queen Charlotte Forest and potential impact on the marine water quality, Marlborough Sounds, New Zealand. *New Zealand Journal of Marine and Freshwater Research*, 26:187-195. Royal Society of New Zealand.

Ferrar, H.T., 1934, The Geology of the Dargaville-Rodney Subdivision, Hokianga and Kaipara Divisions. Bulletin No.34 (New Series). Department of Scientific and Industrial Research, Geological Survey Branch, Wellington.

Forrest, B.M., 1991, Oyster farm impacts on the benthic environment: a study in Mahurangi Harbour. Master of Science (Environmental Science and Zoology), University of Auckland.

Grant, W.D. and Madsen, O.S., 1979. Combined wave and current interaction with a rough bottom. *Journal of Geophysical Research*, 84:1797-1808.

GESAMP, 1993, Anthropogenic influences on sediment discharge to the coastal zone and environmental consequences. GESAMP Reports and Studies No. 52. Joint Group of Experts on the Scientific Aspects of Marine Environment Protection (GESAMP), United Nations.

Gibb, J.G., 1986, A New Zealand regional Holocene eustatic sea level curve and its application to determination of vertical tectonic movements: contribution to IGCP-Project 200. *Royal Society of New Zealand Bulletin 24*.

Harris, T.F.W., 1993, The Mahurangi System. Environment and Planning Division, Auckland Regional Council.

Herald, J.R., 1989, Hydrological impacts of urban development in the Albany Basin, Auckland. Doctor of Philosophy (Geography), University of Auckland.

Hicks, D.M., 1994, Storm sediment yields from basins with various landuses in Auckland area. Miscellaneous Report No. 183, National Institute of Water and Atmospheric Research Ltd, Christchurch.

Hume, T.M., 1983, Upper Waitemata Harbour sediments and the inferred impacts of future catchment and estuary use change. Auckland Regional Authority.

Hume, T.M. and Dahm, J., 1992, An investigation of the effects of Polynesian and European land use on sedimentation in Coromandel estuaries. Prepared for Department of Conservation, Hamilton Regional Office. Water Quality Centre, DSIR Consultancy Report No. 6104.

Hume, T.M. and McGlone, M.S., 1986, Sedimentation patterns and catchment use change recorded in the sediments of a shallow tidal creek, Lucas Creek, Upper Waitemata Harbour, New Zealand. *New Zealand Journal of Geology and Geophysics*, 22:1-19.

Johnston, R.M.S., 1984, Sediments and sedimentary processes in Mahurangi Harbour. Master of Science thesis, Department of Earth Sciences, University of Waikato.

Kingett Mitchell and Associates, 1988, Manukau Harbour Action Plan: Assessment of recent sedimentation of the Manukau Harbour.

Meade, R.H., 1982, Sources, sinks and storage of river sediments in the Atlantic drainage of the United States. *Journal of Geology*, 90:235-252.

McGlone, M.S., 1994, Unpublished report on the pollen analysis of cores from the Mahurangi Estuary. Landcare Research, Lincoln.

Morrisey, D.J. and Swales, A., 1996, Towards the development of guidelines for the sustainable management of aquaculture in the Auckland region. Consultancy Report ARC304/1, National Institute of Water and Atmospheric Research Limited.

Morton, J.E. and Miller, M.C., 1973, The New Zealand Sea Shore, Second Edition. William Collins and Sons, Glasgow.

Nichols, M.M., 1977, Response and recovery of an estuary following a river flood. *Journal of Sedimentary Petrology*, 47: 1171-1186.

Oldman, J.W. and Black, K.P, 1997, Mahurangi Estuary numerical modelling. NIWA Client Report ARC60208/1.

Powell, A.W.B., 1979, New Zealand Mollusca: marine, land and freshwater shells. Collins, Auckland.

Sale, E.V., 1978, Quest for Kauri. A.H. and A.W. Reed, Wellington.

Schubel, J.R. and Pritchard, D.W., 1986, Responses of Upper Chesapeake Bay to variations in discharge of Susquehanna river, *Estuaries*, 9(4A): 236-249.

Sheffield, A.T., 1991, The sedimentology and hydrodynamivcs of the Whangamata Harbour. Master of Science (Earth Sciences), University of Waikato.

Strachan, C.J., 1977, Landuse, sediment yield and solute load: a case study from the Auckland region. Master of Science thesis, Department of Geography, University of Auckland.

Stroud, M.J. and Cooper, A.B., 1997, Modelling sediment loads to the Mahurangi. Prepared for ARC Environment. Niwa Client Report ARC60211.

Stuvier, M. and Pearson, G.W., 1993, Modelling atmospheric ^{14}C and ^{14}C ages of marine samples to 10000 years BC, *Radiocarbon*, 35(1):137-189.

Swales, A., 1989, The effects of urbanisation and consequent sediment generation on the Upper Pakuranga Estuary, Auckland. Master of Science thesis, Department of Geography, University of Auckland.

Swales, A. and Hume, T.M., 1994, Sedimentation history and potential future impacts of catchment logging on the Whangamata Estuary, Coromandel Peninsula. Consultancy Report CHH003, National Institute of Water and Atmospheric Research Limited.

Swales, A. and Hume, T.M., 1995, Sedimentation history and potential future impacts of production forestry on the Wharekawa Estuary, Coromandel Peninsula. Consultancy Report CHH004, National Institute of Water and Atmospheric Research Limited.

Trotter, S.A., 1990, Estuarine sedimentation and land cover history: The case of the Mahurangi. Master of Science thesis, Departments of Geography and Environmental Science, University of Auckland.

Van Roon, M., 1981, Calculation of mass transport by streams, and yields under a variety of landuses. *Working report No. 28, Upper Waitemata Harbour Catchment Study.*

Vant, W.N., Williamson, R.B., Hume, T.M. and Dolphin, T.J., Effects of future urbanisation in the catchment of Upper Waitemata Harbour. Prepared for Environment and Planning Division, Auckland Regional Council. NIWA Consultancy report ARC220.

Williams, P.W., 1976, Impact of urbanisation on the hydrology of Wairau Creek, North Shore, Auckland. *Journal of Hydrology (N.Z.)*, 15:81-99.

9. APPENDICES

APPENDIX A: METHODS

A.1 Coring

Background

Analysis of various sediment layers in the cores using sedimentological, palynological (pollen) and radiocarbon dating techniques, enabled historical catchment landcover changes to be correlated with estuarine sedimentation rates. This information was used to assess the potential impacts of future catchment landcover changes on estuarine sedimentation.

Field Method

Twelve sites were selected for coring to represent the diversity of sedimentary environments (e.g., estuary tidal creek, sheltered embayments, main channel and intertidal flats) and provide appropriate spatial coverage of sedimentation in the estuary (Fig. 2.1).

Most cores where taken from locations remote from the main channel where there is less reworking by currents and therefore the sediment stratigraphic record is likely to be complete. In this respect cores from tidal arms and embayments are the sites where the most complete sediment sequences are likely to be found. In the vicinity of Dawsons Creek (Core M6) a site near the channel was selected because anecdotal evidence suggested rapid sedimentation.

Cores were taken from a boat using a Livingston piston corer to drive PVC pipe (50 mm internal diameter) into the unconsolidated estuarine sediments. This technique is particularly suitable for shallow estuarine applications because the piston system minimises compression of the sediments during core penetration. Core lengths are limited to about 5 metres.

Prior to coring, sediment thickness was measured by pushing gum spears (steel rods) into the sediment column. At many of the sites a sudden resistance - indicating contact with basement rock did not occur because of the substantial depth of sediment accumulation (e.g., 10 m+). However, the gum spears confirmed the general suitability of a particular site for extracting long cores.

Core penetration varied from 3.25 metres (Core M1) to 3.92 metres (Core M2). Total core compression was calculated by comparing the total length of core penetration with the actual length of core retained. The length of core retained was measured in the field and again in the laboratory. Core compression occurs during coring, particularly as water filled voids (e.g., animal burrows) collapse and compact.

Compression in the Mahurangi Estuary sediment cores varied from 0-8% and averaged 5%.

Laboratory Method

In the laboratory, each PVC core barrel was partially cut through using a skill-saw. The last few millimetres being split by hand to avoid disturbing sediment in the core. The cores where then logged with major stratigraphic units being determined on the basis of colour and textural characteristics. Further information for paleo-environmental interpretation was provided by the occurrence and type of common bivalve and gastropod species found in the cores. The level of sample preservation was used to determine the degree to which these skeletal components had been reworked by tidal currents and waves. Samples were taken from the cores for sediment textural analysis and ^{14}C dating.

A.2 Sediment physical characteristics

Background

Sediment texture (grain size distribution and morphology) reflects the nature of the sediment source and sorting by waves and currents in the estuary. Changes in sediment texture over time, as preserved in cores, is indicative of environmental change. In the catchment, rainfall events deliver predominantly fine clay and silt to the estuary, in addition to a much smaller amount (<10%) of sand and gravel. Following native forest clearance by European settlers we would expect increasing proportions of sand and gravel to be delivered to the Mahurangi Estuary, resulting from erosion of less weathered, deep regolith by sheet and gully erosion and hillslope failure.

Method

Sediment texture was determined on 10 mm thick slices taken from each of the major stratigraphic units in the core. The samples were pre-treated to remove organics (6% weight/volume hydrogen peroxide: 24 hours) then flushed with de-ionised water and dispersed (0.5% weight/volume sodium hexametaphosphate). The proportion of mud (< 0.0625 mm), sand (0.0625 - 2.0 mm) and gravel (> 2.0 mm) was determined by wet and dry sieving.

The dry bulk density (mass/unit volume) of sediments is measured at various depths in the sediment column so that the mass of sediment deposited in the estuary can be calculated. Sediment bulk density was determined in 10 mm thick slices, taken from each unit by drying (24 hours at 120°C) and weighing.

A.3 Pollen dating

Background

The pollen types present at various depths in the sediments reflects the catchment landcover at the time the sediment was deposited. In many New Zealand estuaries the succession of pollen types, associated with landcover changes, is well documented. A succession from native forest species (e.g., Rimu, Kauri) that changes to bracken, fern pollen and spores with Polynesian settlement, followed by the appearance of exotic species (e.g., grasses, willow, pine etc.) and the decline of native species with European settlement is typical (Hume, 1983; Hume and Dahm, 1992; Hume and McGlone, 1986; Kingett-Mitchell Limited, 1988; Sheffield, 1991; Swales and Hume, 1994,1995).

The application of palynology as a dating tool depends on the availability of a reliable catchment landcover history. This includes dates for Polynesian settlement, the initiation of large scale forest clearance during European settlement, pastoral landuse and in many catchments, the planting of exotic (pine) forests. Given this information it is possible to date horizons in the pollen record and derive net-sedimentation rates for each phase of landcover change.

A primary limitation of this technique is caused by the vertical mixing of sediments. Physical mixing (i.e., wave and tidal-current action) and bioturbation (mixing by organisms) may erase evidence of localised or relatively short phases of landcover disturbance (e.g., Polynesian forest clearance for gardens) by blending these horizons with older and/or more recent sediments (Hume and Dahm, 1992; Hume and McGlone, 1986; Swales and Hume, 1994, 1995).

The pollen dating technique also assumes that pollen deposited in estuarine sediments is solely derived from the adjacent catchment. However, the pollen assemblage will be influenced to some degree by wind, fluvial (river) and tidal-current transport pathways, but mainly the quantity of pollen in estuarine sediments is related to the distance from the catchment source (Hume and Dahm, 1992; Vant et al., 1993). In the Mahurangi Estuary the proximity of a large catchment indicates that most pollen will be locally derived.

The general provenance of pine pollen is a measure of local versus external sources. At concentrations of 5-10% the pollen may be derived from local or regional sources while at concentrations of 20-40% (e.g. Core M1) or more, there is a high degree of certainty that the pollen is derived from a local source, within the catchment (Dr M. McGlone, Landcare Research, Lincoln, pers. com., 1994).

In interpreting the pollen record, allowance must also be made for the time lag between event and effect. An example of this is the time lag between pine planting and the development of a significant pollen rain that is detectable in sediment deposits, which is in the order of one decade. Thus, this correction must be applied when determining time horizons based on this indicator species.

Method

The analysis of pollen in the cores concentrated on the upper part of the sediment column. Samples were taken at 100 mm intervals down to the base of each core. The general abundance of pollen types in samples (cores M1, M2, M3, M4, M6, M12) and a detailed count (pollen concentrations) of cores M1 and M8 was used to identify time horizons in the sediment column. Palynological analysis of the sediment column was conducted by Dr Matt McGlone of Landcare Research, Lincoln.

A.4 Radiocarbon dating

Background

Radiocarbon dating was used to provide absolute dates on shell layers in the cores. This technique is suitable for material older than 250 years BP (Hume and Dahm, 1992) and therefore for dating layers further down in the core. The carbonate shells of benthic organisms, such as bivalves, are particularly suitable for analysis.

In dating material at a particular depth in the sediment column it is assumed that this dates the time of initial deposition. This may not always be the case if older shells have been eroded, re-worked and redeposited in younger sediment at a higher level. In this situation under-estimation of sedimentation rates results. This is most likely to occur in the vicinity of channels where meandering and scour by tidal-currents may erode the sediment column.

Caution is also required where intact bivalves are present (both valves joined) in sediment cores. Dating of those animals which burrowed to considerable depth immediately prior to death results in overestimation of net-sedimentation rates. As such, whole dis-articulated valves are most suitable for radiocarbon dating. Comparison of radiocarbon dates with horizons dated using palynological techniques reduces the likelihood of error in estimating estuarine sedimentation rates.

The measured radiocarbon ages need to be calibrated to take into account several effects:

(1) Fluctuations in the production of atmospheric radiocarbon (^{14}C), related to solar and geomagnetic influences and the apparent differences (offset) in atmosphere-ocean carbon reservoirs and activity (Stuiver and Braziunas, 1993) which converts a radiocarbon age to a solar (calendar) date.

(2) The time lag between atmospheric ^{14}C entering the oceans (the global marine offset) and the mixing of deep 'old' seawater with 'young' surface waters in the coastal zone requires a reservoir correction in the order of -336 years. Without this correction present-day shell or organic material would provide an age up to several hundred years old.

(3) The absence of an absolute dating method for the ocean (e.g., c.f. dendrochronology from tree rings on land) requires the modelling of atmospheric-ocean carbon exchange, based on actual variations in the former. Because of the uncertainties inherent in this approach a local correction factor (DR), which in New Zealand is +30 years, is included in the reservoir correction (McFadgen and Manning, 1990). This is the difference between the radiocarbon age for the modelled surface layers of the world ocean (1950 A.D.) and that derived locally by an independent source, and is applied prior to calibration.

(4) The historical fluctuations in atmospheric carbon demonstrated by dendrochronological studies produces characteristic 'wiggles' in the radiocarbon-calendar age curves (see Stuiver and Braziunas, 1993). Consequently, for any given radiocarbon date there may be several calibrated ages (intercepts), any of which could be the true date. Given this and other errors inherent in the analysis the 'wiggle effect' can result in substantial total errors and a wide age range.

In this study ^{14}C ages were calibrated to take account of the above effects using a probability distribution method. This method is favoured by many workers because the relatively higher probabilities in the vicinity of curve intercepts is explicitly recognised. This enables the range (% area under the probability curve) within which the 'true' age is likely to fall to be quantified.

Laboratory Method

Samples of shell material were selected from cores M1, M6, M8 and M9 where it occurred in relatively thin (10-15 cm) sand and shell units. Bivalve and gastropod species favoured for dating where *Austrovenus stutchburyi* (cockle), *Macomona lilliana* (large wedge shell), *Paphies australis* (Pipi). In the distinctive, massive green-grey mud unit, which dominates the Holocene sedimentation record in the Mahurangi Estuary, the turret shell *Maoriculpus roseus* is abundant. Skeletal remains of *Maoriculpus* were used to date time horizons, and thereby derive 'background' sedimentation rates for the Mahurangi Estuary.

Radiocarbon dating of the shell samples, and calibration of radiocarbon ages, was conducted by the University of Waikato Radiocarbon Dating Laboratory using a standard level of precision. Standard errors were in the order of $\pm$ 45 to 130 years. As the samples were dated at between 931 and 7345 years BP, these errors have a negligible effect on the accuracy of calculated sedimentation rates.

A.5 Estimating catchment flood inputs

Method

Measurements of river flow and suspended sediment concentrations (ssc) at the Mahurangi River College site during floods were used to compute flood sediment loads. Two events were considered; a 62.3 m^3/s (peak flow) flood in July 1994 (2.2 year return period) and a 137.6 m^3/s flood in March 1995 (9 year return period).

The measurements show that high ssc coincided with the flood peak and that generally ssc were significantly higher on the rising limb of the flood hydrograph (Fig. A.1). Although the flood hydrograph is relatively well defined, sampling of ssc is less frequent - particularly for the July 1994 flood event. Calculation of the flood sediment load requires flow and ssc time series to be interpolated at a regular, frequent time increments and then integrated.

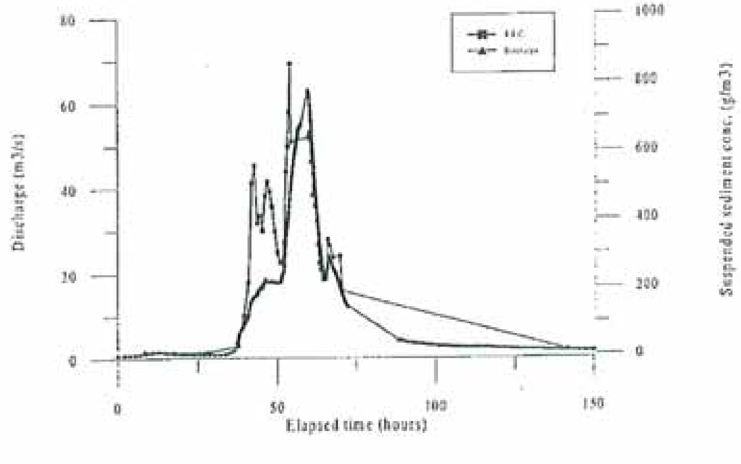

Figure A.1: July 1994 flood, discharge and suspended sediment concentration measured at Mahurangi River College site.

<u>July 1994 Flood</u>

A linear regression was applied (natural log) to instantaineous flow (x) and ssc measurements (y), and subsequently the relationship was used to predict ssc at regular time increments. Although the correlation coefficient was high ($r^2 = 0.93$), it was apparent that predictions of ssc in some cases diverged markedly (50-200%) from measured ssc. This was due to the significant scatter (residuals) of data, as a result of higher ssc's on the rising limb (c.f., falling limb) of the flood hydrograph.

Consequently, a cubic-spline function was fitted to the flood-hydrograph and flow and ssc regularly interpolated at 0.25 hour intervals. In some cases interpolation of data is a more robust approach than the use of a statistical model, because of the scatter inherent in the flow-ssc relationship. Cubic-splines locally fit a smoothly defined curve between (raw) data points which provides a more realistic interpolation of the time series (Davis, 1986). This interpolation method was used to compute flood sediment loads, whereas regression relationships were only used when the record was too sparse to fit a spline curve (i.e., at low flows and on falling limb of hydrograph).

<u>March 1995 Flood</u>

The more frequent sampling of ssc during this event provided a good curve fit over a large proportion (75%) of the flood hydrograph. The initial low flow and early phase of the flood hydrograph (0-19.75 h) ssc was estimated using the <25 cumec regression relationship. The sediment load for this event can be accurately estimated because of the high frequency of raw ssc over the entire flood hydrograph. The interpolated flow and ssc time series enabled the flood hydrograph segments (Δt, 0.25

hours) to be integrated and a cumulative sediment load computed by the mid-point method (flow and ssc at Δt mid-point).

NO CHART FOR HERE.

Figures A.1 Flood discharge and suspended sediment concentration measured at the college site, Mahurangi River, July 1994.

A.6 Estuarine hydrodynamics and sediment entrainment

Introduction

The fate of catchment sediment runoff to the Mahurangi Estuary will depend to a large extent on the ability of tidal currents and waves to entrain and transport sediments. Estuarine surficial sediments are mostly fine-grained mixtures of mud (grain size <62.5 μm), sand and organic detritus. In many places the sediments are cohesive.

Predicting the transport of cohesive sediments is much more difficult than it is for noncohesive sediments. Cohesive-sediment transport is complicated by various factors including the aggregation and disaggregation of flocs ('clumps' of cohesive sediments), which affects the settling velocity, and hence sedimentation rate. Generally, faster flows are required to entrain cohesive sediments, but cohesive sediments settle out of the flow much more slowly than non-cohesive sediments.

Because of the many uncertainties associated with predicting cohesive sediment transport, the approach taken in this study is to estimate an "entrainment potential" based on sediment grain size and density. While this approach ignores some processes which influence the behaviour of cohesive sediments, it nevertheless provides a first approximation of the potential for waves and currents to rework bed sediments. The entrainment potential estimated herein is likely to overestimate actual sediment entrainment in Mahurangi Estuary.

A.6.1 Computing sediment entrainment thresholds

The initiation of noncohesive grain motion at the bed is determined by the balance between the bed shear stress and the resistance of the sediment grains to disturbance. The latter is, conferred by the grains' submerged weight, which is a function of grain size and density. The bed shear stress (t_b), which acts to dislodge grains from the bed, is a function of the current speed and hydraulic bed roughness. The "wall law" or von Karman-Prandtl law describes the relationship between flow speed, bed shear stress and bed roughness in a steady, turbulent boundary layer:

$U_Z = U_* / \kappa \, . \ln (z/z_0)$

where U_Z = mean flow speed at height z above the bed

U_* = shear velocity ($=\sqrt{t_b/\rho}$, where t_b = bed shear stress and ρ is fluid density)

κ = von Karman's constant (0.41)

z = height above bed

z_0 = roughness length, which in fully rough turbulent flow equals $K_s/30$

where K_s is the bed roughness, which is a function of grain size and bedform geometry.

The critical shear velocity U_{*cr}, which is the value of U_* at which sediments are just dislodged from the bed by the flow, can be found from Shield's empirical relationship and the "wall law" can be used to convert U_{*cr} to Uz_{cr}, the flow speed at elevation z above the bed at which sediments are dislodged from the bed. In this study, we assume the seabed is flat. Bedforms generally increase bed shear stress relative to a flat bed under the same flow, however it is not clear how much, if any, of the increase in bed shear stress acts to entrain bed sediment.

By comparing measured current velocities with estimates of Uz_{cr} it is possible to make a preliminary assessment of the potential for sediment to be entrained by tidal currents in the estuary.

Sediment Entrainment by Waves

The skin friction exerted at the bed by combined currents and waves was calculated using Grant and Madsen's (1979) model using appropriate sediment grain size (to represent the hydraulic roughness) and density data. The calculated skin friction values were then compared to the threshold value for entrainment. When the combined flow skin friction exceeds the threshold value for a sediment particle then it is entrained by the flow and sediment transport may occur. In the case of bedload, the transport rate is proportional to the cube of the current velocity. Therefore, small changes in current speed have a significant effect on the rate of sediment transport.

Hydrodynamic and wave models were used to compute the peak depth-averaged tidal current and maximum wave bed-orbital velocities in each grid cell. The combined current and orbital velocities were then compared to (theoretical) critical values at the bed to determine zones where sediment is likely to be entrained at some point during the tidal-cycle. In grid cells where sediment entrainment was predicted to occur, the duration of entrainment was estimated by integrating potential entrainment at each half hour time-step over the entire tidal cycle.

A.6.2 Estuary modelling

Hydrodynamic Modelling

A comprehensive hydrodynamic, wave and sediment modelling study has been conducted. The models used in the Mahurangi Estuary sedimentation study include :

- 3DD (Black, 1995), a layered, 3-dimensional hydrodynamic model. In this study 3DD is used in the two-dimensional (vertical averaged) mode and predicts water levels and circulation within the estuary;

- 3DD_WGEN, a wind wave model which is used to predict wave height, period and bed orbital velocities in the estuary. The model includes terms for shoaling and energy losses due to friction and wave breaking.

The hydrodynamic model (3DD) was constructed on a regular (100x100 m) grid, covering the entire estuary downstream of the weir at Warkworth, where the Mahurangi River enters the estuary. Because of the spatial resolution of the model, the area upstream of Vialls Landing (upper estuary above core M8) was schematised as a straight channel one cell in width.

The bathymetry of the estuary was derived from published Navy charts, fair sheets and dedicated surveys of areas in the estuary conducted by NIWA for this study. The raw bathymetry were combined with a digitised shoreline and gridded using a kriging interpolation technique (Davis, 1986).

The tidal boundary for the hydrodynamic model was set offshore at approximately the 20m contour. A tide gauge deployed for 3 months at the entrance to the estuary was used to determine the harmonic constituents of the tides so that the offshore boundary condition for any particular tide could be modelled. Freshwater input to the model estuary was simulated by discharging daily freshwater flows from the Mahurangi River at the head of the model estuary.

Field Data Collection

A field program to collect hydrodynamic data was conducted from November 1993 to August 1994. Instruments were deployed throughout the estuary measuring water levels, current velocities and various water quality parameters. Surveying of cross sections at Scotts Landing and Mahurangi Heads was conducted in preparation for tidal gauging of ebb/flood tide discharge. Additional water samples, velocity, temperature and salinity profile data were collected at other selected sites around the estuary under a variety of freshwater inflow conditions.

Calibration and Verification of the Hydrodynamic Model

The hydrodynamic model was calibrated using the tidal gauging data. Good agreement between field measurements of water levels, velocities and discharges and modelled values was achieved. The similarity of the modelled and observed ebb and flood tide discharges is especially encouraging because modelled discharge combines velocity predictions, water level predictions and bathymetry data to give the total flux of water entering or exiting the estuary. Using the same model parameters, other periods were then modelled and similar agreement between field and modelled values was achieved.

Modelling Wind Generated Waves

Initial investigations had shown that tidal currents by themselves (i.e., no waves) were not sufficient to entrain intertidal sediments in the Mahurangi Estuary. Field observations had also indicated that waves are an important process by which sediment is resuspended in the estuary. Therefore, waves were also modelled. Scenarios were based on a 24 year local wind record and combined with tidal currents to assess the ability of combined waves and currents to entrain estuary sediments.

The model 3DD_WGEN which employs the Jonswap or SMB wave generation formulae was used to predict waves. Shoaling and energy losses due to friction and wave breaking are treated. Linear wave theory is used to predict orbital velocities under waves at any depth down to the bed.

Three wave parameters were calculated for each 100x100 m grid cell in the Mahurangi Estuary. These parameters are:

- **Significant Wave Height**: A commonly used measure of wave amplitude. It can be defined in a number of ways [Komen *et al*, 1994]. Historically, the significant wave height is defined as the average of the largest one third of wave heights recorded ($H_{1/3}$) or alternatively $H_s = 4m_0^{1/2}$ where m_0 is the zeroth moment or variance of the time series of sea-surface elevation relative to mean sea level. It can be shown that $H_{1/3}$ is approximately equal to H_s. Both definitions of significant wave height are average heights weighted towards the largest waves.

- **Peak Spectral Period**: A measure of the maximum period (time between successive wave peaks). It is calculated directly from the wave spectrum. The significant wave period (which is the period corresponding to the significant wave height) can also be calculated, however this requires the conversion of the wave spectrum into the time domain. This can result in a resolution problem if the wave period is small, as in the Mahurangi Estuary.

- **Orbital Velocity at the Bed**: The orbital velocity is the oscillating current generated by the wave orbital motions. The orbital velocity amplitude decreases with depth underneath the water surface.

In shallow coastal waters, such as estuaries, water depth is an important factor influencing wave height and bed orbital velocities. When the wave height becomes a significant portion of the depth (0.8 of depth) breaking will occur. The water depth in each grid cell is dependent on the local bathymetry and tide both of which are extracted from the hydrodynamic model.

Sediment Entrainment

The hydrodynamic model was used to compute peak tidal currents for the neap and spring tide conditions in each 100x100 m cell in the model grid. In the main channel, peak velocities occur at mid tide when flow is concentrated (in the channel) whereas on the intertidal flats peak velocities occur immediately prior to exposure of the flats by ebb tides.

The threshold at which sediment is dislodged from the seabed by currents and waves were computed for each grid cell (sediment entrainment thresholds). The threshold values were computed using sediment grain-size and density derived from the surficial sediment data (Fig. 5.4). A single measure of sediment grain size, the volume weighted mean diameter, was specified for each grid cell (Appendix A.6.3). Sediment bulk density was derived from the surface layer of the cores, and appropriate values applied to each grid cell.

The peak current velocities in each cell were compared to the predicted threshold currents required to entrain sediment from the bed. From those data, we identified model cells where sediment would be entrained as well as the duration (percentage of tidal cycle) of sediment entrainment.

A.6.3 Sediment texture

Surficial sediments were sampled at 50 sites, in all of the major sedimentary environments (i.e., channels, intertidal flats, inlets, embayments) found in the Mahurangi Estuary.

Sediment grain-size distributions were determined using a Malvern laser-diffraction system (Department of Earth Sciences, University of Waikato), which calculates the equivalent spherical volume of particles. The technique uses the principle of light diffraction, in which particle size (volume) is determined by the pattern of light diffraction from particles. It is reasonable to assume that sand-sized particles approximate a spherical shape, however, clay particles are more likely to be flat plates with large surface aspect ratios. This implies that measurement of clay particle size may be less accurate than for sand, depending on the orientation of the particle.

Volume-based measures of grain size distribution are also strongly influenced by large particles. Most of the volume of a mixed sand-mud sample will be held by the coarse particles, however this does not reflect the fact that the sample is mainly composed of clay particles in terms of the number of individual particles. Deriving a one-dimensional measure for a three-dimensional object is a fundamental problem in sedimentology but, despite its limitations, the technique does provide a consistent approach to particle sizing with the clay-sand size range.

Sediment Distribution throughout Mahurangi Estuary

To estimate thresholds for sediment entrainment, a single measure of sediment grain size was specified for each cell in the hydrodynamic model grid (Fig A.2). The volume-weighted mean diameter grain size was used to represent sediment texture. In the Mahurangi Estuary, surficial sediments are often bimodal, with a dominant coarse mode (55-300 µm) and secondary fine mode (6-10 µm). The volume-weighted mean diameter is influenced by modal peaks, in particular, by the coarse modal peak. The result of this approach was that in many cases the particle size specified was that of a noncohesive sediment. The cohesive size fraction present in most samples suggests that actual sediment entrainment will be less than that predicted for grain-size values used in our estimates.

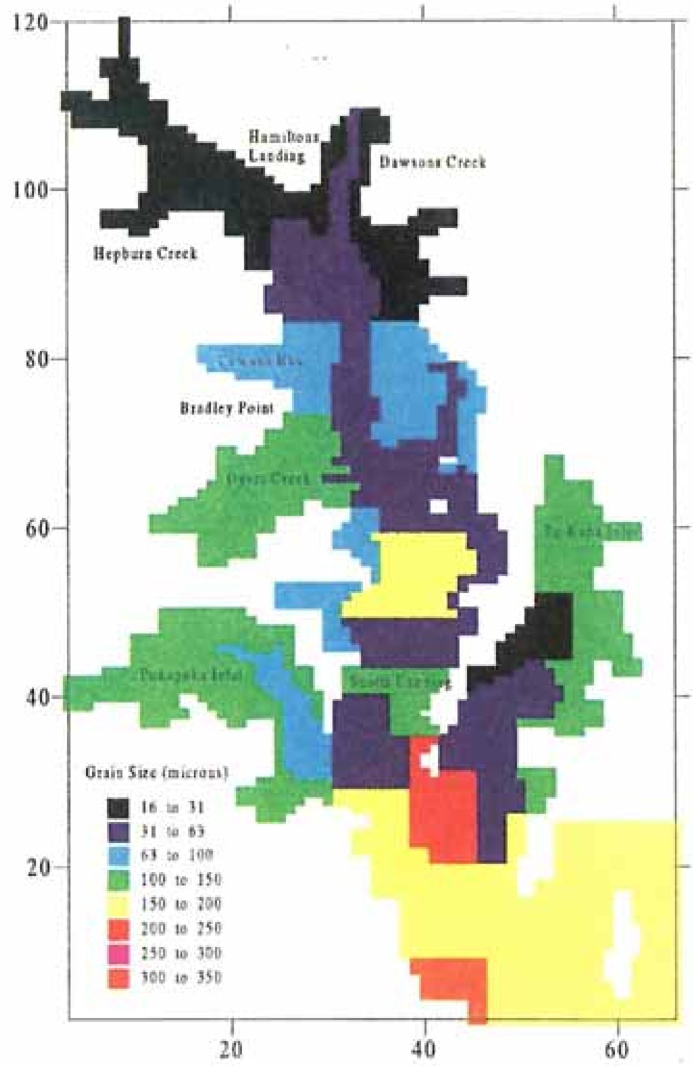

Fig. A.2: Spatial pattern of mean grain size (microns), represented by the volume-weighted mean diameter, used to model sediment entrainment in the Mahurangi Estuary.

f

APPENDIX B: SEDIMENT CORE LOGS (M1-M12)

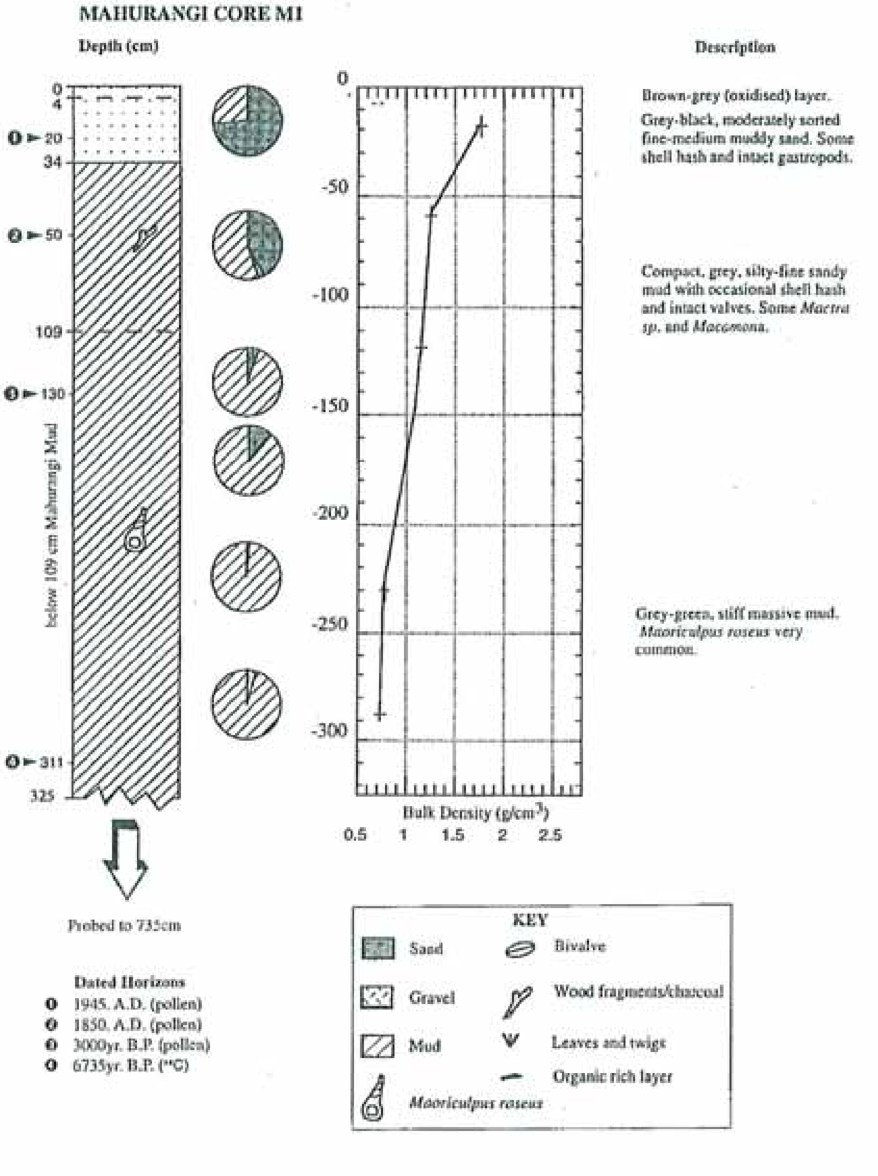
MAHURANGI CORE M1
Depth (cm)
Description
Brown-grey (oxidised) layer.
Grey-black, moderately sorted fine-medium muddy sand. Some shell hash and intact gastropods.
Compact, grey, silty-fine sandy mud with occasional shell hash and intact valves. Some Mactra sp. and Macomona.
Grey-green, stiff massive mud. Maoriculpus roseus very common.
below 109 cm Mahurangi Mud
Bulk Density (g/cm3)
Probed to 735cm
Dated Horizons
1945. A.D. (pollen)
1850. A.D. (pollen)
3000yr. B.P. (pollen)
6735yr. B.P. (14C)
KEY
Sand
Gravel
Mud
Maoriculpus roseus
Bivalve
Wood fragments/charcoal
Leaves and twigs
Organic rich layer

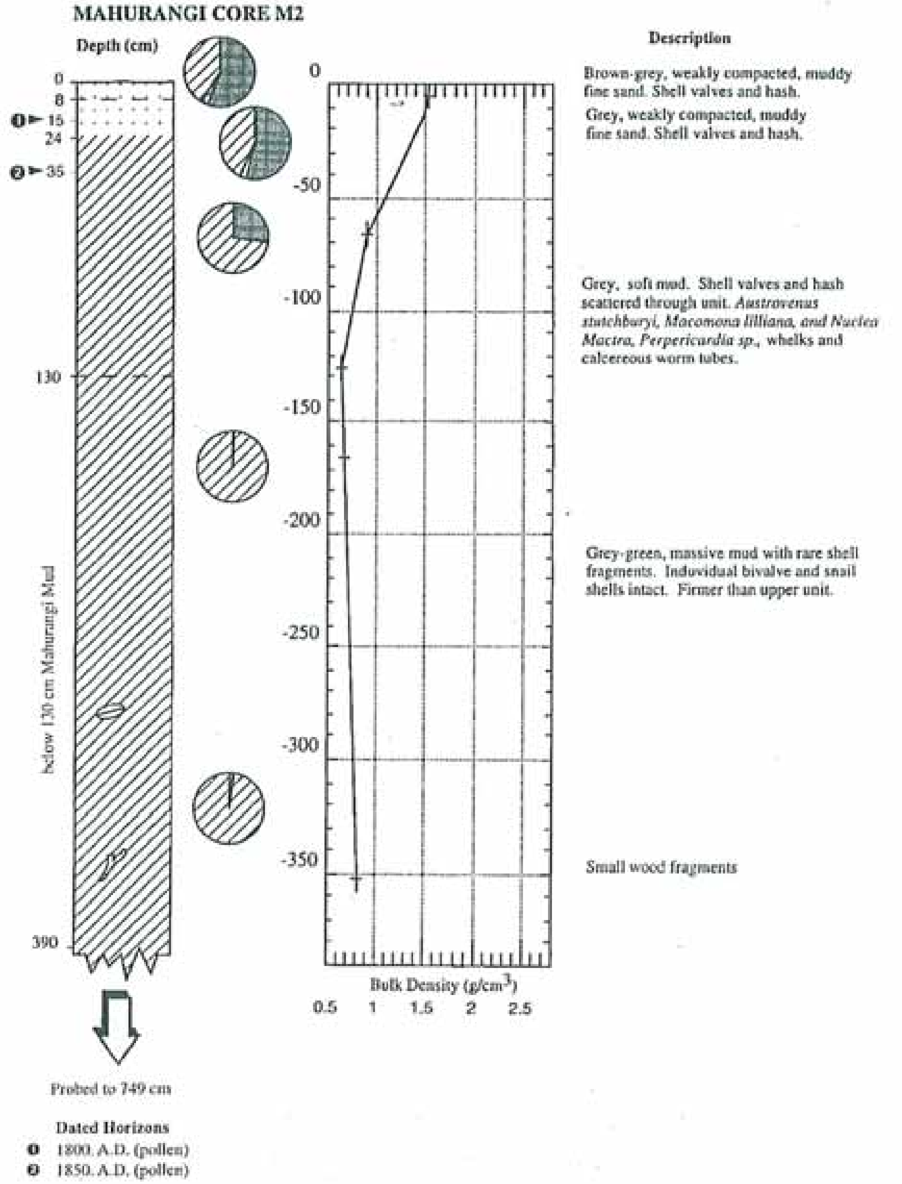
MAHURANGI CORE M2
Depth (cm)
0
8
15
24
35
130
390
below 130 cm Mahurangi Mud
Probed to 749 cm
Dated Horizons
❶ 1800. A.D. (pollen)
❷ 1850. A.D. (pollen)
0
-50
-100
-150
-200
-250
-300
-350
Bulk Density (g/cm³)
0.5 1 1.5 2 2.5
Description
Brown-grey, weakly compacted, muddy fine sand. Shell valves and hash.
Grey, weakly compacted, muddy fine sand. Shell valves and hash.
Grey, soft mud. Shell valves and hash scattered through unit. Austrovenus stutchburyi, Macomona lilliana, and Nuclea Mactra, Perpericardia sp., whelks and calcereous worm tubes.
Grey-green, massive mud with rare shell fragments. Induvidual bivalve and snail shells intact. Firmer than upper unit.
Small wood fragments

MAHURANGI CORE M3

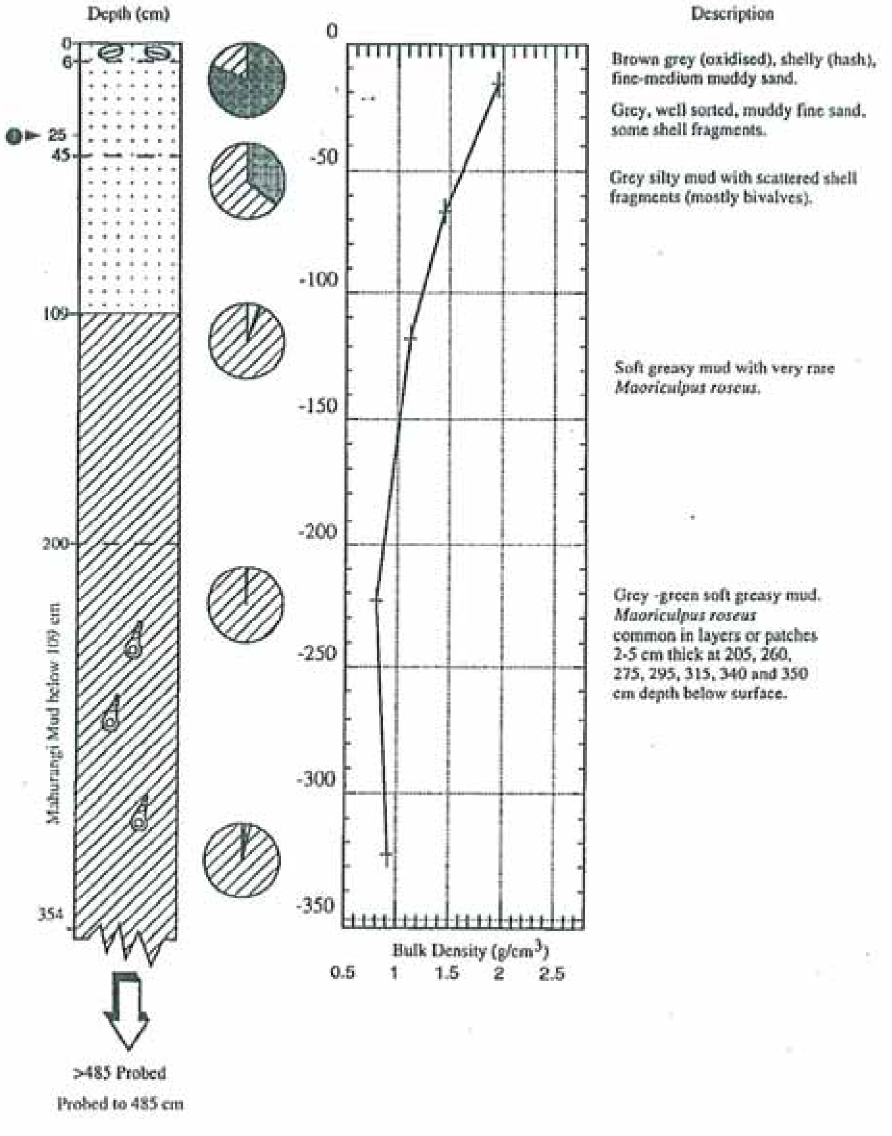

Dated Horizons

❶ 1900. A.D. (pollen)

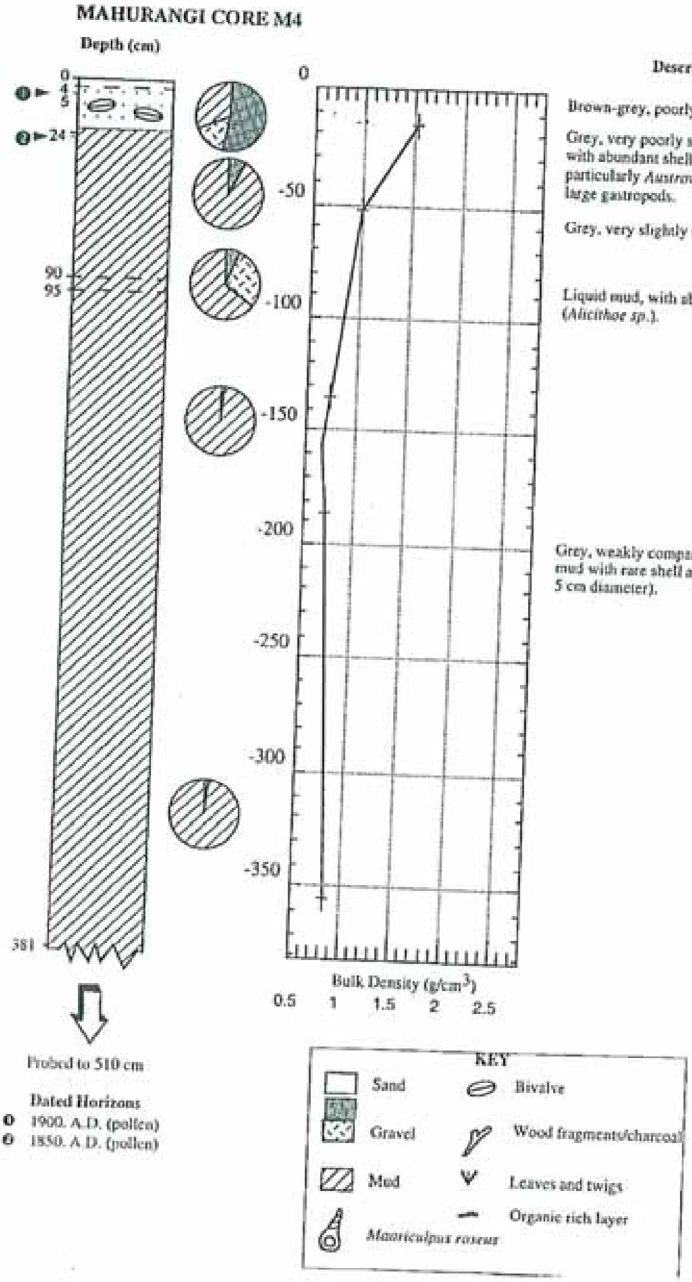
MAHURANGI CORE M4
Depth (cm)
0
4
5
24
90
95
381
Probed to 510 cm
Dated Horizons
1900. A.D. (pollen)
1850. A.D. (pollen)
0
-50
-100
-150
-200
-250
-300
-350
Bulk Density (g/cm³)
0.5
1
1.5
2
2.5
Description
Brown-grey, poorly sorted muddy fine sand
Grey, very poorly sorted muddy fine sand, with abundant shell valves and hash, particularly Austrovenus stutchburyi and large gastropods.
Grey, very slightly sandy mud, soft.
Liquid mud, with abundant gastropods (Alicithoe sp.).
Grey, weakly compacted, slightly sandy mud with rare shell and pebbles (up to 5 cm diameter).
KEY
Sand
Gravel
Mud
Mauriculpus roseus
Bivalve
Wood fragments/charcoal
Leaves and twigs
Organic rich layer

MAHURANGI CORE M5

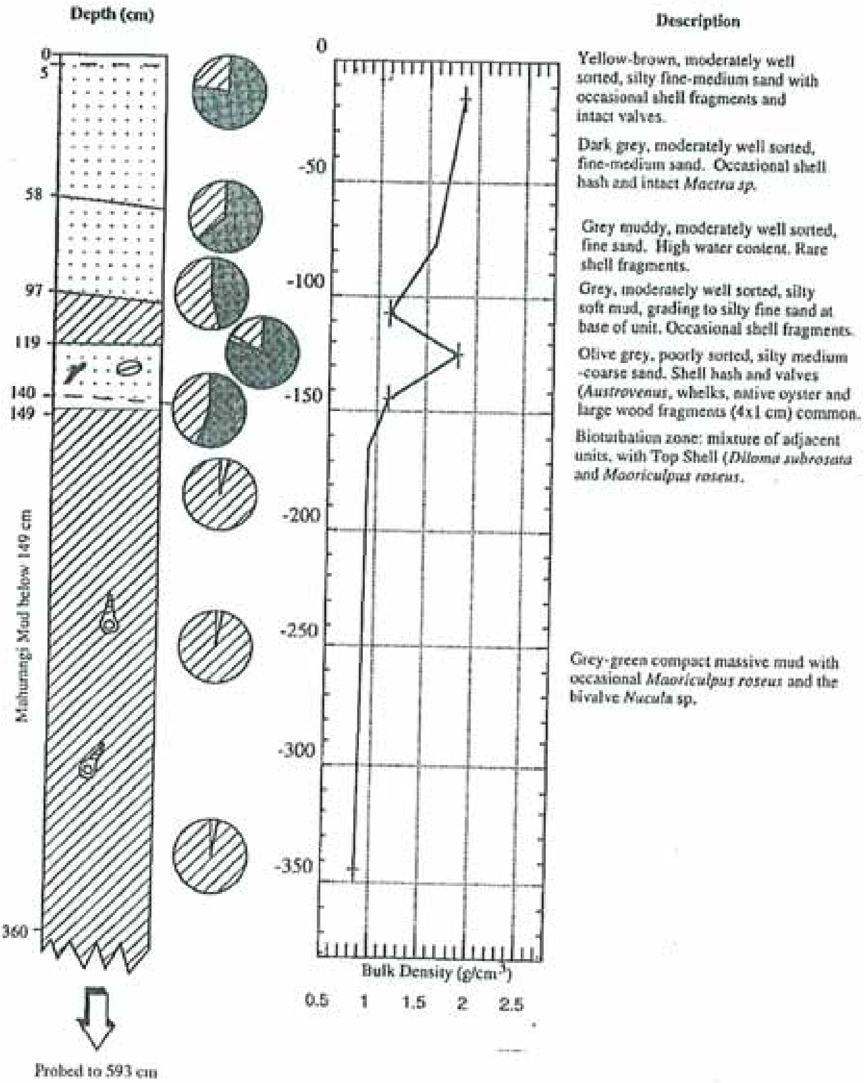

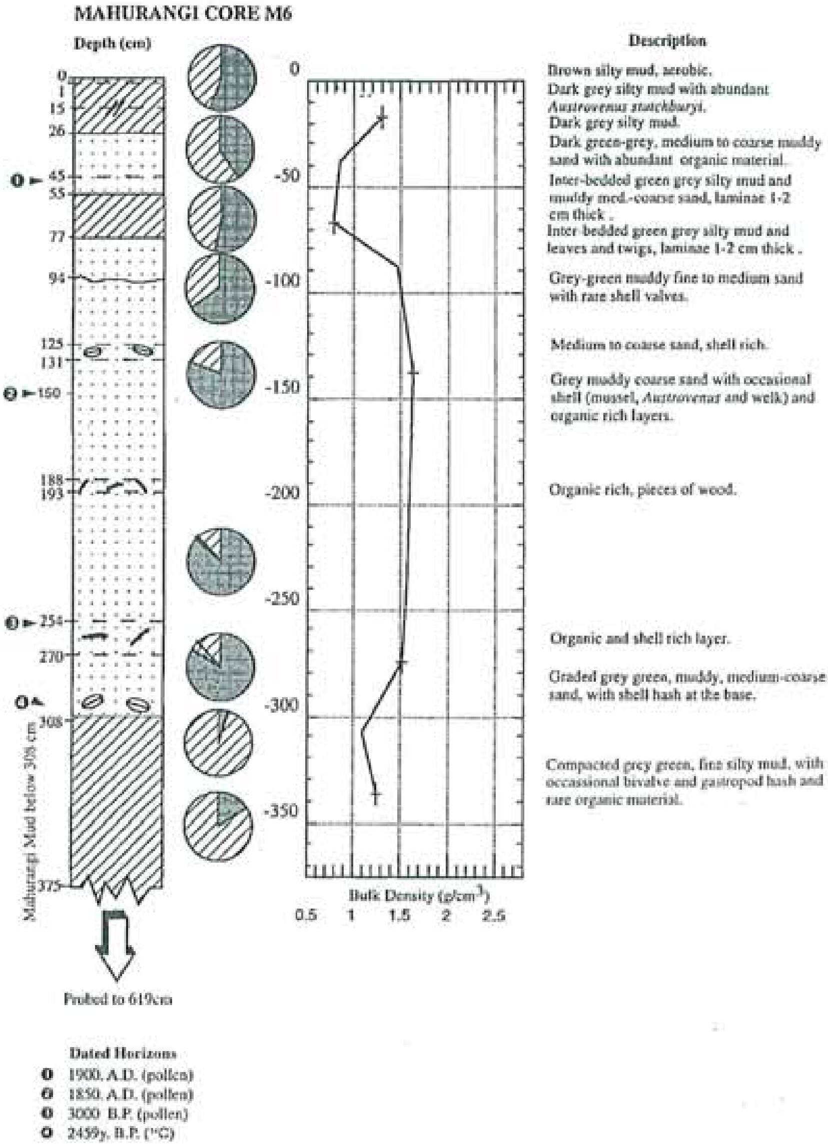
MAHURANGI CORE M6
Depth (cm)
0
1
15
26
45
55
77
94
125
131
150
188
193
254
270
308
375
Mahurangi Mud below 308 cm
Probed to 619cm
0
-50
-100
-150
-200
-250
-300
-350
Bulk Density (g/cm^3)
0.5
1
1.5
2
2.5
Description
Brown silty mud, aerobic.
Dark grey silty mud with abundant *Austrovenus statchburyi*.
Dark grey silty mud.
Dark green-grey, medium to coarse muddy sand with abundant organic material.
Inter-bedded green grey silty mud and muddy med.-coarse sand, laminae 1-2 cm thick.
Inter-bedded green grey silty mud and leaves and twigs, laminae 1-2 cm thick.
Grey-green muddy fine to medium sand with rare shell valves.
Medium to coarse sand, shell rich.
Grey muddy coarse sand with occasional shell (mussel, *Austrovenus* and welk) and organic rich layers.
Organic rich, pieces of wood.
Organic and shell rich layer.
Graded grey green, muddy, medium-coarse sand, with shell hash at the base.
Compacted grey green, fine silty mud, with occassional bivalve and gastropod hash and rare organic material.
Dated Horizons
1900 A.D. (pollen)
1850 A.D. (pollen)
3000 B.P. (pollen)
2459y. B.P. (^{14}C)

MAHURANGI CORE M7

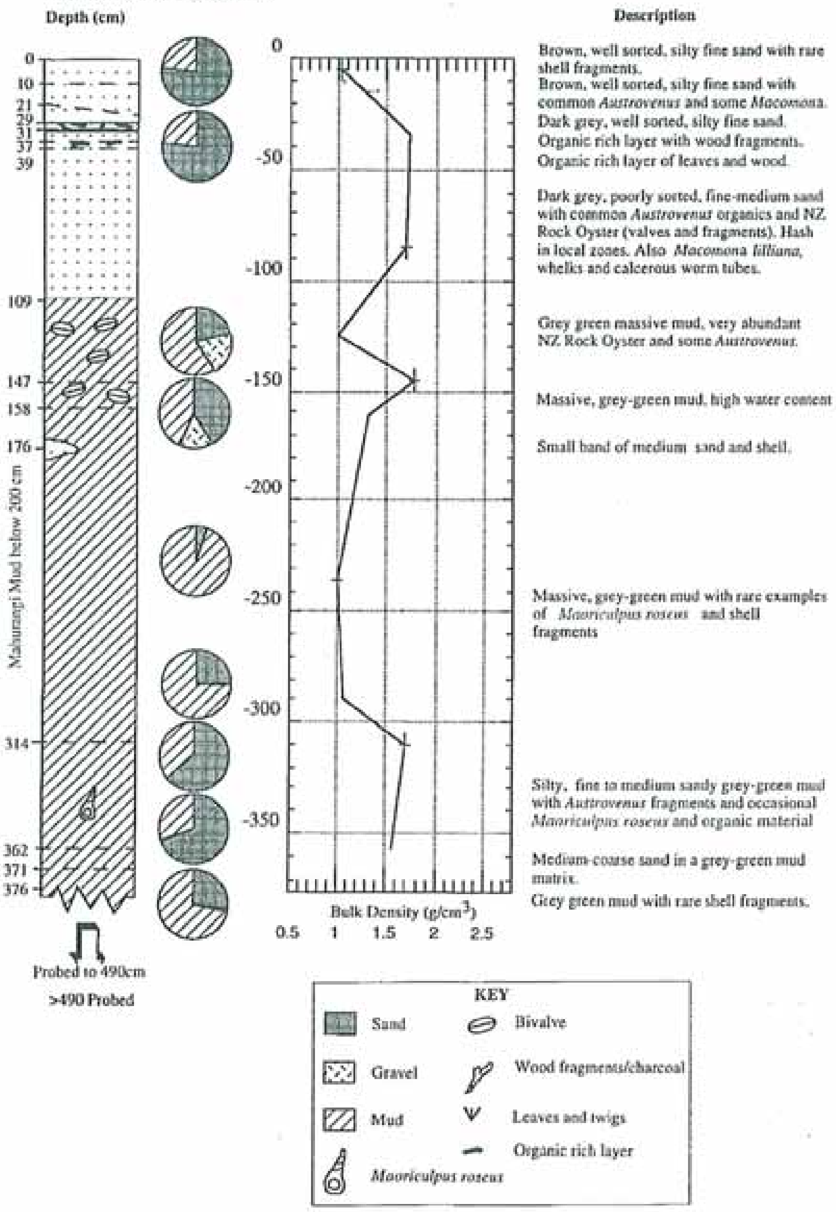

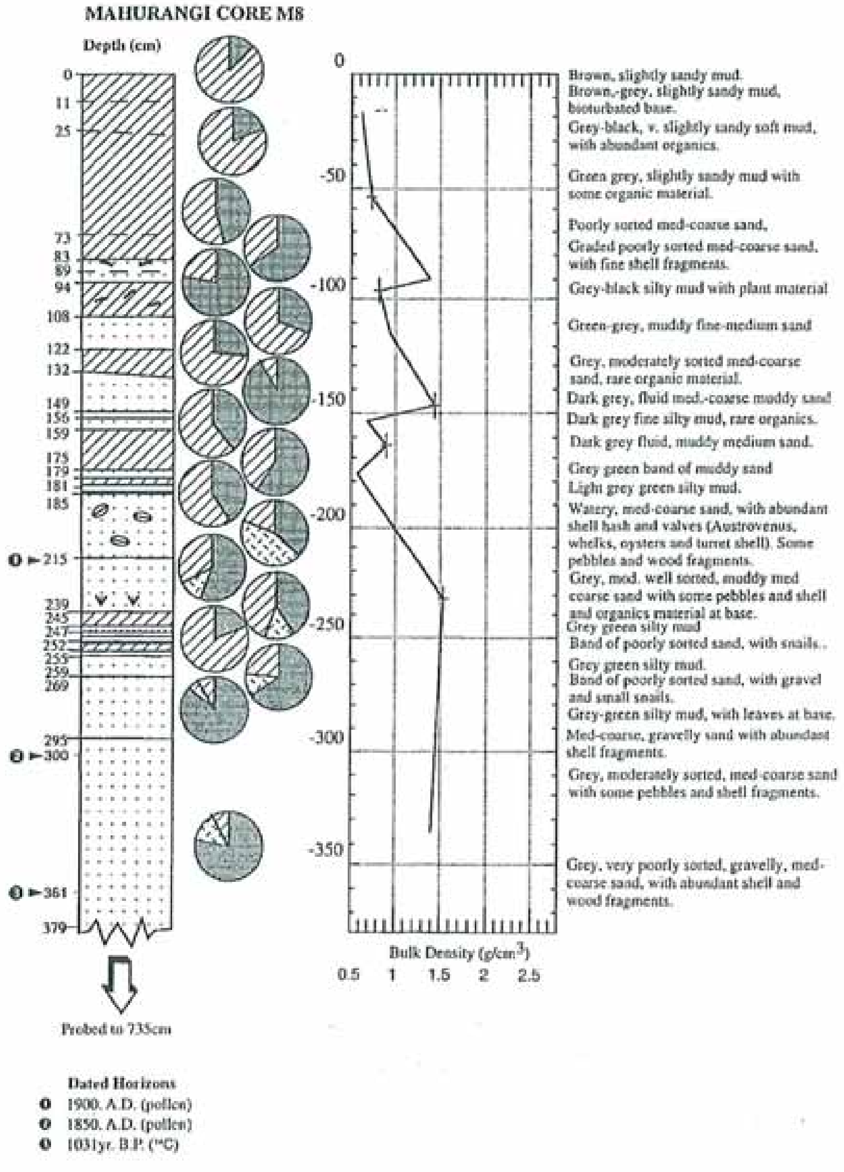
MAHURANGI CORE M8
Depth (cm)
Probed to 735cm
Dated Horizons
1900. A.D. (pollen)
1850. A.D. (pollen)
1031yr. B.P. (14C)
Bulk Density (g/cm3)
0.5 1 1.5 2 2.5
Brown, slightly sandy mud.
Brown,-grey, slightly sandy mud, bioturbated base.
Grey-black, v. slightly sandy soft mud, with abundant organics.
Green grey, slightly sandy mud with some organic material.
Poorly sorted med-coarse sand,
Graded poorly sorted med-coarse sand, with fine shell fragments.
Grey-black silty mud with plant material
Green-grey, muddy fine-medium sand
Grey, moderately sorted med-coarse sand, rare organic material.
Dark grey, fluid med.-coarse muddy sand
Dark grey fine silty mud, rare organics.
Dark grey fluid, muddy medium sand.
Grey-green band of muddy sand
Light grey green silty mud.
Watery, med-coarse sand, with abundant shell hash and valves (Austrovenus, whelks, oysters and turret shell). Some pebbles and wood fragments.
Grey, mod. well sorted, muddy med coarse sand with some pebbles and shell and organics material at base.
Grey green silty mud
Band of poorly sorted sand, with snails..
Grey green silty mud.
Band of poorly sorted sand, with gravel and small snails.
Grey-green silty mud, with leaves at base.
Med-coarse, gravelly sand with abundant shell fragments.
Grey, moderately sorted, med-coarse sand with some pebbles and shell fragments.
Grey, very poorly sorted, gravelly, med-coarse sand, with abundant shell and wood fragments.

MAHURANGI CORE M9

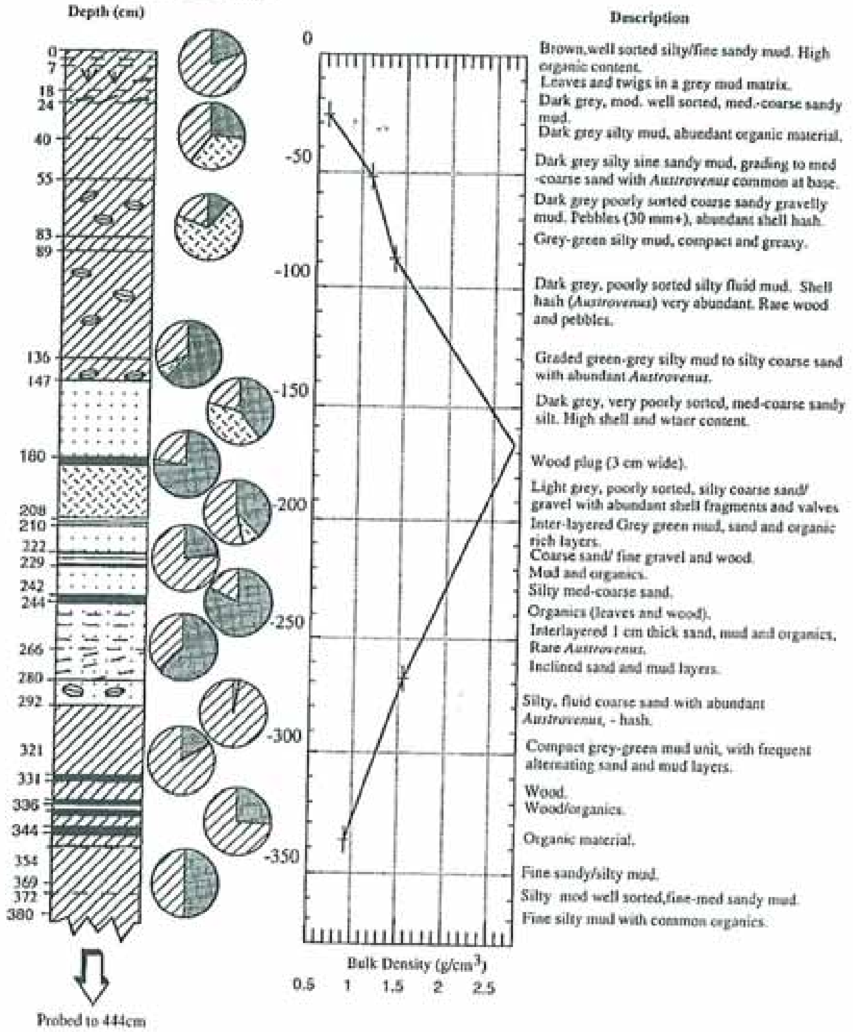

MAHURANGI CORE M10

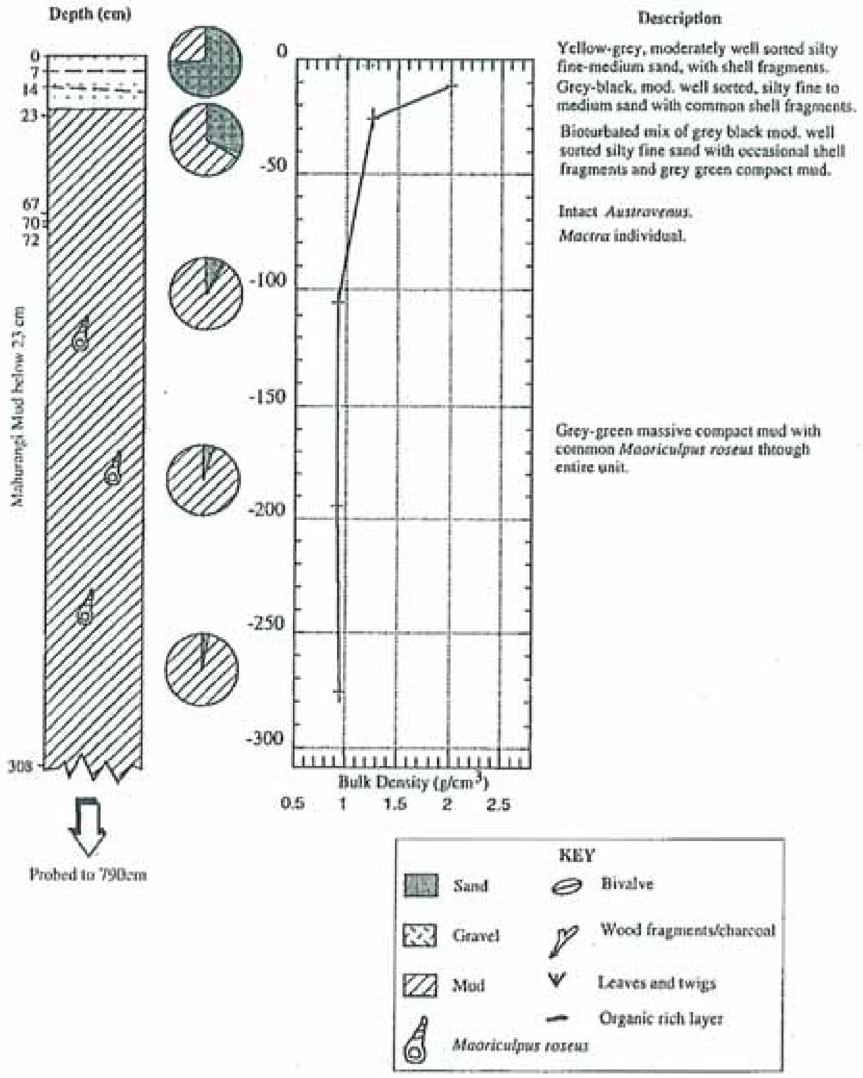

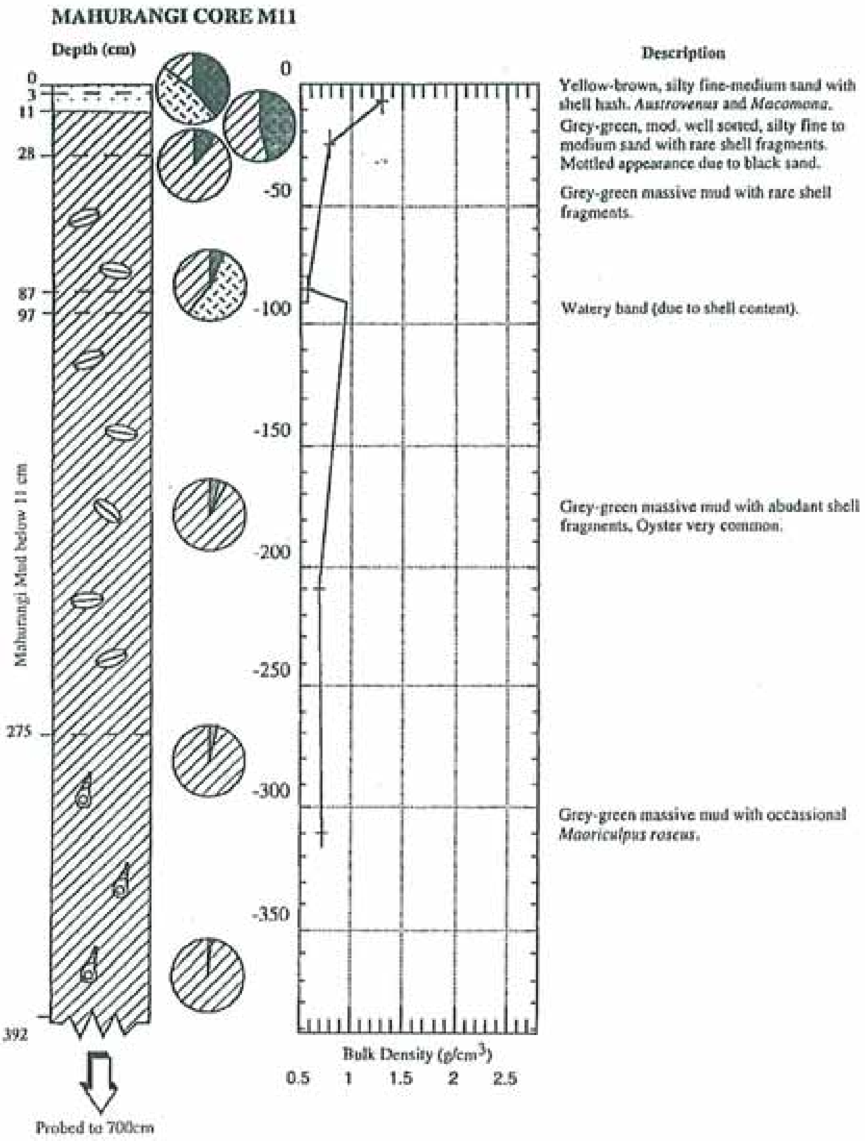
MAHURANGI CORE M11
Depth (cm)
0
3
11
28
87
97
275
392
Mahurangi Mud below 11 cm
Probed to 700cm
0
-50
-100
-150
-200
-250
-300
-350
Bulk Density (g/cm3)
0.5 1 1.5 2 2.5
Description
Yellow-brown, silty fine-medium sand with shell hash. Austrovenus and Macomona.
Grey-green, mod. well sorted, silty fine to medium sand with rare shell fragments. Mottled appearance due to black sand.
Grey-green massive mud with rare shell fragments.
Watery band (due to shell content).
Grey-green massive mud with abudant shell fragments. Oyster very common.
Grey-green massive mud with occassional Maoriculpus roseus.

MAHURANGI CORE M12

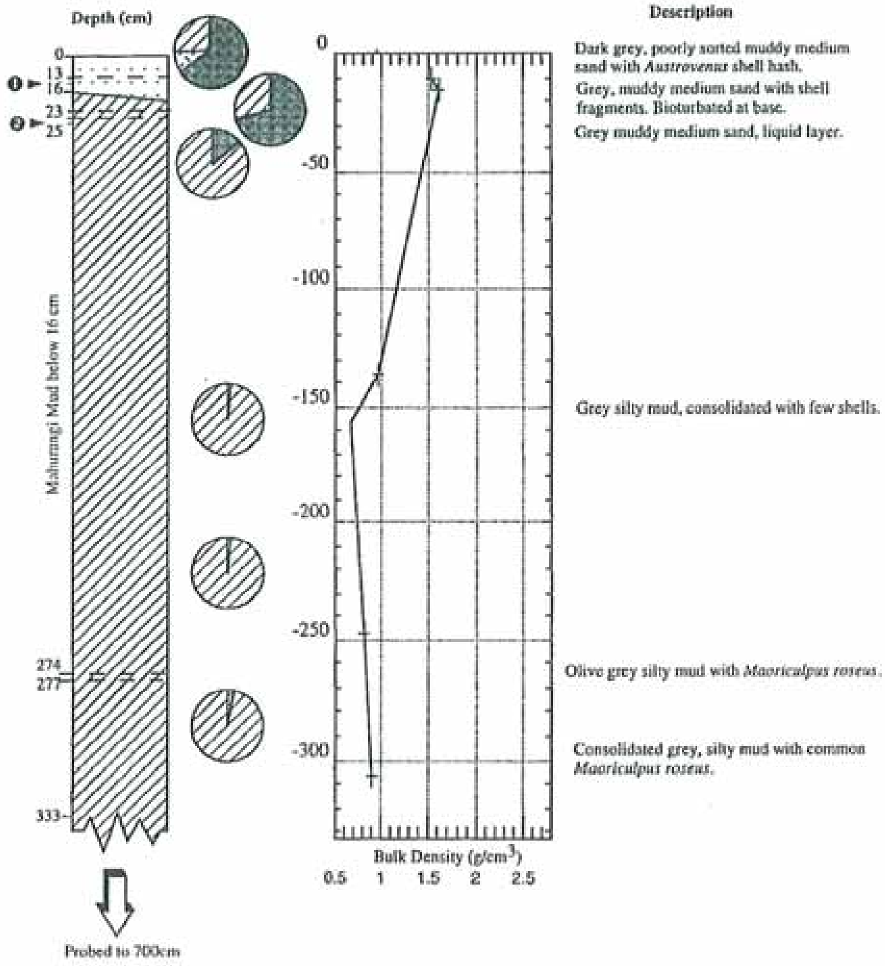

Dated Horizons
❶ 1900. A.D. (pollen)
❷ 1850. A.D. (pollen)

APPENDIX C: POLLEN DATING REPORT

REPORT ON POLLEN ANALYSIS OF CORES M1,M2,M3,M4,M5,M6,M8 & M12 FROM MAHURANGI HARBOUR

Preparation and pollen analysis

Samples taken as one cm thick slices were prepared for pollen analysis by the standard method of digestion in hydrofluoric acid, acetolysis, and chlorine bleach. Pollen rich residue for analysis was mounted in glycerine jelly. Pollen preservation was excellent, and all but one sample had adequate pollen and spore spectra for analysis. Two cores were selected for detailed analysis (Core M1 & M8). Sufficient samples were made up from the remaining cores to permit estimate of zone boundaries from scanning of slides, but no detailed analysis was undertaken on these samples.

Vegetation history

The pollen samples fall into 4 broad assemblage groups, and these are marked on the two analysed pollen diagrams (Fig 1 and Fig 2). From the base of the core they are:

Zone D: estimated age 6000 BP - 3000 BP
Assemblages marked by complete dominance of forest trees and tree ferns, but with low amount of kauri (*Agathis australis*). Forest dominants include kauri, rimu (*Dacrydium cupressinum*), kahikatea (*Dacrycarpus dacrydioides*), totara (*Podocarpus*), matai (*Prumnopitys taxifolia*), miro (*Prumnopitys ferruginea*), hard beech (*Nothofagus fusca* type) This zone represents undisturbed conifer/hardwood forest before the rise of kauri.

Zone C: estimated age 3000 BP - 1850 AD
Pollen assemblages of this zone are the same as the last, with the exception that kauri and matai have become more common. In the upper half of this zone in Core M1 there is a slight increase in bracken (*Pteridium esculentum*) that may possibly indicate some early Polynesian distfirbance of the catchment, although it is equally possible that it is simple the effect of natural disturbance.

Zone B: estimated age 1850 AD - 1900 AD
In the course of this zone all forest dominants decline steeply, disturbance indicators bracken and tutu (*Coriaria*) increase rapidly. Traces of pine (*Pinus*) pollen are encountered.

Zone A: estimated age 1900 AD - present.
Pine, grass (Poaceae) and weeds increase steeply, while bracken decreases.

Zone ages

Sea level rise constrains the age of the undisturbed forest Zone D to around 6-7000 BP, although similar forest has dominated this region since about 10 000 BP (Newnham & Lowe, 1991). Kauri had been increasing in the Auckland region since about 6000 BP (Newnham & Lowe; Ogden *et al.* 1992), but peaking only after 3000 BP. Zone D therefore probably dates from around 6000 BP to about 3000 BP. Zone C is characterised by abundant kauri and undisturbed forest. The rapid rise of bracken and decline of forest that begins Zone B indicates massive forest disturbance including the destruction of the kauri forest. A similar event in Lucas Core 12 was interpreted as the beginning of Maori burning of the Auckland

Isthmus at around 700 BP (Hume & McGlone, 1986). However, this event at Lucas Creek was not accompanied by total destruction of the kauri forest, which came later in the profile at the point that other signs of European influence such as weeds and pine became apparent. Logging of kauri in the Warkworth area began in the late 1820s , but in 1840 the hills on the sides of the Mahurangi Harbour are described as being covered with kauri down to the water's edge (see references in Beever 1981). This being the case, it seems unlikely that Zone B represents Maori deforestation of the area, but rather the intensive logging that began in the 1850s. Zone A is characterised by the simultaneous increase of pine, grass and weeds of arable land - plantain (*Plantago lanceolata*), sorrel (*Rumex acetosella*), clover (*Trifolium*). The pollen in the Cupressaceae can belong either to the native cedar (*Libocedrus*), or to a number of introduced trees, most probably macrocarpa (*Cupressus macrocarpa*). In Core M8 there is a strong increase in Cupressaceae that probably reflects farm hedges and plantations of macrocarpa. Tree fern spore levels do not fall as perhaps would have been expected from the destruction of forest in the district. Tree fern spores resist corrosion, and their continuing high levels indicate reworking and erosion of soils and sediments in the catchment. The beginning of Zone A probably dates from the end of the kauri extraction phase in this district. The high levels of pine however can only date from the establishment of substantial pine plantations in the region which is likely to be in the 1950s and 1960s.

There seems to be only a weak relationship between stratigraphy and pollen assemblages.

Table and Figures

In the Table, and Figs 1 & 2, the zonation of the pollen assemblages in the cores is indicated. Pollen percentages in the figs are as a proportion of a pollen sum that excludes tree ferns and wetland plants. In the Table, "5" indicates as high a porportion of the pollen sum as has been noted in cores, and "1" indicates a low percentage of 5-1%. "+" indicates the pollen type was seen, but probably in not enough quantity to be registered as a percentage. "-" pollen type absent.

References

Beever, J. 1981. A map of the pre-European vegetation of lower Northland, New Zealand. *New Zealand Journal of Botany* 19: 105-110.

Hume, T.M.; McGlone, M.S. 1986. Sedimentation patterns and catchment use change recorded in the sediments of a shallow tidal creek, Lucas Creek, Upper Waitemata Harbour, New Zealand. *New Zealand Journal of Marine and Freshwater Research* 20: 677-687.

Newnham, R.M.; Lowe, D.J. 1991. Holocene vegetation and volcanic activity, Auckland Isthmus, New Zealand. *Journal of Quaternary Science* 6: 177-193.

Report prepared for Dr Terry Hume, NIWA Ecosystems, PO Box 11-115 Hamilton.

Matt McGlone
Landcare Research
PO Box 69, LINCOLN

21 September 1994

Table 1: Mahurangi pollen results

Site & depth (cm)	pine	grass & weeds	bracken	kauri	other forest	Zone
M2 (X94/2)						
10	5	5	4	+	1	A
20	+	+	5	4	4	B
30	-	-	5	4	4	B
40	-	-	-	5	5	C
M3 (X94/3)						
10	5	5	2	+	1	A
20	2	4	3	4	4	A
30	-	-	-	5	5	C
40 - 60	-	-	-	5	5	C
M4 (X94/4)						
1	5	5	3	+	2	A
5	+	+	3	2	4	B
10	+	+	3	3	4	B
20	-	-	2	5	4	B
30-50	-	-	1	5	5	C
60	-	-	-	5	5	C
M6 (X94/5)						
10	4	4	3	+	2	A
20	3	4	3	+	2	A
30	3	3	4	+	2	A
40	2	3	4	+	3	A
50	+	+	4	3	4	B
60-100	+	-	4	3	4	B
200	-	-	-	5	5	C
300	-	-	-	1	5	D
M12 (X94/7)						
10	5	4	2	1	1	A
20	+	+	2	4	5	B
30	+	-	-	5	5	C
40	-	-	-	5	5	C

FIG.1: Mahurangi Core M1

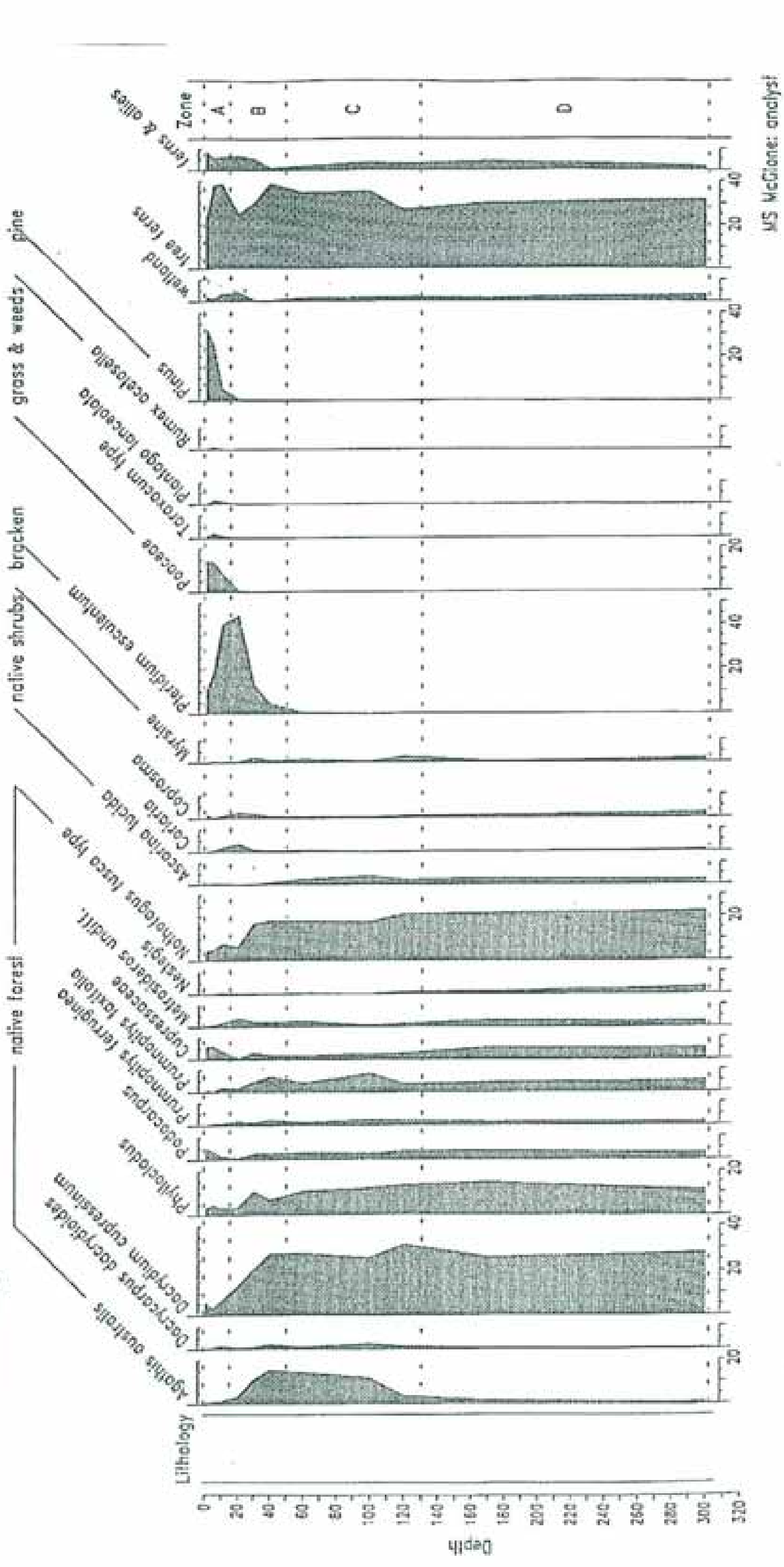

FIG 2: Mahurangi Core M8